Chapter 1

Introduction

Physiological functions of arachidonic acid (AA) metabolism and phospholipase A_2 (PLA_2) family of enzymes

Essential fatty acids, including omega-3 and omega-6, can not be synthesized *de novo* by humans and therefore must be obtained from the diet. In addition to providing energy, essential fatty acids and/or their metabolites serve multiple functions in the body , including: 1) regulation of inflammation and clotting; 2) involvement of cell death and aging; 3) acting as neuronal messengers; 4) formation of lipid rafts and affecting cellular signaling; and 5) modulation of transcription factors. The biological effects of essential fatty acids are mediated by the balance between omega-3 and omega-6 fats and their mutual interactions . Omega-3 fatty acids are generally less inflammatory, or anti-inflammatory; while omega-6 fatty acids, especially AA, is a key inflammatory intermediate.

AA, which is present in the phospholipids of the cellular membranes, is released by the cleavage action of the PLA_2 family of enzymes. AA is then further metabolized by cyclooxygenases (COX), lipoxygenases (LOX) and cytochrome P450s into prostanoids (e.g., prostaglandins, prostacyclins, and thromboxanes), leukotrienes, epoxyeicosatrienoic and hydroxyeicosatetraenoic acids, respectively .

Prostanoids and leukotrienes, collectly called eicosanoids, are involved in the modulation of all cardinal signs of inflammation, namely, redness, swelling, pain and fever . Proinflammatory eicosanoids promote dilation and increase the permeability of blood vessels near the site of injury, thus causing redness and swelling. Leukocytes, which are attracted to local tissue by leukotrienes, further promote inflammation by producing proinflammatory

cytokines and other mediators. Prostaglandin E_2 (PGE_2) can sensitize pain neurons and promote fever by acting on the hypothalamus. Glucocorticoid steroids and non-steroidal anti-inflammatory drugs (NSAIDS) are used to suppress inflammation by limiting production of inflammatory eicosanoids through the inhibition of PLA_2 and the COX family of enzymes. However, it is worth noting that not all effects of eicosanoids are inflammatory; since eicosanoids derived from omega-3 fatty acids can function as anti-inflammatory mediators. Further, the net effect of a certain eicosanoid on inflammation is dependent on the target tissue/ cell type involved, the stimulus given, and the interaction with other lipid mediators. As an example, PGE_2 can either promote or suppress inflammation with variation in the cellular milieu .

Changes in AA metabolism are often involved in cell death and AA accumulation can directly induce cell death *via* a mitochondrial-mediated pathway . Indeed, the chemopreventive benefits of COX inhibitors (non-steroid, anti-inflammatory drugs) against cancers may be at least partially due to their ability to promote intracellular AA accumulation . Further, oxidized metabolites of AA produced by LOX and cytochrome P450 can also induce apoptosis.

In addition to its role in inflammation and cell death, AA participates in cellular signaling as a secondary messenger and regulates multiple signaling enzymes, notably phospholipase C (PLC) and protein kinase C (PKC). De-regulation of AA metabolism has been implicated in many diseases, notably sepsis , arthritis , inflammatory bowel disease (IBD) , atherosclerosis , neurodegenerative diseases and cancer .

The PLA_2 family of enzymes, including calcium-dependent, cytosolic PLA_2 ($cPLA_2$) and secretory PLA_2 ($sPLA_2$), as well as calcium-independent PLA_2 ($iPLA_2$), are the rate-limiting enzymes involved in the first step of AA metabolism . In line with the physiological functions of AA and eicosanoids, all three groups of PLA_2 play important roles in inflammation , cell

death/apoptosis and other cellular functions . The enzymatic activities of the PLA_2 family of enzymes are tightly regulated by multiple factors. Full activation of $cPLA_2$ involves phosphorylation by MAPK and translocation of $cPLA_2$ from the cytosol to the plasma membrane, where it hydrolyzes phospholipids to generate AA . In the context of inflammation, PLA_2 activities can be modulated by cytokines (e.g., TNF-α and IL-1β) and microbial products (e.g., lipopolysacchride [LPS]) . In the context of cellular stress, PLA_2 activities can be modulated by reactive oxygen species (ROS), radiation and chemotherapeutic drugs (e.g., cisplatin) . Further, PLA_2 activities can also be modulated by hormones (e.g., oxytocin), mitogens, second messengers (e.g., eicosanoids and Ca^{2+}) and protein regulators (e.g., annexins and PLAA) .

Review of literature regarding PLAA

PLAA is a novel activator of PLA_2 that regulates the production of PGE_2, TNF-α, and IL-1β . The cDNA of murine PLAA was originally cloned from a smooth muscle-like cell line, BC_3H1, using antibodies to melittin , a peptide component (26-amino acid long) of bee venom known to activate PLA_2 and phospholipase D . Within murine PLAA, a stretch of amino acid residues between positions 503-538 exhibit 42% identity with mellitin. Subsequently, a 28-kDa fragment of murine PLAA was partially purified from BC_3H1 cells by using anti-melittin antibody affinity chromatography, which was shown to stimulate PLA_2 activity in an *in vitro* assay system . Later, the cDNA encoding the rat *plaa* gene was cloned . This led to our cloning and characterization of the human *plaa* gene from a human macrophage/monocyte cell line U937 . The full length human PLAA contains 738 amino acid residues with a predicted molecular mass of 82 kDa, sharing over 90% similarity at the amino acid level with murine and rat PLAA . In its amino terminal region, the human PLAA contains G protein beta domain (G_β) (amino acid residues 1- 250) , which is involved in protein-protein interaction and signaling functions such as activating phospholipase C . Within amino acid residues 503-538, human PLAA exhibits 39% identity with melittin .

Expression of the *plaa* gene in host cells (e.g., macrophages and intestinal epithelial cells) can be induced rapidly by bacterial products, such as cholera toxin (CT) and LPS , as well as by proinflammatory cytokines, such as TNF-α and IL-1β . As demonstrated by our antisense knockdown experiment, expression of the murine *plaa* gene is required for AA production in RAW 264.7 murine macrophages stimulated with LPS and CT . The gene encoding human PLAA is expressed in the majority of body tissues at different levels , with high expression observed in spleen, tonsil, blood vessel, cervix, prostate, bone and adipose tissue.

The potential role of PLAA in inflammation

Our earlier studies indicated increased levels of PLAA in biopsy specimens of patients with IBD in concurrence with the induction of COX-2 and PLA_2 . Likewise, monosodium urate crystals, the etiological agent of gout, also induced the expression of the *plaa* gene and activated PLA_2 . Consistent with the induction of PLA_2 activity in patients with adult respiratory distress syndrome (ARDS) and atherosclerosis , LPS increases *plaa* mRNA abundance in murine and rat alveolar macrophages and human endothelial cells (unpublished results from our laboratory). In turn, induction of PLAA can modulate inflammatory responses. For example, injection of a 28-kDa murine PLAA polypeptide into rabbit knee joints resulted in acute inflammatory arthritis with increased eicosanoid production and synovial leukocyte count . Treatment of human neutrophils with the same PLAA polypeptide increased neutrophil degranulation and production of lysosomal enzymes and superoxide anions . In addition, the 28-kDa murine PLAA polypeptide, as well as the human PLAA synthetic peptide (36-amino acid long [position 503-538]) spanning the melittin homology domain, also induced the production of TNF-α and IL-1β in human monocytes and murine RAW 264.7 macrophages . Conversely, blocking expression of the *plaa* gene by using antisense oligonucleotides reduced AA production in RAW 264.7 cells stimulated with LPS and CT .

However, the *in situ* function of PLAA in the context of inflammation is not understood. There is a paucity of information in the following areas: 1) previous functional characterization of PLAA was conducted using either a 28-kDa murine PLAA polypeptide or PLAA synthetic peptides added exogenously to the cell culture. Therefore, the exact role of native full length PLAA (an intracellular protein) within the host cell with respect to its capacity to activate PLA_2 and to regulate eicosanoid production is completely unknown; 2) the mechanism of mutual induction between PLAA and cytokines is not well understood; and 3) the regulation of *plaa* gene expression has not been illustrated.

In our current study, we hypothesized that hyper-expression of the native *plaa* gene induced by inflammatory stimuli further perpetuates inflammation by modulating eicosanoid and cytokine production. This hypothesis was examined with the following aims: 1) to determine whether native PLAA regulates eicosanoid production by overexpressing the *plaa* gene *in situ*; 2) to identify inflammation-associated protein targets modulated by *plaa* gene induction; and 3) to delineate whether native PLAA regulates cytokine production by modulating NF-κB activation. In addition, we characterized the transcriptional regulation of the *plaa* gene and searched for *cis*- and *trans*-acting regulatory elements in its 5' genomic region.

The potential role of PLAA in apoptosis

The gene encoding human PLAA is located on chromosome region 9p21 , a region frequently inactivated in various cancers, including melanoma, glioma, ovarian, lung and breast cancers and lymphoid leukemia . It has been reported that PLAA peptides induced apoptosis of smooth muscle cells and tumor regression in animal models of glioma, lung and breast cancer . $cPLA_2$, $sPLA_2$ and $iPLA_2$ have all been implicated in apoptosis and $iPLA_2$ mediates cisplatin-induced renal cell apoptosis . Interestingly, unpublished data from a study conducted by Peters *et al* showed that carboplatin-sensitive ovarian cancer cells from patients produced higher levels of PLAA than did their resistant control cells. In a cell line derived

from the organ of Corti, cisplatin induced the expression of genes involved in AA metabolism , especially PLAA, PLA_2 group IVA (a cytosolic PLA_2) and group V (a secreted PLA_2). Oxidative stress, potentially induced by oxidized metabolites of AA, was suggested to contribute to the cytotoxicity of cisplatin . Further, AA accumulation can induce apoptosis either directly *via* a mitochondrial-mediated pathway , or indirectly by inducing production of the cytotoxic ceramide .

It is also worth noting that clusterin and interleukin (IL)-32 , both of which are modulated by PLAA , are involved in apoptosis. PLAA induction downregulated expression of clusterin, while upregulating the expression of IL-32 in HeLa cervical cancer cells . Clusterin is a cytoprotective protein known to promote tumor chemo-resistance . IL-32 associated specifically with apoptotic T cells, and the ectopic expression of the *IL-32* gene in HeLa cells induced apoptosis . Based on these previous studies, we believe induction of PLAA by cytotoxic agents such as cisplatin can partially mediate the apoptotic responses in host cells .

However, the detailed mechanism by which PLAA induction modulates apoptosis is not clear, and it remains to be proven whether cisplatin-induced apoptosis is partially mediated by PLAA induction. Therefore, we hypothesized that native PLAA promotes cisplatin-induced apoptosis by modulating AA metabolism and expression/production of clusterin and IL-32.

Chapter 2:

ALTERATION IN THE ACTIVATION STATE OF NEW INFLAMMATION-ASSOCIATED TARGETS BY PLAA

Abstract

Phospholipase A_2 (PLA_2)-activating protein (PLAA) is a novel signaling molecule that regulates the production of prostaglandins (PGE_2) and tumor necrosis factor (TNF)-α. To

characterize the function of native PLAA *in situ*, we generated HeLa (Tet-off) cells overexpressing *plaa* (*plaa* ^{high}) and control (*plaa* ^{low}) cells, with the *plaa* gene in the opposite orientation in the latter construct. The *plaa* ^{high} cells produced significantly more PGE_2 and interleukin (IL)-6 compared to *plaa* ^{low} cells in response to TNF-α. There was increased activation and/or expression of cytosolic PLA_2, cyclooxgenase-2, and NF-κB after induction of *plaa* ^{high} cells with TNF-α compared to the respective *plaa* ^{low} cells. Microarray analysis of *plaa* ^{high} cells followed by functional assays revealed increased production of proinflammatory cytokine IL-32 and a decrease in the production of annexin A4 and clusterin compared to *plaa* ^{low} cells. We demonstrated the role of annexin A4 as an inhibitor of PLA_2 and showed that addition of exogeneous clusterin limited the production of PGE_2 from *plaa* ^{high} cells. To understand regulation of *plaa* gene expression, we used a luciferase reporter system in HeLa cells and identified one stimulatory element, with Sp1 binding sites, and one inhibitory element, in exon 1 of the *plaa* gene. By using decoy DNA oligonucleotides to Sp1 and competitive binding assays, we showed that Sp1 maintains basal expression of the *plaa* gene and binds to the above-mentioned stimulatory element. We demonstrated for the first time that the induction of native PLAA by TNF-α can perpetuate inflammation by enhancing activation of PLA_2 and NF-κB.

Introduction

Inflammatory responses in the host are characterized by a variety of changes, including vasodilation, leukocyte extravasation, and an increase in vascular permeability. These changes are induced by inflammatory mediators, such as lipids (e.g., prostaglandins, leukotrienes and platelet-activating factor) , pro-inflammatory cytokines (e.g., tumor necrosis factor-alpha [TNF-α], interleukin [IL]-1β and IL-6) and chemokines (e.g., IL-8 and macrophage chemoattractant protein [MCP]-1) .

Induction of systemic proinflammatory cytokines, such as TNF-α, contributes to the development of acute and chronic inflammatory conditions (e.g., trauma, infection, and rheumatoid arthritis). The effect of TNF-α is partially mediated by PLA_2 and COX-2, which promote a shift towards a proinflammatory lipid profile (e.g., leukotriene B_4 and PGE_2) to further perpetuate inflammatory responses . TNF-α activates both NF-κB and MAPK signaling, which in turn lead to induction of PLA_2 and COX-2. In this study, we examined the inflammatory responses modulated by *plaa* gene expression induced by TNF-α. To accomplish this goal, we established HeLa (cervical carcinoma) Tet-off cells overexpressing the native *plaa* gene and compared their inflammatory responses induced by TNF-α to that of the control cells stimulated the same way (Material and Methods section). In addition, we characterized the transcriptional regulation of the *plaa* gene in HeLa cells.

Materials and Methods

Overexpression of the plaa gene in HeLa Tet-off cells

Using the following forward and reverse primers: 5' TGCACGCGTATGCACTGTATGAGCGGCCACTCCAAT 3' and 5' TATGCTAGCTACAGCAAATTTAGGATAAATCTACAGC 3', the human *plaa* gene was cloned into the pBI-EGFP vector (ClonTech Laboratories, Inc., Mountain View, CA) at the *Mlu*I/*Nhe*I restriction sites to form pBI-EGFP-PLAA recombinant plasmid. The underlined bases in the primer sequences represent the respective restriction sites. The enhanced green fluorescent protein (EGFP) open reading frame is contained in the pBI-EGFP-PLAA plasmid as a reporter. HeLa Tet-off cells (G418 resistant, ClonTech) were co-transfected with plasmids pBI-EGFP-PLAA and pTK-Hyg. This HeLa cell line provides the transcriptional activator to bind the promoter in pBI-EGFP-PLAA, and the pTK-Hyg vector provides a hygromycin resistance selection marker. Three weeks after transfection, stable transfectants that were resistant to hygromycin (200 μg/ml) and G418 (200 μg/ml) (ClonTech) were individually

selected based on intensity of green fluorescence and expanded. Five selected clones were screened by Northern blot analysis for the expression of the *plaa* gene. The clone that consistently showed the highest levels of expression of the *plaa* gene was designated as *plaa* ^{high} and was used throughout these studies. A clone in which the *plaa* gene was inserted in the opposite orientation and exhibited the lowest level of *plaa* gene expression (representing expression of the native *plaa* gene in the HeLa cells) was referred to as *plaa* ^{low}, and used as a negative control in all subsequent experiments.

Cell culture

The human cervical epithelial cell line HeLa was purchased from American Type Culture Collection (Manassas, VA). The cells were cultured in Dulbecco's Modified Eagle Medium (DMEM) with 10% fetal bovine serum (FBS) supplemented with penicillin (100 U/ml)-streptomycin (100 U/ml) (Invitrogen, Carlsbad, CA). HeLa Tet-off (*plaa* ^{high} and *plaa* ^{low}) cells were maintained in DMEM with 10% tetracycline-free FBS supplemented with hygromycin (100 μg/ml) and G418 (100 μg/ml). Both cell lines were cultured at 37°C with 5% CO_2. For each experiment, cells were plated in either 25- or 75- cm^2 tissue culture flasks or 6-well tissue culture plates and allowed to attach overnight.

Northern blot analysis

Total RNA was isolated from HeLa cells using a RNAqueous kit (Ambion, Inc., Austin, TX) and then subjected to electrophoresis on 1.0% formaldehyde agarose gels, blotted onto nylon membranes, and probed with ^{32}P-labeled human *plaa* cDNA (10^5 cpm/ng) . The filters were subsequently prehybridized (using Quickhyb, Strategene, La Jolla, CA), hybridized, and washed using 2X SSC (consisting of 0.3M trisodium citrate and 3.0M sodium chloride in dH2O, pH 7.0) with 0.2% sodium dodecyl sulfate (SDS) at 68^{o}C as recommended by the manufacturer. After washing, the filters were dried and exposed to X-ray film at -70^{o}C for 12 hr. The ^{32}P-labeled *plaa* gene probe was subsequently stripped from the filters using 50%

formamide (incubated at 68°C for 2 hr), and the latter re-probed with a ^{32}P-labeled glyceraldehyde-3-phosphate dehydrogenase (GAPDH) cDNA probe (ClonTech) as an internal control to normalize RNA loading onto each lane of the gel.

Western blot analysis

Host cell lysis was accomplished in RIPA buffer (Pierce, Rockford, IL). Western blot analysis was performed by established procedures with slight modifications according to specifications of the antibody manufacturer. Polyclonal antibodies against COX-2, $cPLA_2$, β-tubulin, calnexin and annexin A4 were purchased from Santa Cruz Biotechnology, Inc., Santa cruz, CA. Monoclonal antibody against the PLAA peptide was purchased from Epitomics, Burlingame, CA. Equal amounts of protein (30-100 μg) were separated on 4-20% gradient SDS-polyacrylamide gels. We used antibodies to β-tubulin and calnexin as loading controls for host cell lysates and membrane fractions, respectively. The blots were scanned using the Gel Doc 2000 scanner and Quantity One (Bio-Rad, Hercules, CA) software to calculate fold increase in antigen levels.

Microarray analysis

Total RNA (10-15 μg) was labeled and hybridized to human GeneChip arrays in the Molecular Genomics Core at the University of Texas Medical Branch, Galveston. Briefly, cDNA synthesis, *in vitro* transcription, labeling and fragmentation of the oligonucleotide probes were performed as instructed by the GeneChip manufacturer (Affymetrix, Sata Clara, CA). The probes were hybridized to the human genome HG-U133 Plus 2 GeneChip using the GeneChip Hybridization Oven 640. The chips were washed in a GeneChip Fluidics Station 400 (Affymetrix) and the results visualized with a Gene Array scanner using the Affymetrix software. Data from four replicates were analyzed using GeneSifter (VizX Labs, Seattle, WA), Significance Analysis of Microarrays (SAM; Stanford, CA) and Spotfire DecisionSite 9.0 (Spotfire Inc., Somerville MA). The data discussed in this publication was deposited in NCBIs

Gene Expression Omnibus (GEO, http://www.ncbi.nlm.nih.gov/geo/) and accessible through GEO series accession number.

Real-time reverse transcriptase-polymerase chain reaction (RT-PCR)

RNA samples for Real Time PCR Analysis were quantified using a Nanodrop Spectrophotometer (Nanodrop Technologies, Wilmingon, DE) and qualified by analysis on an RNA Nano chip using the Agilent 2100 Bioanalyzer (Agilent Technologies, Santa Clara, CA). Synthesis of cDNA was performed using 1 µg of total RNA in a 20 µl reaction using the reagents in the Taqman Reverse Transcription Reagents Kit from Applied Biosystems Inc., Foster City, CA. The reaction conditions were as follows: 25ºC, 10 min, 48ºC, 30 min, and 95ºC, 5 min. Real-time RT-PCR amplifications (in triplicate) were performed using 2 µl of cDNA in a total volume of 25 µl using SYBR green and the SYBR Green PCR Master Mix (Applied Biosystems) as specified by the manufacturer. The final concentration of the cDNA was 250 nM and of the primers was 900 nM. Real-time RT-PCR assays were performed with 18S RNA as a normalizer. All PCR assays were run in the ABI Prism 7000 Sequence Detection System and the conditions were as follows: 50ºC, 2 min, 95ºC, 10 min; and then 40 cycles of the following: 95ºC, 15 sec, and 60ºC, 1 min. Primers used in gene amplification were synthesized by Integrated DNA Technologies (Coralville, IA) and are listed in **Table 2.1**.

Table 2.1: Sequences of primers used for amplification of selected genes by real-time RT-PCR.

Gene designation	Primer sequences
plaa-Forward	5′-GGAAAGCTATTAACTGTCCTGAAGATATT-3′
plaa-Reverse	5′-TCATTGCAGAAGTTCTCATTCACA-3′
il32-Forward	5′-TGGAGACAGTGGCGGCTTAT-3′
il32-Reverse	5′-GGCACCGTAATCCATCTCTTTCT-3′
clu-Forward	5′-CTCAGCAGGCCATGGACAT-3′
clu-Reverse	5′-CGGTCATCGTCGCCTTCT-3′
plcB4-Forward	5′-CGAGCACACCAGGCTAAGATT-3
plcB4-Reverse	5′-GCAAGTCTCTTTCTTTCTTCCAGAA-3″
pde1A-Forward	5′-CTGAACTGGAAATTTTAGCAATGGT-3′
pde1A-Reverse	5′-TTATACAAAATGGCAACATCTGACCTT-3′

ctsB-Forward	5′-CCCCGTGGAGGGAGCTT-3′
ctsB-Reverse	5′-ATCATCTCTCCGGTGACGTGTT-3′
mfap2-Forward	5′-AGTGTCTCAACGAGGTCTGCTTCT-3′
mfap2-Reverse	5′-TGGGCACACACTGTACGAACA-3′
rad1-Forward	5′-GCCAGGGACTTTAACTGCACTT-3′
rad1-Reverse	5′-AGACTGTCACCACTCCTCCTTCTT-3′
slc43A3-Forward	5′-CTTGTCGGCTGTGGTGTCTCT-3′
slc43A3-Reverse	5′-GCAAGCATGAACATCACATTCAC-3′
cxcr4-Forward	5′-CACCGAGGCCCTAGCTTTC-3′
cxcr4-Reverse	5′-CGTGCTGGGCAGAGGTTT-3′
klf5-Forward	5′-AGAAGGAGTAACCCCGATTTGG-3′
klf5-Reverse	5′-AGAAGACTTGGTATAAACTTTTGTGCAA-3′
nr2F1-Forward	5′-CACATGCCGTGCCAACAG-3′
nr2F1-Reverse	5′-AGGCATTCTTCCTCGCTGAA-3′
16S rRNA-F	5′-AGTCACCGCTGAAGGCTACGAT-3′
16S rRNA-R	5′-CAAATGCATCTTTCAGGTTCGC-3′

Measurement of PGE_2

HeLa Tet-off cells (*plaa* ^{high} and *plaa* ^{low}) were treated with 30 ng/ml of TNF-α for 8 hr and the cell culture supernatants collected. When indicated, $cPLA_2$ inhibitor methyl arachidonyl fluorophosphonate (MAFP) (Cayman, Ann Arbor, MI) was added to the cells at indicated concentrations 1 hr prior to TNF-α stimulation, and was present throughout the 8 hours' stimulation. Dimethyl sulfoxide (DMSO) was used to dissolve MAFP before addition to cells and was used as a vehicle control for the treatment. For pre-treatment of cells with clusterin antibody or recombinant clusterin (Biovendor, Candler, NC), increasing amounts were added to cells 4 hr before TNF-α stimulation (30 ng/ml) and were present throughout the 8 hours'

stimulation. The final concentrations of clusterin antibody in the supernatants were 31.25, 62.5, 125, 250, and 500 ng/ml. The final concentrations of recombinant clusterin in the supernatants were 5, 10, 20, 40, 80, 160, and 320 ng/ml. PGE_2 levels in the supernatant were determined using a commercially available competitive ELISA kit (Assay Designs, Ann Arbor, MI) according to the manufacturer's instructions. PGE_2 standards were provided in the kit and were used in each assay.

Preparation of membrane fractions

Membrane fractions from HeLa Tet-off cells (*plaa* ^{high} and *plaa* ^{low}) were isolated by using established procedures . Briefly, cells were washed and suspended in ice-cold homogenization buffer (50 mM Tris–HCl pH 8.0, 1 mM EDTA, 1 mM EGTA, 20% glycerol, freshly added 1 mM dithiothreitol (DTT), and Protease Inhibitor Cocktail [Roche, Mannheim, Germany] at 1:100 dilution). Cell suspensions were sonicated on ice using a Branson sonicator (15 second burst for 4 cycles at 30% output) and sonicates centrifuged at 1000 x *g* for 5 min at 4°C to remove unbroken cells and debris. The low speed supernatant, designated as crude homogenate, was further centrifuged at 100,000 x *g* for 1 hr at 4°C. The high speed supernatant was designated as the cytosolic fraction. The high speed pellet, designated as the membrane fraction, was washed 3 times with homogenization buffer to remove cytosolic protein contaminants and was suspended in 400 µl of ice-cold homogenization buffer containing 0.1% Triton X-100. The pellet was then sonicated on ice for 4 cycles of 15 s each. The cytosolic and membrane fractions were aliquoted and stored at -80 °C until used for PLA_2 assays or Western blot analysis. Protein concentrations in various fractions were determined using the Bradford Protein Reagent (Bio-Rad, Hercules, CA).

Measurement of PLA_2 activity

PLA_2 activity in the membrane fractions of HeLa cells was determined using a commercially available PLA_2 activity kit (Cayman, Ann Arbor, MI) according to the

manufacturer's instructions . Equal amounts of membrane proteins (20-40 μg) were used for each sample. When inhibitors were used, they were dissolved in DMSO and incubated with membrane samples at indicated final concentrations for 30 min at 25°C. DMSO was used as a vehicle control for the treatment. Included inhibitors (Cayman) were: $cPLA_2$ inhibitor MAFP (used at concentrations of 1.2 μM, 0.6 μM, and 0.3 μM), $iPLA_2$ inhibitor Bromoenol lactone (BEL) (used at concentrations of 140 nM, 70 nM, and 35 nM) , $cPLA_2$ and $sPLA_2$ inhibitor 7,7-dimethyl-5,8-Eicosadienoic acid (DMEDA, used at a concentration of 35 μM) and $sPLA_2$ inhibitor 1-Palmitylthio-2-palmitoylamido-1,2-dideoxy-sn-glycero-3-phosphorylcholine (TPC, used at a concentration of 5 μM) . Bee venom PLA_2 (Cayman) was used as a positive control. To measure inhibition of PLA_2 activity by annexin A4, membrane proteins were pre-incubated with increasing amounts of recombinant annexin A4 (Novus Biologicals, Littleton, CO) for 30 min at 25°C. The final concentrations of annexin A4 in the PLA_2 activity reaction mixtures were 31.25, 62.5, 125, 250, 500, 1000, 2000 ng/ml. Bovine serum albumin (BSA) was used as a negative control. The units of PLA_2 activity in the membrane fractions were expressed as μmole/min/mg. One unit of PLA_2 enzyme hydrolyzes one μmole of the substrate arachidonoyl thio-phosphatidylcholine per minute at 25°C.

Phosphorylation profiles of signaling proteins

Bio-Plex phosphoprotein assays (Bio-Rad) were performed at the Gastrointestinal Immunology Core of the University of Texas Medical Branch at Galveston. Included human signaling targets were: p65, I-κBα, ERK-1, p38 MAPK, JNK, c-jun, CREB, Akt, GSK 3α and β), TrkA, HSP27, and histone 3. Equal amounts of protein samples were used in each measurement and phosphorylated protein standards were employed in the assay.

Measurement of nuclear translocation of NF-κB p65 by confocal immunofluoresence

The nuclear translocation of NF-κB p65 induced by TNF-α was detected by established procedures with slight modifications. Briefly, HeLa Tet-off cells (*plaa* ^{high} and *plaa* ^{low}) were

treated with 30 ng/ml of TNF-α for 0, 15 or 60 min before fixation. Subsequently, 4% freshly prepared paraformaldehyde and 0.5% Triton X-100 were used to fix and permeablize the cells, respectively. Goat anti-p65 C-20 antibody (Santa Cruz Biotechnology) and Alexa Fluor 488 (green) donkey anti-goat antibody (Molecular Probes, Carlsbad, CA) were used as primary and secondary antibodies, respectively. Samples stained with secondary antibody alone were used as negative controls. Mounting medium with DAPI (Vector Laboratories, Burlingame, CA) and Alexa Fluor 568 (red) phalloidin (Molecular Probes) was used to stain the nucleus and actin, respectively.

Measurement of DNA binding activity of NF-κB p50

HeLa Tet-off cells (*plaa* ^{high} and *plaa* ^{low}) were treated with 30 ng/ml of TNF-α for 0, 15 or 60 min before nuclear isolation using the NE-PER™ kit (Pierce, Rockford, IL). Nuclear extracts were assayed for DNA binding activity using the TransAM™ p50 kit (Active Motif, Carlsbad, CA) according to the manufacturer's instructions. Briefly, DNA oligonucleotides containing p50 consensus sites were used to pre-coat plate wells and to capture p50 from the samples. Primary antibody against human p50 and secondary antibody conjugated with horse-radish peroxidase (HRP) were employed for the detection of p50. DNA oligonucleotides containing either wild type (WT) or mutated (MT) p50 consensus sites were used as competitors to ensure specificity of the assay. WT oligonucleotides were: 5'-AGTTGAGGGGACTTTCCCAGGC-3' (forward sequence) and 5-GCCTGGGAAAGTCCCCTCAACT-3' (reverse sequence). MT oligonucleotides were: 5'-AGTTGAGGCCACTTTCCCAGGC-3'(forward sequence) and 5'-GCCTGGGAAAGTGGCCTCAACT-3' (reverse sequence). Stimulated Jurkat (TPA+CI) cell nuclear extract was used as a positive control. The reaction mixture without nuclear extract was used as a negative control.

Cytokine profiles

Bio-Plex cytokine assays (Bio-Rad) were performed at the Gastrointestinal Immunology Core of the University of Texas Medical Branch at Galveston as described by the manufacturer. Included human cytokine targets were: IL-1β, IL-2, IL-4, IL-5, IL-6, IL-7, IL-8, IL-10, IL-12, IL-13, IL-17, TNF-α, MCP-1, MIP-1β, G-CSF, GM-CSF, and IFN-γ. Cytokine standards were used in the assay.

Measurement of clusterin concentration

Clusterin concentration in culture supernatants and in cellular and nuclear fractions of HeLa Tet-off cells (*plaa* ^{high} and *plaa* ^{low}) was measured using a commercially available sandwich ELISA kit (Biovendor), according to the manufacturer's instructions. Recombinant clusterin protein was used to generate a standard curve.

Measurement of IL-32 concentration

A sandwich ELISA method was used to measure the concentration of IL-32 in cellular lysates and supernatants of HeLa Tet-off cells (*plaa* ^{high} and *plaa* ^{low}). Briefly, mouse antiserum against IL-32 (CIM Antibody Core, Arizona State University, Tempe, AZ) was diluted 1:200 in binding solution (0.1 M Na_2CO_3, pH 9.0) and incubated in a high-binding microtiter plate overnight at 4°C. An aliquot (10 μg) of total cellular proteins were diluted in phosphate-buffered saline (PBS) and subsequently incubated in the microtiter plate overnight at 4°C. Wells were incubated with freshly made 1% bovine serum albumin (BSA) in PBS and washed in PBS-Tween 20 (0.05%). The plate was then incubated with detection antibody (developed in rabbits) against IL-32 (ProSci, Poway, CA) at 10 μg/ml for 3 hr at room temperature. Subsequently, HRP-conjugated goat anti-rabbit antibody (Santa Cruz) and TMB (3,3′,5,5′-tetramethylbenzidine) substrate were applied. The color reaction was stopped with 50 μl of 1 M H_2SO_4 and read with a microtiter ELISA plate reader (Molecular Devices Corp., Sunnyvale, CA) at 450 nm. BSA was used as a negative control. A 15-amino acid long peptide from the

carboxyl terminal of IL-32 (ProSci) was serially diluted (100 to 6400 pg/ml) and used to generate a standard curve.

Construction of luciferase reporter plasmids for mapping the 5' genomic region of the plaa gene

We mapped the DNA sequence ranging from 4008 base pairs (-4008 bp) upstream to the 1st ATG (0 bp) of exon I in the *plaa* gene. This 4008 bp sequence was progressively truncated into smaller fragments using a PCR-based strategy and the latter inserted in front of the firefly luciferase gene in the pGL3-Basic vector (Promega, Madison, WI). The pGL3-Basic vector without insert was used as a negative control in the luciferase reporter assay. The pGL3-Control vector, which contains a SV40 promoter and SV40 enhancer in addition to the backbone structure of pGL3-Basic, was used as a positive control. All of the plasmid constructs were prepared in the Molecular Genomics Core facility, University of Texas Medical Branch, Galveston. All of the plasmids were purified using cesium chloride density gradient centrifugation and sterilized (through 0.22 μm filters) prior to transfection of HeLa cells.

Transfection of HeLa cells with luciferase reporter plasmids and measurement of luciferase activity

The luciferase reporter plasmids were transfected into HeLa cells using Transfast™ reagent (Promega), according to the manufacturer's instructions. The charge ratio of transfection reagent to DNA was 1:1. A pRL-TK vector expressing the *Renilla* luciferase reporter was transfected together with the firefly luciferase plasmid as a control for luciferase activity, transfection efficiency, and cell viability. Twenty-four hr after transfection, the HeLa cells were lysed and assayed for luciferase activity using the Dual-Luciferase Reporter Assay kit (Promega), according to the manufacturer's instructions. Luciferase activities of various

constructs were measured by luminometer LB 953 (Berthold, Australia). Individual firefly luciferase activity was normalized against the *Renilla* luciferase activity.

Generation of Sp1 decoy oligonucleotides and transfection

Double-stranded DNA oligonucleotide containing the consensus Sp1 binding sequence (underlined) was designated "Wild Type (WT) Sp1 decoy" and synthesized by Bio-Synthesis (Lewisville, TX). Mutated (MT) Sp1 decoy was altered at two positions (shown as lower case letters) in the WT Sp1 decoy. WT Sp1 decoy was (complementary strand not shown), 5'-ATTACCGGGCGGGCGGGCTAC-3' and MT-Sp1 decoy was 5'-ATTACCGGtaGGtaGGGCTAC-3'. No binding sites for other known transcription factors were detected in these sequences . The decoy oligonucleotides were HPLC purified and contained three pairs of phosphorothioate bonds at both ends. The decoy oligonucleotides were transfected together with the firefly luciferase plasmids at a molar ratio of 50:1 to compete for Sp1 binding. Resulting luciferase activities were measured as described above.

Generation of the core stimulatory element of the plaa gene and competitive binding assay

The double-stranded DNA oligonucleotide, which resides between 255 to 277 bp upstream of the ATG start codon in exon I of the *plaa* gene, was designated "Wild Type (WT) element" and synthesized by Bio-Synthesis. Mutated (MT) element was altered at five positions (shown as lower case letters) in the WT element. The WT element (complementary strand not shown) had the following sequence: 5'-CCGCATCGGCGTCGGCGGTTGGG-3' and MT-Sp1 decoy had the following sequence: 5'- CCaCATCGaCGTCGtCaGTTGGa -3'. The competitive binding assay was performed using a Sp1 ELISA kit (Panomics, Fremont, CA) according to manufacturer's instruction. Briefly, a biotinylated oliogonucleotide containing Sp1 consensus binding site (labeled Sp1 probe) was used to bind and immobilized recombinant Sp1 protein to

streptavidin coated wells. The bound Sp1 protein was then detected by primary antibody against Sp1 and HRP-conjugated secondary antibody. When indicated, the WT or MT element was used to compete with the Sp1 probe for Sp1 binding. A Sp1 probe without biotin label (unlabeled Sp1 probe) was used as a positive control for the competitive binding assay.

Statistical analysis

The data were analyzed using Student's t test, with a p value of < 0.05 considered significant.

Results

Overexpression of the plaa gene in HeLa Tet-off cells

The expression of the *plaa* gene is rapidly induced by TNF-α, LPS and CT in murine RAW 264.7 macrophages and human colonic epithelial Caco-2 cells ; however, PLAA-induced functional changes in host cells are unknown.

To address this question, we established HeLa Tet-off cells that overexpressed the *plaa* gene using a bidirectional promoter in vector pBI which also expresses EGFP as a reporter (methods section). Individual stable transfectants were selected based upon the intensity of green fluoresence and expanded. Five cell clones were screened for *plaa* gene expression by Northern blot analysis. As shown in **Fig. 2.1A**, the clone F13 designated as *plaa* ^{high} had the highest level of *plaa* expression with a 7.5-fold higher abundance of the *plaa* transcript as compared to the control clone R19 (designated as *plaa* ^{low}) in which the *plaa* gene inserted in the opposite orientation was expressed from the pBI vector. We used expression of GAPDH as a loading control. This induction in the expression of the *plaa* gene was confirmed by mRNA microarray analysis (10.1-fold increase, **Table 2.2**) and real-time RT-PCR (2.2-fold increase, **Table 2.3**).

In addition, Western blot analysis confirmed an increasing trend of the *plaa* gene expression when unstimulated *plaa* ^{high} and *plaa* ^{low} cells were compared, with a 2 fold increase in the PLAA level in the former cells (**Fig. 2.1B**). This trend intensified after stimulation with 30 ng/ml of TNF-α for 8 hr, with *plaa* ^{high} cells producing 4-5-fold more PLAA than *plaa* ^{low} cells, based on Western blot analysis (**Fig. 2.1B**). The host cells were stimulated with TNF-α as the latter is known to induce the expression of native *plaa* . Normal HeLa cells expressed similar amounts of *plaa* as the *plaa* ^{low} cells with or without TNF-α stimulation (data not shown). The growth and survival properties of *plaa* ^{high} and *plaa* ^{low} cells were comparable to that of the normal HeLa cells (data not shown). The expression level of *plaa* in *plaa* ^{high} cells is physiologically relevant, as a similar level of PLAA is seen in murine RAW 264.7 macrophages. These macrophages not only produce a high level of PLAA but also other proinflammatory mediators.

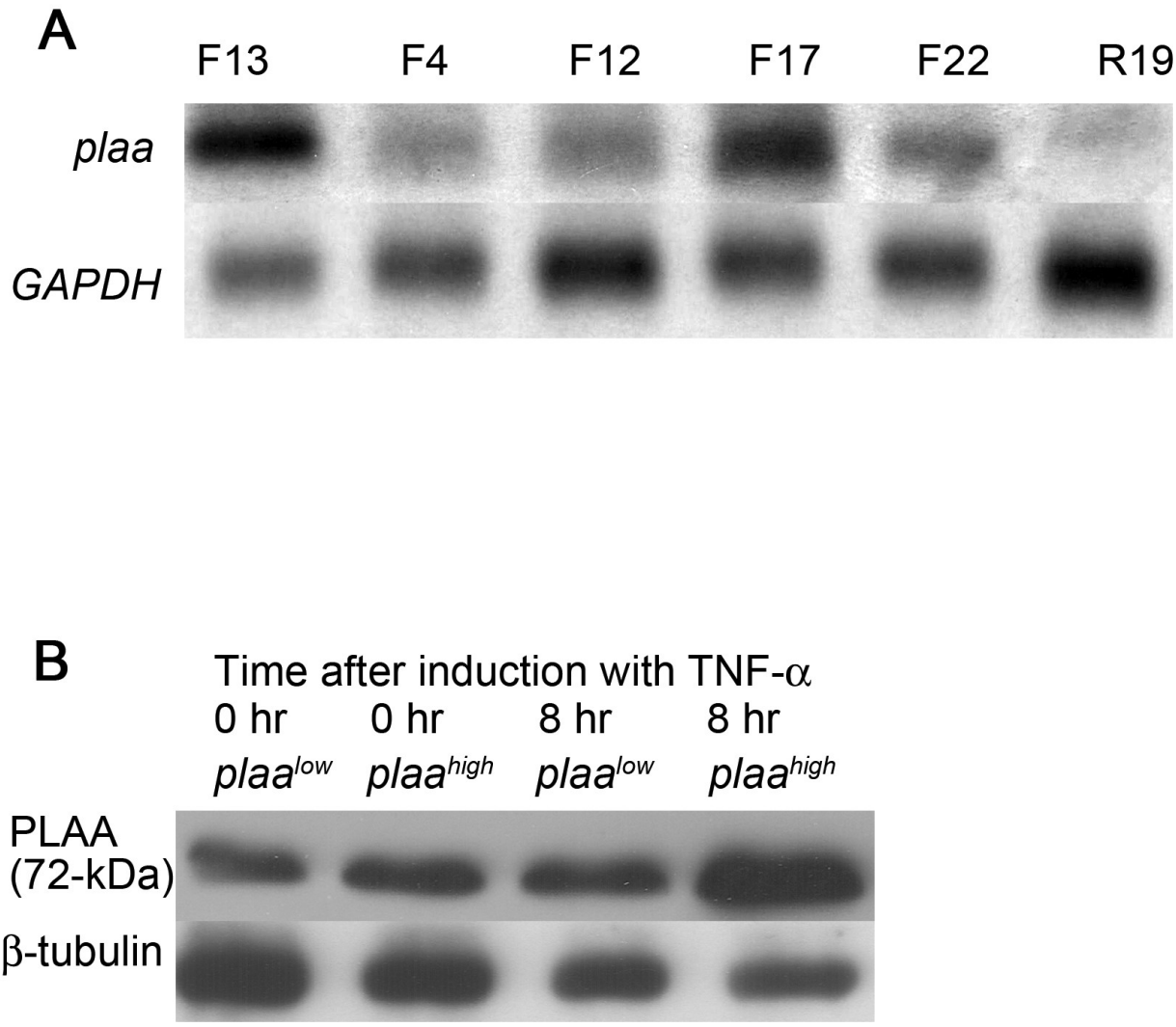

Figure 2.1 Overexpression of the *plaa* gene in HeLa Tet-off cells. (A) Northern blot analysis on clones for *plaa* gene expression. HeLa Tet-off cell clones were cultured in DMEM with 10% tetracycline-free FBS supplemented with hygromycin (100 U/ml) and G418 (100 U/ml) for 8 hr before RNA isolation. The RNA samples were run on 1.0% formaldehyde agarose gels, transferred to nylon membranes, and the membranes then probed with ^{32}P-labeled human *plaa* cDNA. Lane 1 to 5 represent RNA samples from clones overexpressing the *plaa* gene. These clones were designated as F13, F4, F12, F17, and F22, respectively. The F13 clone was designated as *plaa* ^{high} and used in all of the experiments. Lane 6 represents the RNA from the control clone R19 in which the *plaa* gene was inserted in the opposite orientation. The R19 clone was designated as *plaa* ^{low} and used in all of the experiments. A ^{32}P-labeled glyceraldehyde-3-phosphate dehydrogenase (GAPDH) cDNA probe was used to normalize RNA loading. **(B)** Western blot analysis of the PLAA protein from *plaa* ^{high} and *plaa* ^{low} cells stimulated with TNF-α (30 ng/ml) or remained untreated. Aliquots (80 μg) of total proteins were subjected to 4-20% SDS-PAGE and the membranes probed with monoclonal antibody against PLAA. The same amount of proteins were run on a second gel, subjected to Western blot analysis, and the membranes probed with a polyclonal antibody against β-tubulin to normalize protein loading. The blots presented are representative of at least three independent repetitions.

***Global transcriptional profile and real-time RT-PCR analysis of plaa ^{high}* cells**

In order to confirm the differential expression of *plaa* and to identify downstream proteins altered by *plaa* overexpression, we compared the transcriptional profiles of *plaa* ^{high} and *plaa* ^{low} cells using microarray analysis. Resting *plaa* ^{high} and *plaa* ^{low} cells were grown without TNF-α stimulation for 8 and 16 hr in DMEM with 10% tetracycline-free FBS supplemented with hygromycin (100 U/ml) and G418 (100 U/ml), and total RNA were isolated and compared. We did not stimulate these cells with TNF-α to limit the number of variables, which would have made data analysis and interpretation more cumbersome. Each experiment was performed in duplicate, yielding a total of 8 arrays. Data were analyzed by MAS 5.0, and a stringent data analysis approach was subsequently employed in order to minimize the incidence of false positives. Pairwise comparisons and Student's t test were performed using GeneSifter, and genes that were not differentially expressed at least 1.5-fold between *plaa* ^{low} and *plaa* ^{high} cells with a *p* value less than 0.05 were eliminated from further analyses. SAM was also used to perform a two-class unpaired comparison between *plaa* ^{low} and *plaa* ^{high} cells, and only genes that resulted in an FDR (False Detection Ratio) of 5% or less were considered as significantly differentially expressed. Finally, Spotfire DecisionSite was used to perform all 28 possible individual pairwise comparisons between the 8 different samples. The fold-change between any *plaa* ^{low} sample and any *plaa* ^{high} sample was expected to be at least 1.5-fold (up- or down-regulated). Genes that were differentially expressed between early and late time points (e.g., *plaa* ^{low} grown for 8 hr versus 16 hr) were eliminated, as were any genes that differed (1.5-fold or greater) between any replicates (e.g., comparison of *plaa* ^{low} cells grown for 8 hr on different days). This resulted in a highly robust set of 64 probe sets representing 54 different genes that were consistently differentially expressed between *plaa* ^{low} and *plaa* ^{high} cells (**Table 2.2**). As expected, the fluorescence signal intensity for the probe set representing the *plaa* gene was much higher (10.1-fold) in *plaa* ^{high} cells, compared to *plaa* ^{low} cells (**Table 2.2**). In addition to *plaa*, 11 altered genes were selected and verified by real-time RT-PCR (**Table 2.3**).

Table 2.2. Genes differentially expressed between *plaa* ^{low} and *plaa* ^{high} cells, based on microarrays analysis.

GenBank ID	Gene Name	FC
	Cell Adhesion and Migration	
BE875786	Cathepsin B (CTSB)	-1.9
NM_001908	Cathepsin B (CTSB)	-1.6
NM_001908	Cathepsin B (CTSB)	-1.5
AJ224869	Chemokine (C-X-C motif) receptor 4 (CXCR4)	-1.8
AF130082	Collagen, type III, alpha 1 (Ehlers-Danlos syndrome type IV, autosomal dominant) (COL3A1)	-1.9
AU144167	Collagen, type III, alpha 1 (Ehlers-Danlos syndrome type IV, autosomal dominant) (COL3A1)	-1.6
AI983428	Collagen, type V, alpha 1 (COL5A1)	-1.9
AI130969	Collagen, type V, alpha 1 (COL5A1)	-1.5
NM_014333	Immunoglobulin superfamily, member 4 (IGSF4)	-1.8
AI924630	Melanoma antigen family D, 2 (MAGED2)	-1.5
NM_017459	Microfibrillar-associated protein 2	-2.1
NM_004772	Neuronal protein 3.1 (P311)	-2.2
D86862	Paxillin (PXN)	1.6
NM_014459	Protocadherin 17 (PDCH17)	-1.6
D13989	Rho GDP dissociation inhibitor (GDI) alpha (ARHGDIA)	1.7
AI571798	Rho GDP dissociation inhibitor (GDI) alpha (ARHGDIA)	1.9
BF059159	Roundabout, axon guidance receptor, homolog 1 (ROBO1)	-2.0
AF091395	Triple functional domain (PTPRF interacting) (TRIO)	1.8
NM_007118	Triple functional domain (PTPRF interacting) (TRIO)	1.9
AF091395	Triple functional domain (PTPRF interacting) (TRIO)	2.0
	Cell Cycle Arrest and Apoptosis	
NM_021197	WAP four-disulfide core domain 1 (WFDC1)	-2.6
NM_014782	Armadillo repeat protein ALEX2 (ARMCX2)	-1.6
AK021947	Mitofusin 2 (MFN2)	1.7
AF074717	RAD1 (S. pombe) homolog (RAD1)	1.6
	DNA Packaging	
AA451996	Histone 2, H2aa3 (HIST2H2AA3)	1.6
	Energy Production	
NM_001976	Enolase 3, (beta, muscle) (ENO3)	-1.8
	Inflammation and Immune Response	
BC000373	Amyloid beta (A4) precursor-like protein 2 (APLP2)	-1.6
NM_001153	Annexin A4 (ANXA4)	-1.7
AI982754	Clusterin (CLU)	-2.0
BC000055	Follistatin-like 1 (FSTL1)	-1.7
X56210	H factor (complement)-like 2 (CFHR1)	-1.7
AF200348	Melanoma associated gene (PXDN)	-1.8
AF200348	Melanoma associated gene (PXDN)	-1.7
NM_004221	Natural killer cell transcript 4 (IL32)	1.9
	Lipid Metabolism	
AB032261	Stearoyl-CoA desaturase (delta-9-desaturase) (SCD)	-1.7
AF145020	Phospholipase A2-activating protein (PLAA)	10.1

Protein Processing		
M55575	Branched chain keto acid dehydrogenase E1, beta polypeptide (maple syrup urine disease) (BCKDHB)	-1.7
D84294	Tetratricopeptide repeat domain 3 (TTC3)	-1.7
D83077	Tetratricopeptide repeat domain 3 (TTC3)	-1.6
NM_017423	UDP-N-acetyl-alpha-D-galactosamine:polypeptide N-acetylgalactosaminyltransferase 7 (GALNT7)	-1.6
NM_012228	Methionine sulfoxide reductase B2 (MSRB2)	-1.5
Signal Transduction		
NM_024087	Ankyrin repeat and SOCS box-containing 9 (ASB9)	-1.8
AI817041	Chemokine orphan receptor 1 (CMKOR1)	-2.3
L37882	Frizzled (Drosophila) homolog 2 (FZD2)	-1.8
NM_002195	Insulin-like 4 (INSL4)	-1.6
NM_017648	Mucin 13, cell surface associated (MUC13)	1.8
NM_005019	Phosphodiesterase 1A, calmodulin-dependent	-2.1
AL535113	Phospholipase C, beta 4 (PLCB4)	-1.8
NM_016240	Scavenger receptor class A, member 3 (SCARA3)	-1.7
NM_003022	SH3 domain binding glutamic acid-rich protein like (SH3BGRL)	-1.8
Transcription Regulation		
NM_006602	Transcription factor-like 5 (basic helix-loop-helix) (TCFL5)	-1.7
AI951185	Nuclear receptor subfamily 2, group F, member 1 (NR2F1)	-1.7
AI700518	Nuclear factor I/B (NFIB)	-1.5
AB030824	Kruppel-like factor 5 (KLF5)	1.5
NM_006470	Tripartite motif-containing 16 (TRIM16)	1.6
Transport		
AL050002	Olfactomedin-like 2A (OLFML2A)	-1.9
AI630178	Solute carrier family 43, member 3 (SLC43A3)	-2.8
BC003163	Solute carrier family 43, member 3 (SLC43A3)	-1.5
NM_016354	Solute carrier family 21 (organic anion transporter), member 12 (SLC04A1)	1.6
Unknown		
AK025298	Autism susceptibility candidate 2 (AUTS2)	-2.5
NM_024717	Multiple C2 domains, transmembrane 1 (MCTP1)	-2.1
AL049949	Chromosome 10 open reading frame 56 (C10orf56)	-1.6
AL049233	Chromosome 10 open reading frame 18 (C10orf18)	1.6
AW006290	RIO kinase 3 (RIOK3)	1.7

The *plaa* ^{high} and *plaa* ^{low} cells were cultured for 8 or 16 hr in DMEM with 10% tetracycline-free FBS supplemented with hygromycin (100 U/ml) and G418 (100 U/ml) before RNA isolation. Total RNA (25 μg) was processed and hybridized to human GeneChip arrays HG-U133 Plus 2 and the data analyzed using GeneSifter, Significance Analysis of Microarrays and Spotfire DecisionSite 9.0. Genes differentially expressed between *plaa* ^{high} and *plaa* ^{low} cells (8 or 16 hr) are shown. FC = fold-change. Genes listed more than once were represented by more than one probe set, each of which was separately determined to be differentially expressed between *plaa* ^{low} and *plaa* ^{high} cells. Negative (-) sign before fold-change indicates down-regulation of gene in *plaa* ^{high} cells, compared to *plaa* ^{low} cells.

Table 2.3. Verification of microarray analysis results by real-time RT-PCR.

Gene Name	Real-time	Microarray
	FC	
PLAA	2.2	10.1
Interleukin 32 (IL32)	2.1	1.9
Microfibrillar-associated protein 2 (MFAP2)	-2.6	-2.1
Phosphodiesterase 1A calmodulin dependent (PDE1A)	-1.5	-2.1
Phospholipase C beta 4 (PLCB4)	-2.2	-1.8
DNA repair exonuclease (RAD1)	1.7	1.6
Solute carrier family 43 member 3 (SLC43A3)	-22.6	-2.8
Clusterin (CLU)	-1.6	-2.0
Cathepsin B (CTSB)	-1.6	-1.6
Chemokine receptor 4 (CXCR4)	-1.3	-1.8
Kruppel-like factor 5 (KLF5)	1.9	1.5
Nuclear receptor subfamily 2 group F member 1 (NR2F1 or COUP TF1)	-1.4	-1.7

Experiments were performed in parallel, and the fold-change values were calculated using the comparative threshold method, after normalization of each gene to an internal control (18S rRNA). FC = fold-change (expression level of gene in *plaa* ^{high} cells compared to *plaa* ^{low} cells). Negative (-) sign before fold-change indicates down-regulation of gene in *plaa* ^{high} cells, compared to *plaa* ^{low} cells.

Differentially expressed genes were grouped by function based on information available in Medline, NCBI, and Stanford SOURCE databases. Functional categories included cell adhesion and migration (20 probes sets representing 13 different genes), cell cycle arrest and apoptosis (4 genes), inflammation and immune response (7 genes), signal transduction (9 genes), and transcription regulation (5 genes). Differentially expressed immune-related molecules included annexin A4 and clusterin (down-regulated 1.7-fold and 2.0-fold, respectively, in *plaa* ^{high} cells compared to *plaa* ^{low} cells) and interleukin-32 (IL-32; up-regulated 1.9-fold in *plaa* ^{high} cells). The trend of differential expression of annexin A4 (**Fig. 2.2A**), IL-32 (**Fig. 2.6**) and clusterin (**Fig. 2.9A**) were not changed by TNF-α stimulation.

Overexpression of the plaa gene decreases annexin A4 expression in plaa ^{high} cells

Based on our microarray data (**Table 2.2**), the mRNA level of annexin A4 was 1.6-fold lower in *plaa* ^{high} cells compared to *plaa* ^{low} cells. The annexin A4 protein is known to inhibit PLA_2 , possibly by binding and shielding the phospholipid surface . According to our Western blot analysis data (**Fig. 2.2A**), *plaa* ^{high} cells expressed 3-4-fold less annexin A4 antigen than *plaa* ^{low} cells, and this trend of differential expression was not altered by TNF-α stimulation. To determine whether PLA_2 activity in *plaa* ^{high} and *plaa* ^{low} cells was altered by differential expression of annexin A4, we performed an *in vitro* enzymatic assay using membrane-bound PLA_2 from cells. TNF-α was used to stimulate cells because it is known to induce PLA_2 activation . PLA_2 activities were comparable in unstimulated *plaa* ^{high} and *plaa* ^{low} cells but were differentially induced by TNF-α (30 ng/ml) to 3.6- and 2.3- fold of the unstimulated level, respectively, after 8 hr (**Fig 2.2B**). Importantly, addition of annexin A4 exogenously dose-dependently inhibited PLA_2 activity in both *plaa* ^{high} and *plaa* ^{low} cells stimulated with TNF-α, confirming its specificity (**Fig. 2.2B**). We used BSA as a negative control in this assay, and it did not elicit this effect. Since *plaa* ^{low} cells contained

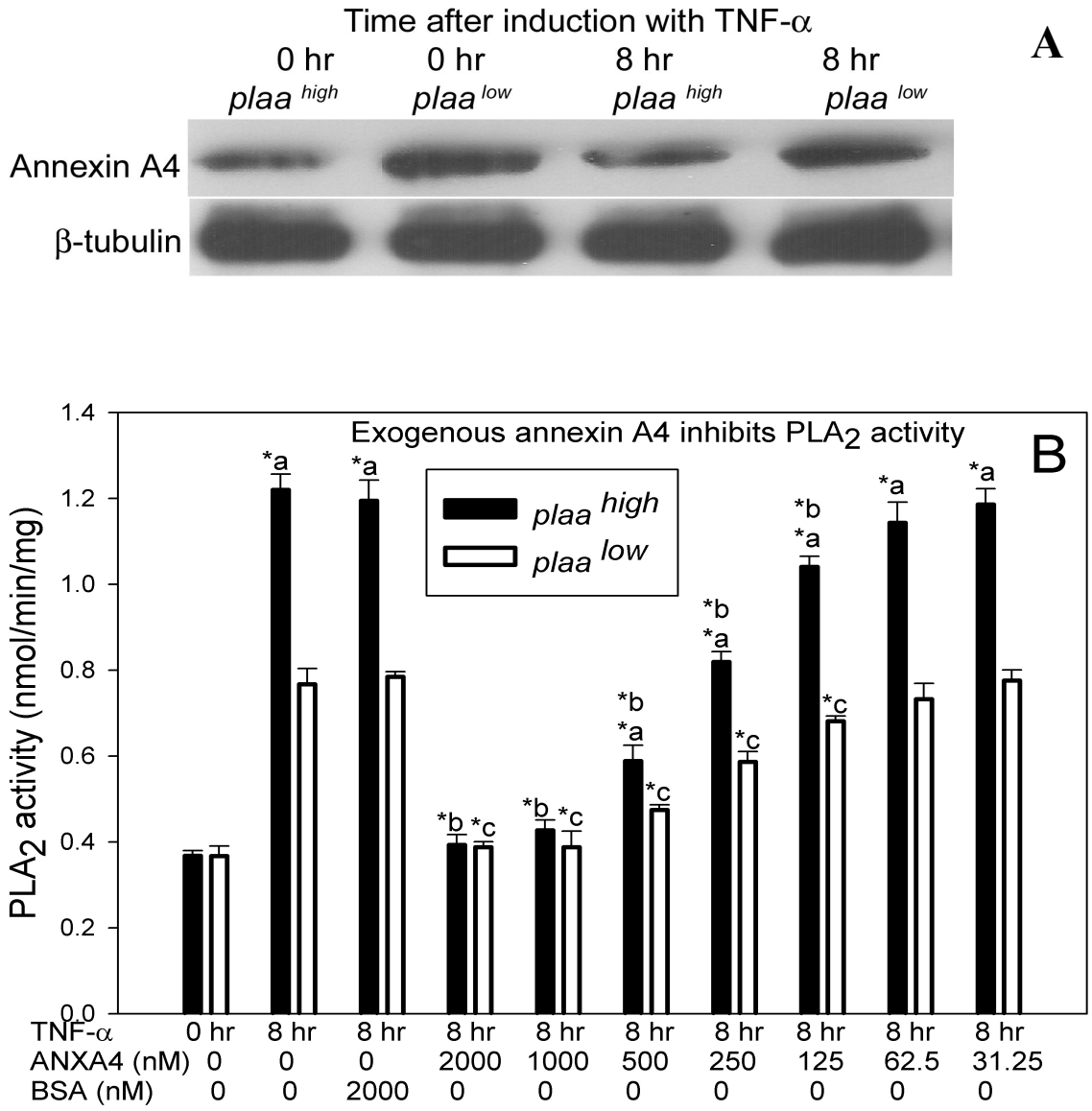

Figure 2.2. Overexpression of the *plaa* gene decreases annexin A4 expression in *plaa* ^{high} cells. The *plaa* ^{high} and *plaa* ^{low} cells were stimulated with TNF-α (30 ng/ml) or left untreated for 8 hr in DMEM with 10% tetracycline-free FBS supplemented with hygromycin (100 U/ml) and G418 (100 U/ml). (**A)** Western blot analysis of annexin A4 from cells. Equal amounts of whole cell lysate (50 μg) were subjected to 4-20% SDS-PAGE and probed with polyclonal antibody against annexin A4. An antibody against β-tubulin was used to normalize protein loading. The blots presented are representative of at least three independent repetitions. (**B)** Recombinant annexin A4 inhibits PLA_2 activity from *plaa* ^{high} and *plaa* ^{low} cells. Membrane fractions from stimulated cells were isolated and incubated with the indicated amounts of recombinant annexin A4 (ANXA4) for 30 min prior to performing the PLA_2 enzyme activity assay. BSA was used as a negative treatment control. PLA_2 activity was expressed as μmol/min/mg, and values were plotted as the mean ± standard deviation of four independent repetitions. *a denotes statistically significant values ($p < 0.05$) compared to that of the *plaa* ^{low} cells. *b denotes statistically significant values ($p < 0.05$) compared to untreated membrane fractions from TNF-α-stimulated *plaa* ^{high} cells. *c denotes statistically significant values ($p < 0.05$) compared to untreated membrane fractions from TNF-α-stimulated *plaa* ^{low} cells.

comparable PLA_2 activity to normal HeLa cells in response to TNF-α stimulation (data not shown), they were used as treatment control cells in the following experiments.

Overexpression of the plaa gene increases PGE_2 production and* induces *$cPLA_2$ and $sPLA_2$ activation by TNF-α in HeLa Tet-off cells

Differential activation of PLA_2 in TNF-α-stimulated *plaa* ^{high} and *plaa* ^{low} cells led us to compare their production of PGE_2 in response to TNF-α (30 ng/ml for 8 hr). Although unstimulated *plaa* ^{high} and *plaa* ^{low} cells produced comparable amounts of PGE_2, stimulation with TNF-α differentially increased PGE_2 production in *plaa* ^{high} and *plaa* ^{low} cell to 5- and 2.5-fold, respectively, as determined by ELISA (**Fig. 2.3A**) . MAFP, a specific $cPLA_2$ inhibitor , dose-dependently reduced PGE_2 production from stimulated *plaa* ^{high} and the *plaa* ^{low} cells. A 4 μM concentration of MAFP essentially reduced PGE_2 to basal levels in *plaa* ^{high} and *plaa* ^{low} cells (**Fig. 2.3B**).

We next determined which PLA_2 subtype was responsible for increased activity in *plaa* ^{high} and *plaa* ^{low} cells. The $cPLA_2$ inhibitor MAFP (1.2 μM), the $iPLA_2$ inhibitor BEL (0.14 μM) and DMEDA (an inhibitor for both $cPLA_2$ and $sPLA_2$, at 35 μM) were able to significantly reduce PLA_2 activity in both *plaa* ^{high} and *plaa* ^{low} cells. However, the $sPLA_2$ inhibitor thioetheramide-PC (TPC) (5 μM) did not alter PLA_2 activity in these TNF-α-induced *plaa* ^{high} and *plaa* ^{low} cells, when compared to cells exposed to only TNF-α (**Fig. 2.3C**), which suggests that $cPLA_2$ and $iPLA_2$ and not the $sPLA_2$ are induced by *plaa* gene overexpression and TNF-α stimulation. In addition, MAFP and BEL dose-dependently inhibited PLA_2 activity in stimulated *plaa* ^{high} and *plaa* ^{low} cells, confirming their specificities (**Fig. 2.3D**). A 1.2 μM ($2*IC_{50}$) of MAFP reduced PLA_2 activity close to that of the unstimulated control, whereas 0.14 μM ($2*IC_{50}$) of BEL was less potent in inhibiting $iPLA_2$ activity. These results indicated a greater induction of $cPLA_2$ than $iPLA_2$ by *plaa* overexpression and TNF-α stimulation.

Upon activation, $cPLA_2$ is known to translocate from the cytosol to the nuclear envelope, endoplasmic reticulum (ER), and Golgi apparatus, where arachidonic acid is produced and presented to cyclooxygenases . Therefore, the membrane localization of $cPLA_2$ in *plaa* ^{high} and *plaa* ^{low} cells was quantified by Western blot analysis (**Fig. 2.4**). Consistently more $cPLA_2$ was present in the membrane fractions of *plaa* ^{high} cells than *plaa* ^{low} cells, irrespective of the TNF-α stimulation time. Without TNF-α stimulation, *plaa* ^{high} cells contained 3-4-fold more $cPLA_2$ antigen in their membrane fraction than *plaa* ^{low} cells (**Fig. 2.4**). After stimulation with 30 ng/ml of TNF-α for 8 hr, *plaa* ^{high} cells contained 3-5-fold more $cPLA_2$ antigen in their membrane fraction than *plaa* ^{low} cells. We used antibodies to membrane-associated calnexin as a loading control for these Western blots .

We also examined expression of COX-2, a major contributor to inducible PGE_2 production (**Fig. 2.5**). Although unstimulated *plaa* ^{high} and *plaa* ^{low} cells did not express COX-2 antigen, based on Western blot analysis, stimulation of cells with TNF-α differentially increased COX-2 expression in *plaa* ^{high} and *plaa* ^{low} cells. As shown in **Fig. 2.5**, expression of COX-2 was consistently higher in *plaa* ^{high} cells than in *plaa* ^{low} cells. After stimulation with 30 ng/ml of TNF-α for 8 hr, *plaa* ^{high} cells expressed 2-3-fold more COX-2 antigen than *plaa* ^{low} cells. Antibodies to β-tubulin were used for Western blot analysis to ensure equal protein load onto the gel.

Overexpression of the plaa gene increases IL-32 expression in plaa ^{high} cells

Our microarray (**Table 2.2**) and real-time RT-PCR data (**Table 2.3**) revealed a significant increase (1.9-fold to 2.1-fold) in IL-32 mRNA in *plaa* ^{high} cells, compared to that of *plaa* ^{low} cells. IL-32 is a novel proinflammatory cytokine implicated in rheumatoid arthritis and known to induce PGE_2 production and NF-κB activation . ELISA assay confirmed a significantly higher level of IL-32 protein in the cytoplasm of resting *plaa* ^{high} cells than resting *plaa* ^{low} cells (**Fig. 2.6**). TNF-α (100 ng/ml) stimulation significantly

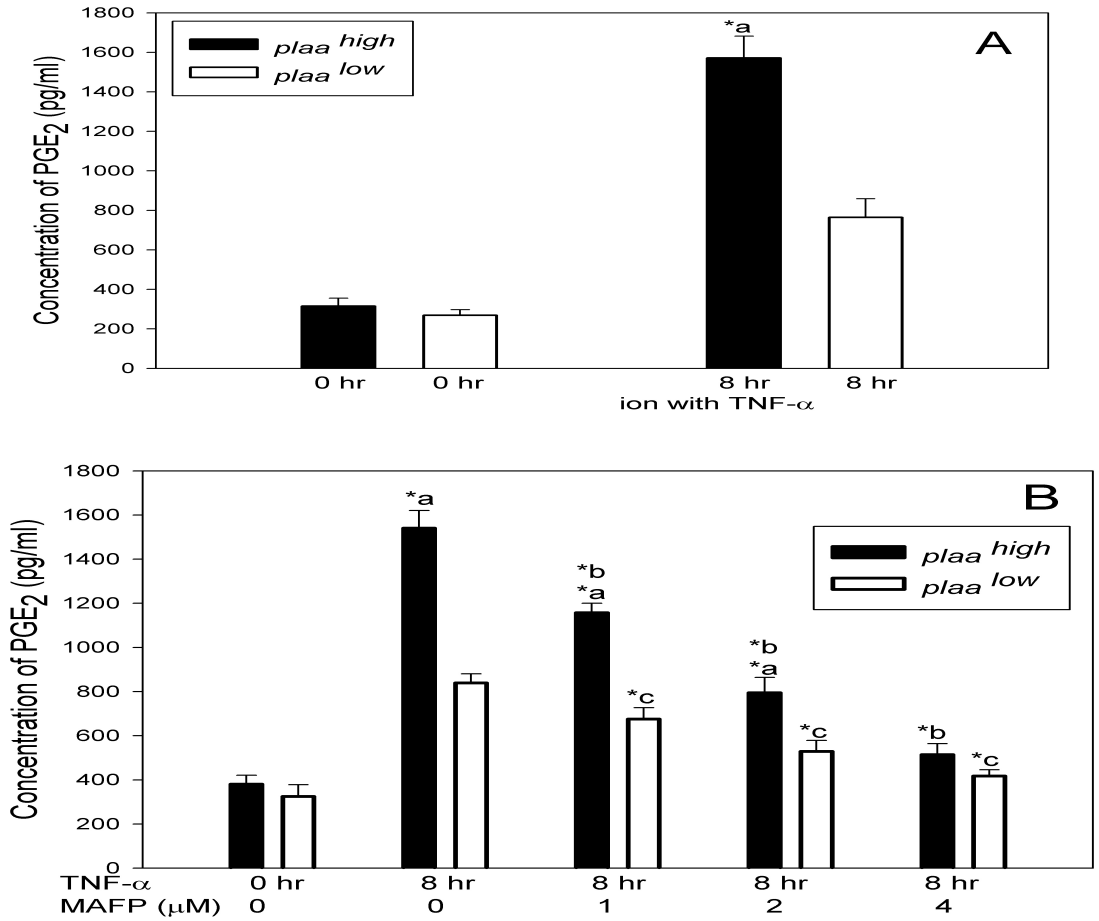

Figure 2.3. Overexpression of the *plaa* gene increases PGE_2 production and PLA_2 activation by TNF-α in HeLa Tet-off cells. Both *plaa* ^{high} and *plaa* ^{low} cells were stimulated with TNF-α (30 ng/ml) or left untreated for 8 hr in DMEM with 10% tetracycline-free FBS supplemented with hygromycin (100 U/ml) and G418 (100 U/ml). **(A)** PGE_2 levels were measured in cell culture supernatants. The PGE_2 values were normalized to the amount of protein in the cell lysates and the data expressed as mean ± standard of four independent repetitions. (**B)** $cPLA_2$ inhibitor MAFP dose-dependently reduced PGE_2 production from stimulated *plaa* ^{high} and *plaa* ^{low} cells. MAFP was added to the cells at indicated concentrations 1 hr prior to TNF-α stimulation and was present throughout the 8 hours' stimulation. DMSO was used to dissolve MAFP before addition to cells and was used as a vehicle control for the treatment.

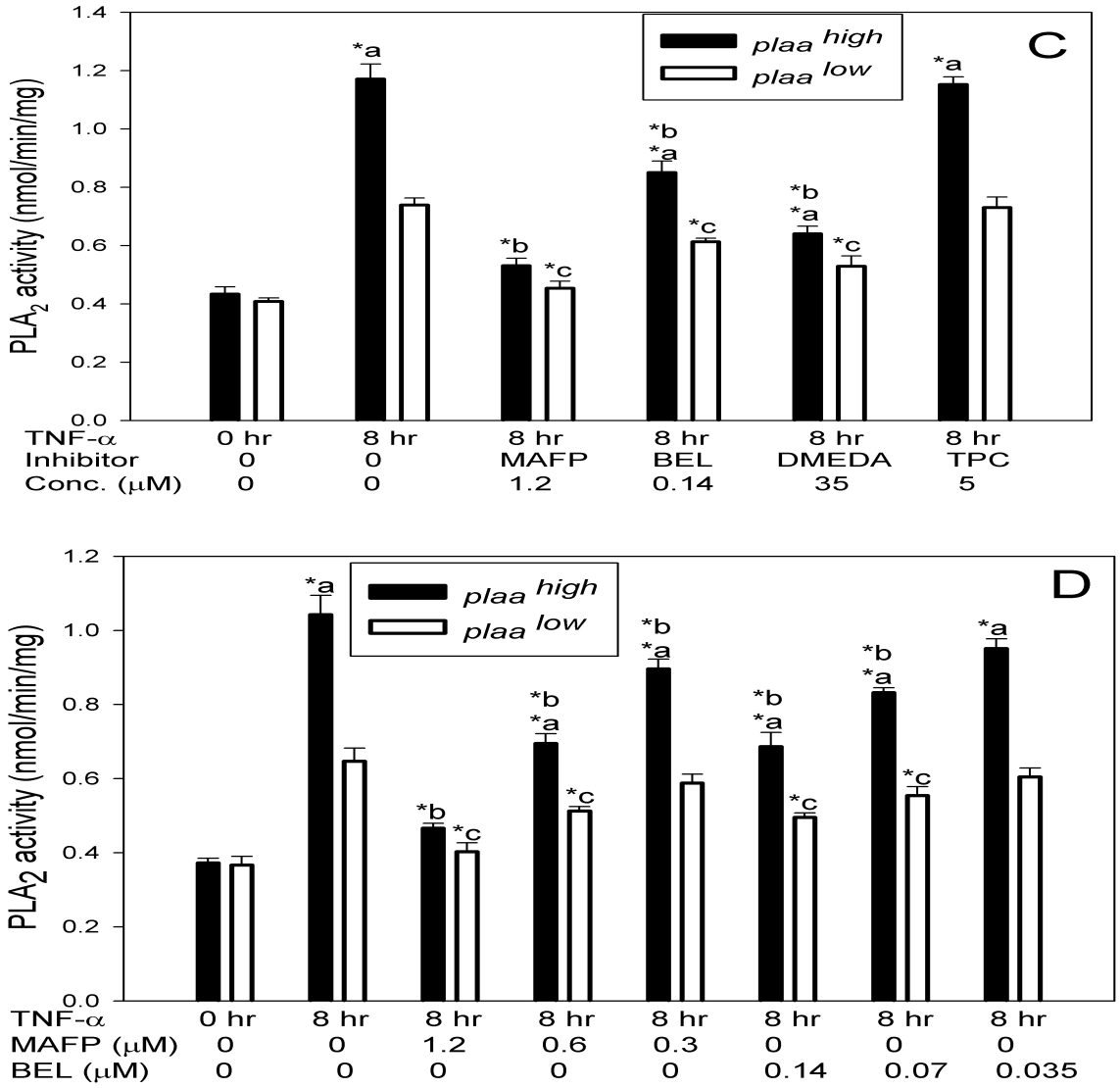

Figure 2.3. Overexpression of the *plaa* gene increases PGE_2 production and PLA_2 activation by TNF-α in HeLa Tet-off cells. *(Continued)* **(C)** $cPLA_2$ inhibitor (MAFP) and $iPLA_2$ inhibitor (BEL) reduced PLA_2 activity from stimulated *plaa* ^{high} and *plaa* ^{low} cells. Equal amounts of membrane proteins of stimulated cells were incubated with inhibitors for 30 min prior to PLA_2 enzyme activity assay. DMSO was used as a vehicle control for the treatment. Included inhibitors were: $cPLA_2$ inhibitor MAFP (1.2 μM), $iPLA_2$ inhibitor BEL (0.14 μM), $sPLA_2$ inhibitor TPC (5 μM), and inhibitor against both $cPLA_2$ and $sPLA_2$ (DMEDA, 35 μM). Titration of the inhibitors MAFP and BEL was also performed to confirm their specificities (**D**). PLA_2 activity was expressed as μmol/min/mg, and values were plotted as the mean ± standard deviation of four independent repetitions. *a denotes statistically significant values ($p < 0.05$) when *plaa* ^{high} cells were compared to that of the *plaa* ^{low}) cells. *b denotes statistically significant values ($p < 0.05$) compared to that of the TNF-α-treated *plaa* ^{high} cells without inhihbitors (vehical control: DMSO). *c denotes statistically significant values ($p < 0.05$)

compared to that of the TNF-α-treated treated *plaa* ^{low} cells without inhihbitors (vehical control: DMSO).

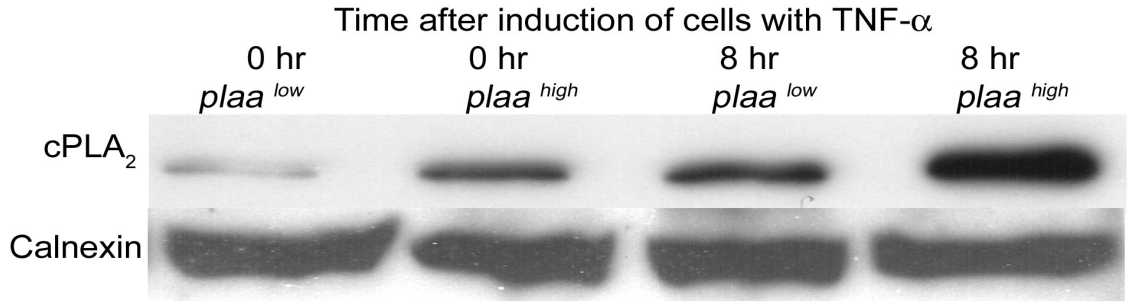

Figure 2.4. Overexpression of the *plaa* gene increases cPLA$_2$ membrane translocation by TNF-α in HeLa Tet-off cells. Western blot analysis of cPLA$_2$ protein from stimulated *plaa* ^{high} and *plaa* ^{low} cells. The *plaa* ^{high} and *plaa* ^{low} cells were stimulated with TNF-α (30 ng/ml) or left untreated for 8 hr. Membrane proteins of cells were prepared, and equal amounts of protein (60 μg) were subjected to 4-20% SDS-PAGE and probed with polyclonal antibody against cPLA$_2$. A polyclonal antibody against calnexin (specific membrane bound host protein) was used to normalize protein loading. The Western blot figure presented is representative of three independent blots.

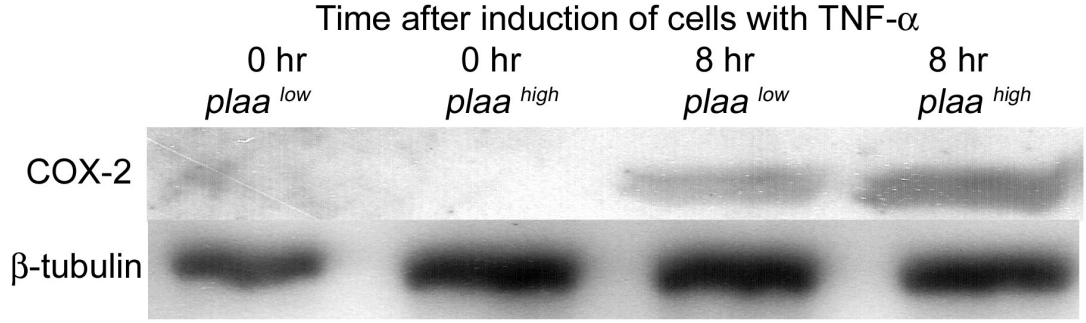

Figure 2.5. Overexpression of the *plaa* gene increases COX-2 expression by TNF-α in HeLa Tet-off cells. Western blot analysis of COX-2 protein from stimulated *plaa* ^{high} and *plaa* ^{low} cells. The *plaa* ^{high} and *plaa* ^{low} cells were stimulated with TNF-α (30 ng/ml) or left untreated for up to 20 hr. An aliquot (40 μg) of total proteins was subjected to 4-20% SDS-PAGE and probed with polyclonal antibody against COX-2. An antibody against β-tubulin was used to normalize protein loading. The Western blot figure presented is representative of three independent blots.

increased the expression of IL-32 in both cells, with consistently higher levels detected in *plaa* ^{high} cells. Consistent with the observations of Goda *et al.* , we found that the majority of IL-32 antigen resided in the cytoplasm, rather than the supernatant. Serial dilutions of the cell lysates were also performed in the ELISA to show specificity of the reaction (data not shown).

Overexpression of the *plaa gene enhances TNF-α-induced NF-κB activation in HeLa Tet-off cells*

The increased expression of COX-2 (**Fig. 2.5**) and IL-32 (**Fig. 2.6**) promoted by PLAA led us to investigate whether overexpression of the *plaa* gene affected the activation of NF-κB. We stimulated *plaa* ^{high} and *plaa* ^{low} cells with 30 ng/ml of TNF-α for up to 60 min, and compared the levels of NF-κB activation using a Bioplex phosphoprotein assay (I-κBα and p65), confocal immunofluoresence (p65), and ELISA (p50). To compare signaling profiles between *plaa* ^{high} and *plaa* ^{low} cells, we performed the Bioplex assay to analyze the phosphorylation levels of NF-κB (p65 and I-κBα) and other signaling proteins including ERK-1, p38 MAPK, JNK, c-jun, CREB, Akt, GSK 3α and β, TrkA, HSP27, and histone 3. We found a significant and consistent difference only for NF-κB (p65 and I-κBα). There were slightly more phosphorylated forms of I-κBα (**Fig. 2.7A-I**) and p65 (**Fig. 2.7B**) in unstimulated *plaa* ^{high} cells than in *plaa* ^{low} cells. These same differences became significant after 15 min (for phospho-IκBα, **Fig. 2.7A-I**) and 5 min (for phospho-p65, **Fig. 2.7B**) of TNF-α stimulation, respectively, and were sustained throughout the rest of the stimulation (60 min). The amount of total IκBα remained comparable between *plaa* ^{high} and *plaa* ^{low} cells, with an overall decreasing trend throughout the stimulation (**Fig. 2.7A-II**).

Confocal immunofluoresence was then performed to trace the translocation of p65 from the cytoplasm to the nucleus. Unstimulated *plaa* ^{high} and *plaa* ^{low} cells exhibited comparable

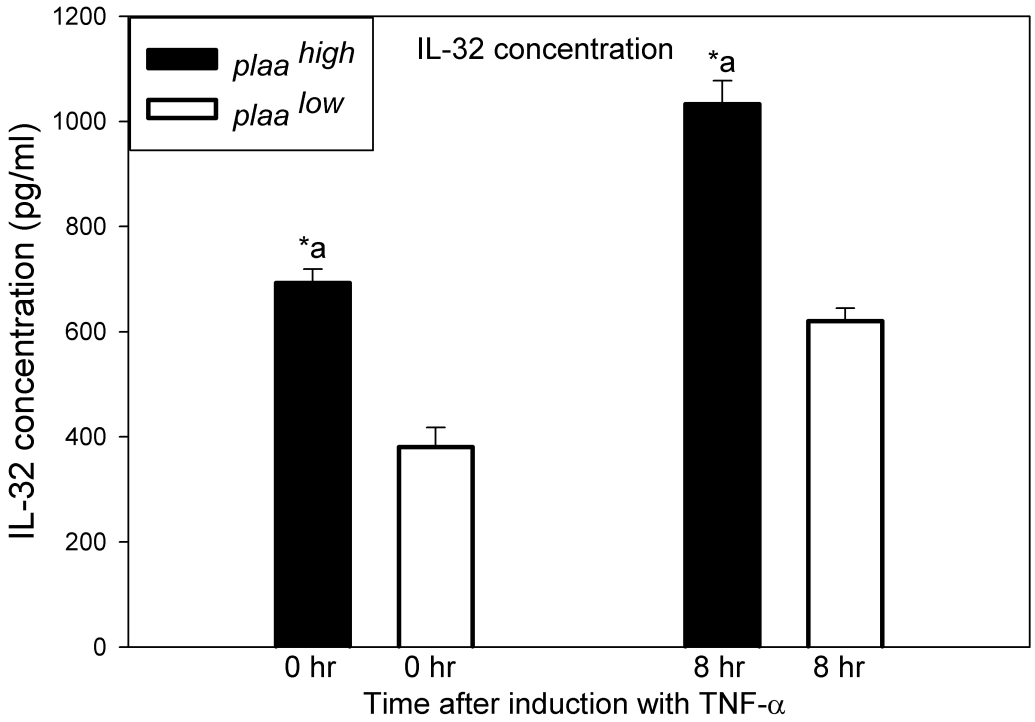

Figure 2.6. Overexpression of the *plaa* gene increases IL-32 expression in *plaa* ^{high} cells. The *plaa* ^{high} and *plaa* ^{low} cells were stimulated with TNF-α (100 ng/ml) or left untreated for 8 hr. A sandwich ELISA method was used to measure the concentration of IL-32 in cellular lysates and supernatants. BSA was used as a negative control. A 15 amino acid-long peptide from the carboxyl terminal of IL-32 was serial-diluted (100 to 6400 pg/ml) and used to generate a standard curve. Values were given as pg/ml and expressed as the mean ± standard deviation of three independent repetitions. *a denotes statistically significant values ($p < 0.05$) compared to that of the *plaa* ^{low} cells.

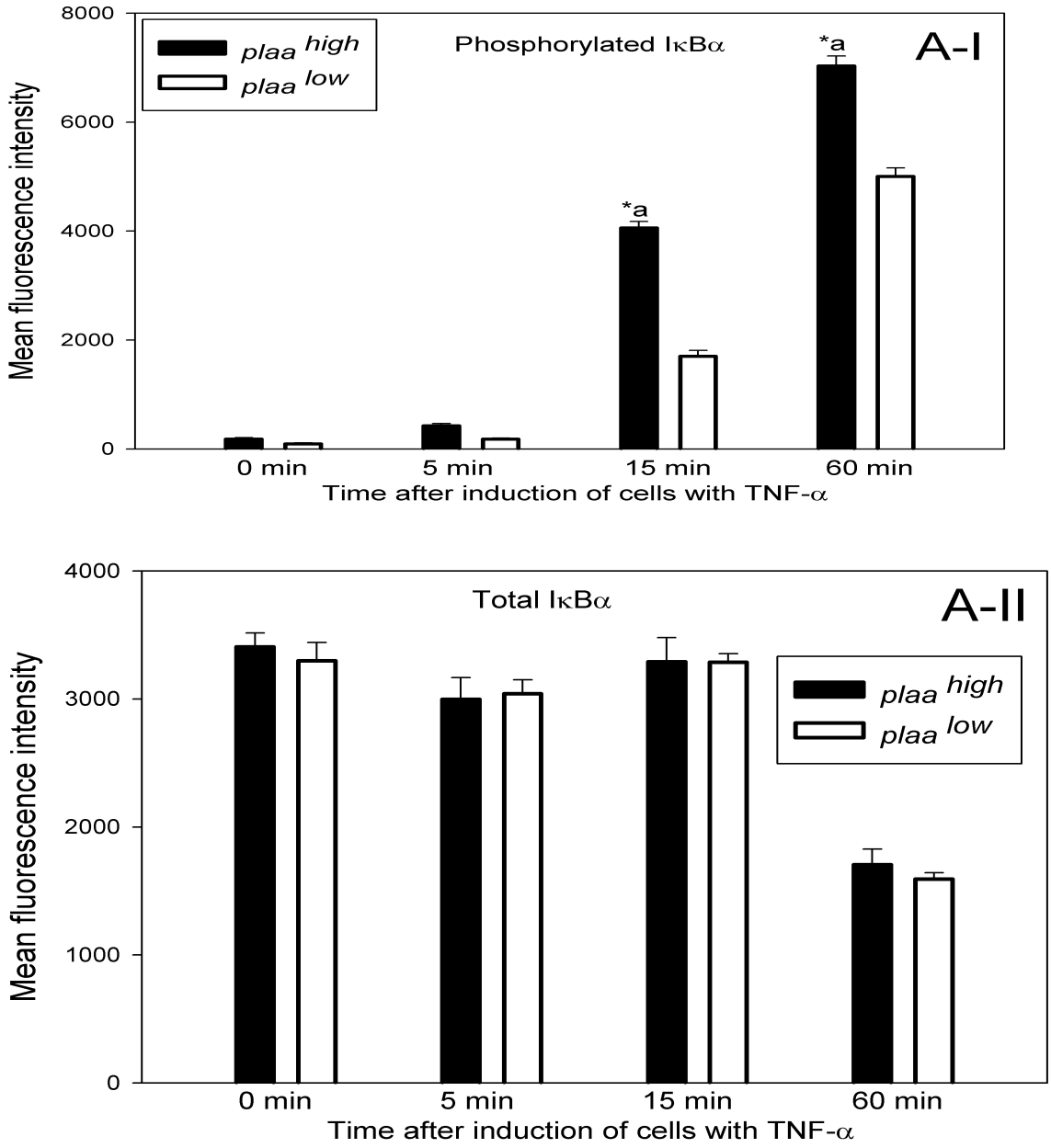

Figure 2.7. Overexpression of the *plaa* gene enhances TNF-α-induced NF-κB activation in HeLa Tet-off cells. The *plaa* ^{high} and *plaa* ^{low} cells were stimulated with TNF-α (30 ng/ml) or left untreated for up to one hr. (**A) I.** Phosphorylation analysis of IκBα. A total of 200 μg of proteins from cells was prepared and phosphorylation of protein targets in these samples was measured using the Bio-plex phosphoprotein assay. Phosphorylated protein standards were used in the assay. The amount of total IκBα (**II**) and phosphorylated p65 (**B**) was also measured in the same samples using Bio-plex phosphoprotein assay (*continued*).

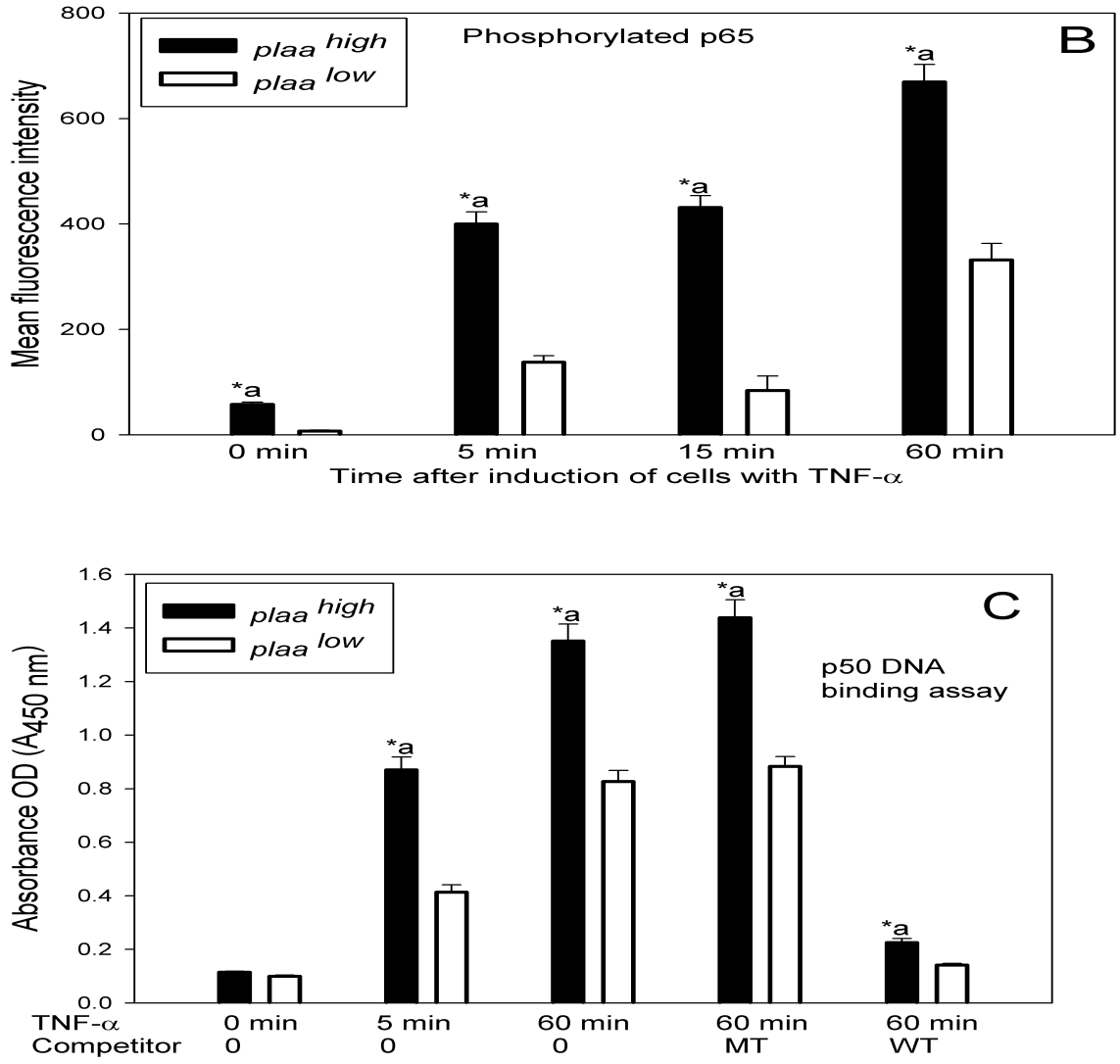

Figure 2.7. Overexpression of the *plaa* gene enhances TNF-α-induced NF-κB activation in HeLa Tet-off cells. *(continued)* The amount of total IκBα (**II**) and phosphorylated p65 (**B**) was also measured in the same samples using Bio-plex phosphoprotein assay. Values were given as relative fluorescence units, and bars represent means of duplicates ± standard deviation of three independent repetitions. *a denotes statistically significant values ($p < 0.05$) compared to that of the *plaa* ^{low} cells. (**C**) Measurement of DNA binding activity of p50. Nuclear fractions from stimulated *plaa* ^{high} and *plaa* ^{low} cells were prepared and used in similar amounts (1 μg each well) and subjected to DNA binding assay. DNA oligonucleotides containing either wild type (WT) or mutated (MT) p50 consensus sites were used as competitors to ensure specificity of the assay (for sequences see "Materials and Methods" section). Values are presented as the mean optical density at $A_{450\ nm}$ (OD A_{450}) and expressed as the mean ± standard deviation of three independent repetitions. *a denotes statistically significant values ($p < 0.05$) compared to that of the *plaa* ^{low} cells.

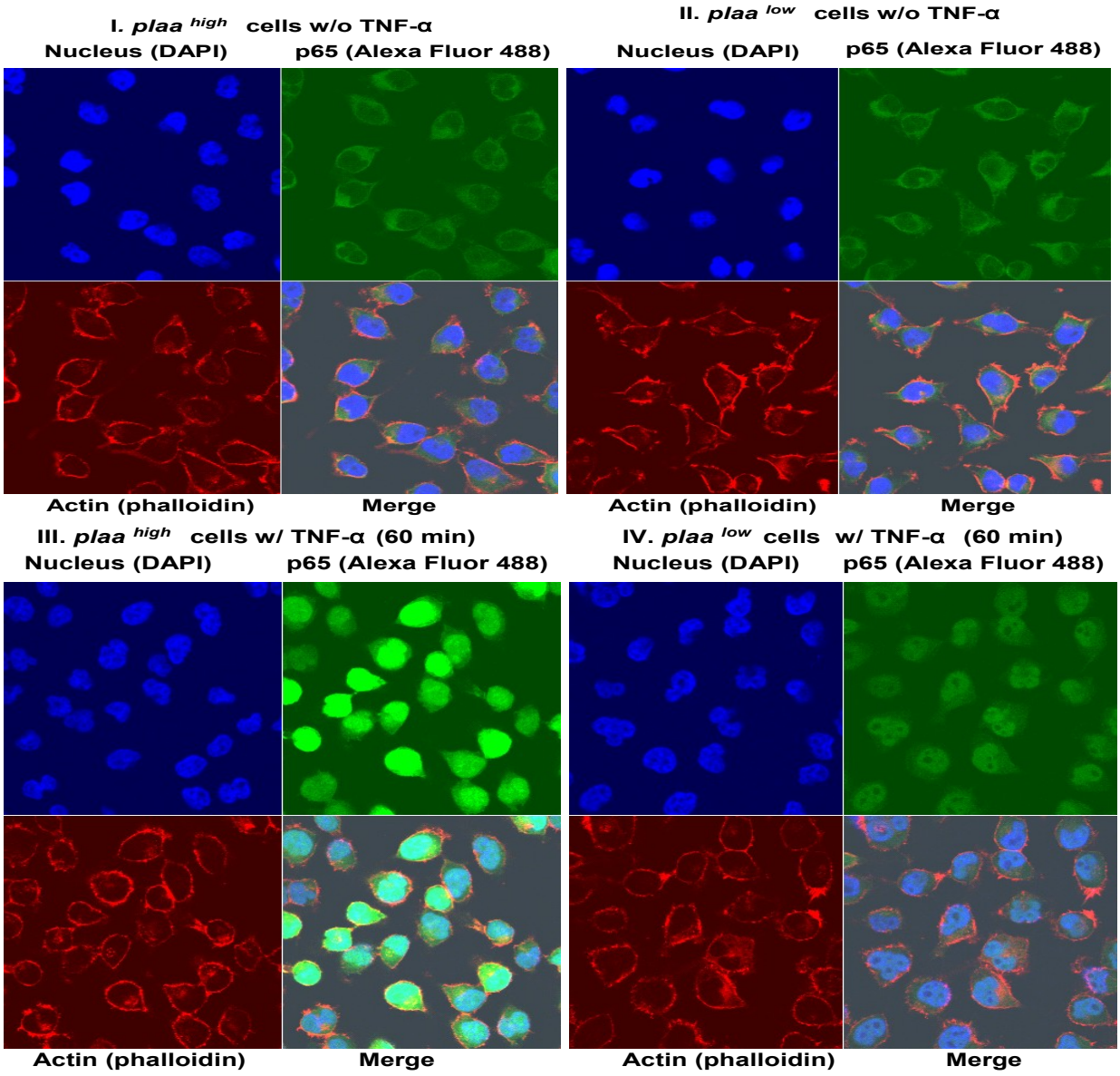

Figure 2.7. (*continued*) **(D)** Immunofluroresence staining was used to visualize nuclear translocation of p65 by confocal microscopy. An Alexa Fluor 488-conjugated primary antibody was used to stain p65 (green). The nuclei were stained blue using DAPI. The actin filaments were stained red using Alexa Fluor 568-conjugated phalloidin. The images showing the staining of p65, nuclei and actin filaments were merged and shown in the lower right panels. The images are representative of one experiment, although three independent experiments were performed.

fluorescence staining of p65 in the cytoplasm only, with no nuclear staining (**Fig. 2.7D-I and II**). Stimulated (with TNF-α for 60 min) *plaa* ^{high} and *plaa* ^{low} cells showed localized staining mainly in the nucleus, with significantly more staining in *plaa* ^{high} cells than in *plaa* ^{low} cells (**Fig. 2.7D-III and IV**). We noted a time-dependent increase of p65 in the nucleus after TNF-α stimulation (from 5-60 min [only data at 60 min were shown]).

To confirm the nuclear translocation and DNA binding of the NF-κB p50 subunit, we isolated nuclear proteins from *plaa* ^{high} and *plaa* ^{low} cells and performed the Trans^{AM} p50 assay, which is an ELISA equivalent of the electrophoretic mobility shift assay (EMSA) . There were comparable levels of nuclear protein binding to p50-specific oligonucleotides from unstimulated *plaa* ^{high} and *plaa* ^{low} cells; however, a significantly higher level of p50-specific binding occurred in stimulated *plaa* ^{high} cells (with TNF-α for 5 or 60 min) compared to stimulated *plaa* ^{low} cells (**Fig 2.7C**). To confirm the specificity of the Trans^{AM} p50 assay, we performed parallel competition assays using competitor oligonucleotides containing either the specific p50-binding consensus sequence (wild-type [WT] competitor) or the mutated sequence (MT). The WT competitor oligonucleotides significantly decreased p50 binding for both *plaa* ^{high} and *plaa* ^{low} cells, whereas the MT competitor did not (**Fig 2.7C**).

Overexpression of the plaa gene increases IL-6 production in TNF-α-stimulated HeLa Tet-off cells

Since NF-κB regulates the expression of many cytokine genes, we performed the Bioplex cytokine assay to compare the cytokine production profiles between *plaa* ^{high} and *plaa* ^{low} cells. The *plaa* ^{high} and *plaa* ^{low} cells were stimulated with 30 ng/ml of TNF-α for 8 hr, and then their supernatants were collected and analyzed using the Bioplex cytokine assay. We found a significant and consistent difference only in the case of IL-6. IL-6 is a proinflammatory cytokine involved in both acute (e.g., sepsis) and chronic inflammation (e.g., rheumatoid arthritis) . Unstimulated *plaa* ^{high} cells produced approximately 8 fold more IL-6 than

unstimulated *plaa* ^{low} cells (**Fig. 2.8**). After stimulation with TNF-α, IL-6 production from *plaa* ^{high} cells was consistently 2.5-fold higher than that of *plaa* ^{low} cells. Compared to their unstimulated states, *plaa* ^{high} and *plaa* ^{low} cells produced 46- and 150-fold more IL-6, respectively.

Overexpression of the plaa gene decreases clusterin expression in plaa ^{high} ***cells.***

Our microarray (**Table 2.2**) and real-time RT-PCR data (**Table 2.3**) revealed a significant decrease (1.6-fold to 2-fold) of clusterin mRNA in *plaa* ^{high} cells, compared to that of *plaa* ^{low} cells. Decreased expression of clusterin is involved in rheumatoid arthritis . Disruption of the clusterin gene promotes NF-κB activation and IL-6 production A sandwich ELISA assay confirmed the microarray and real-time RT-PCR results. The *plaa* ^{high} cells expressed significantly less secreted clusterin (sCLU) antigen than *plaa* ^{low} cells, both in the cell culture supernatant and in the cytoplasm (**Fig 2.9A**). TNF-α stimulation did not change this trend of differential expression. Recombinant clusterin was employed to generate a standard curve and to determine the specificity of the assay (data not shown). Slightly lower nuclear clusterin (nCLU) levels were noted in the nucleus of *plaa* ^{high} cells than that of *plaa* ^{low} cells.

Interestingly, sCLU is involved in lipid transport and can be induced by nefiracetam, a drug that inhibits canine renal prostaglandin synthesis and COX-2 expression through an unknown mechanism . We therefore examined whether reduction in extracellular levels of sCLU in *plaa* ^{high} cells contributed to the induction of PGE_2 production. Indeed, after antibody against clusterin was supplied to the cell culture medium, a dose-dependent induction of PGE_2 was observed for both *plaa* ^{high} and *plaa* ^{low} cells stimulated with TNF-α (**Fig. 2.9B**). An antibody against β-tubulin did not induce any PGE_2 production, which confirmed the specificity of the assay. Conversely, we examined whether extracellularly supplied clusterin is sufficient to reduce PGE_2 production stimulated by TNF-α. As shown in

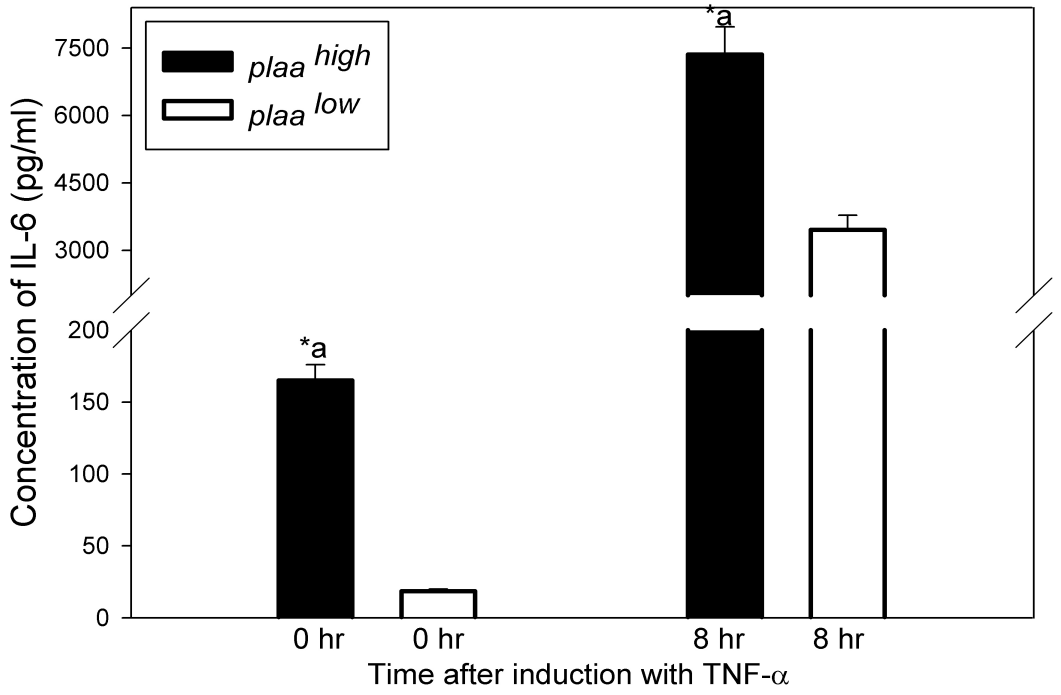

Figure 2.8. Overexpression of the *plaa* gene increases IL-6 production in TNF-α-stimulated HeLa Tet-off cells. IL-6 levels were measured using Bio-plex cytokine assay in culture supernatants of *plaa* ^{high} and *plaa* ^{low} cells stimulated with TNF-α (30 ng/ml) or left untreated for 8 hr. IL-6 values were normalized with amounts of protein in the cell lysates and expressed as the mean ± standard deviation of four independent repetitions. *a denotes statistically significant values ($p < 0.05$) compared to that of the *plaa* ^{low} cells.

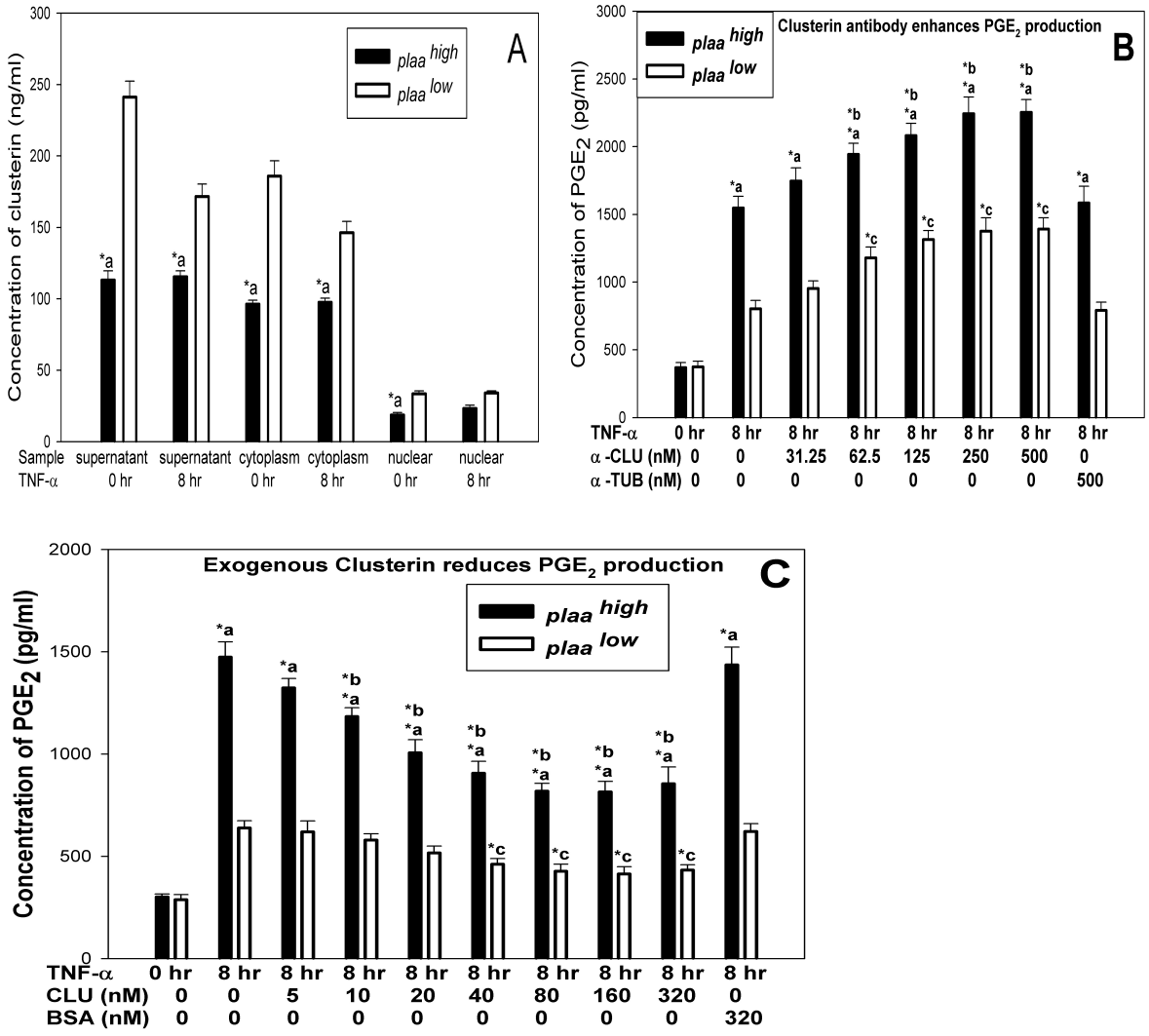

Figure 2.9. Overexpression of the *plaa* gene decreases clusterin expression in *plaa* ^{high} cells. The *plaa* ^{high} and *plaa* ^{low} cells were stimulated with TNF-α (30 ng/ml) or left untreated for 8 hr. (**A)** ELISA analysis of clusterin concentration from cells. Supernatants, cytoplasmic fractions, and nuclear fractions from cells were isolated and assayed for clusterin concentration. Values were expressed as the mean ± standard deviation of three independent repetitions. To determine the effect of clusterin on PGE_2 production from stimulated cells, antibodies against clusterin (α-CLU) (**B**) and exogenous clusterin (CLU) (**C**) were supplied to the culture supernatant after 4 hr of TNF-α stimulation and were present throughout the 8 hours' stimulation. Supernatants from cells were then assayed for PGE_2 levels. Antibodies against β-tubulin (α-TUB) (**B**) and BSA (**C**) were used as negative treatment controls. Values were expressed as the mean ± standard deviation of four independent repetitions. *a denotes statistically significant values ($p < 0.05$) compared to that of the *plaa* ^{low} cells. *b denotes statistically significant values ($p < 0.05$) compared to that of the TNF-α-stimulated *plaa* ^{high} cells. *c denotes statistically significant values ($p < 0.05$) compared to that of the TNF-α-stimulated *plaa* ^{low} cells.

Fig. 2.9C, addition of exogenous clusterin partially reduced PGE_2 production from both stimulated *plaa* ^{high} and *plaa* ^{low} cells in a dose-dependent manner. Saturation points were reached when 20-40 ng/ml of clusterin was supplied to the culture medium. As a control, BSA did not exert this effect (**Fig. 2.9C**). Neither clusterin antibody nor clusterin protein interfered with the results of the PGE_2 ELISA (data not shown).

A Sp1-binding stimulatory element and an inhibitory element are responsible for the transcriptional regulation of the plaa gene.

To search for *cis*- and *trans*-acting regulatory elements of the *plaa* gene, we performed luciferase reporter assays on progressive deletion mutants spanning the 5' genomic region of the *plaa* gene. The luciferase activities correlated with the ability of different elements from the *plaa* gene to stimulate transcription. In HeLa cells, we identified two important regulatory elements (**Fig. 2.10A**); one inhibitory element located between -901 to -1204 bp (upstream of the ATG start codon in exon I of the *plaa* gene) and a stimulatory element located between -252 to -418 bp. The position -252 bp denoted 252 bp remaining upstream to the initiation codon (0 bp) in the *plaa* gene. Luciferase assays with the same constructs performed in murine RAW 264.7 macrophages produced similar results (data not shown).

Deletion of the inhibitory element between -901 to -1204 bp resulted in ~33% increase in luciferase activity (**Fig. 2.10A**). Fusion of the inhibitory element (-901 to -1204 bp) in front of the -488 bp construct created a new recombinant clone which had ~67% less luciferase activity than that of the -488 bp construct. An even greater reduction in luciferase activity was observed when the inhibitory element was fused in front of the -545 bp construct. These results suggested that the inhibitory element is both sufficient and necessary to inhibit the expression of the *plaa* gene. In this inhibitory element (-901 to -1204 bp), 32 potential transcription factor binding sites were predicted by *in silico* analysis, using the online transcription factor binding site prediction tool, "AliBaba2" (data not shown).

Serial deletions within the stimulatory element (-252 to -418 bp) of the *plaa* gene defined a core promoter between -252 to -293 bp (**Fig. 2.10A**). Deletion of the element between -252 to -293 bp resulted in ~80% reduction in luciferase activity (**Fig. 2.10A**). Using *in silico* analysis, we identified one potential binding site for Sp1 between -252 to -293 bp and six other Sp1 sites between -294 to -418 bp (**Fig. 2.11**). Sp1 is a transcription factor known to regulate the activities of proteins involved in eicosanoid production, such as $cPLA_2$, $sPLA_2$, platelet-activating factor acetylhydrolase (PAF-AH) , and 12(S)-lipoxygenase .

To examine whether Sp1 binds to the stimulatory element and maintains basal transcription of the *plaa* gene, we employed decoy DNA oligos to compete for Sp1 binding with the stimulatory element (-252 to -418 bp) of the *plaa* gene in our luciferase assay. As shown in **Fig. 2.10B**, the WT Sp1 decoy significantly reduced the luciferase activity associated with the stimulatory element. The luciferase activity from this element was reduced to 20% of its original value and was similar to that of the -252 construct (which did not contain the element between -252 to -418 bp). A scrambled (MT) decoy, on the other hand, had no effect. To prove the specific binding between Sp1 and the core promoter element (-252 to -293 bp) of the *plaa* gene, we performed a competitive binding assay using a 23 bp fragment of the core promoter element (-255 to -277 bp). As shown in **Fig. 2.10C**, the WT fragment of the core promoter element (WT element) dose-dependently inhibited the binding between Sp1 and the probe containing Sp1 site (biotin-labeled Sp1 probe). The inhibitory potency of the WT element was similar to that of the unlabeled Sp1 probe. Conversely, the MT element, whose Sp1 binding site was mutated, could not inhibit the binding between Sp1 and the labeled Sp1 probe. These results suggest that Sp1 maintains basal expression of the *plaa* gene and binds to the stimulatory element.

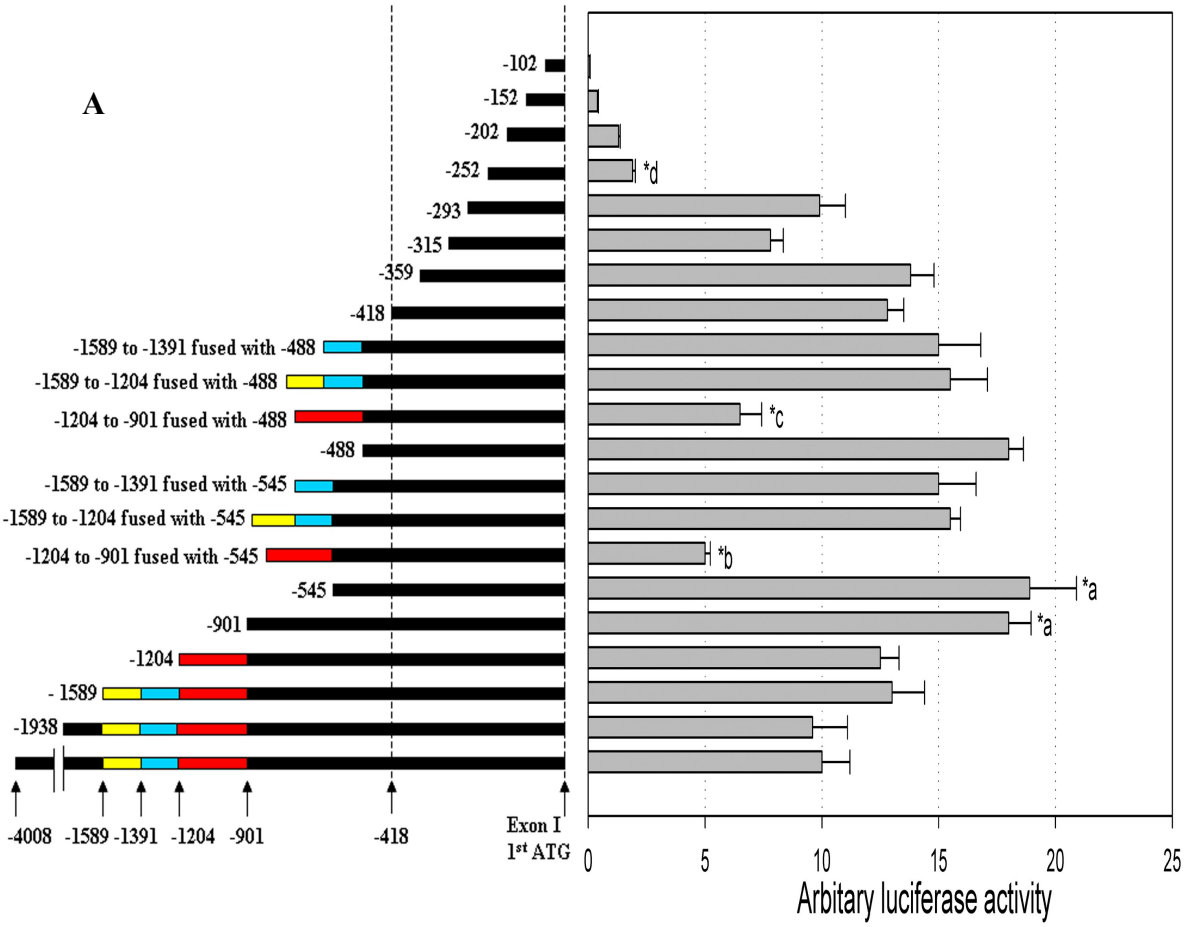

Fig 2.10. An Sp1-binding stimulatory element and an inhibitory element are responsible for the transcriptional regulation of the *plaa* gene. (A) Mapping of the 5' genomic region of the *plaa* gene using luciferase assays. –4008 denotes 4008 base pairs remaining upstream to the 1st ATG codon (0 bp) of exon I in the *plaa* gene, while the rest of the DNA sequence (upstream of 4008 bp) was deleted. This 4008 bp-sequence was progressively truncated into smaller DNA fragments and the latter inserted in front of the firefly luciferase gene in the pGL3-Basic vector. The region colored in red represents sequence between -901 to -1204. The red element was moved forward and fused with the -545 or -488 element to determine whether spacing affects its inhibitory activity. A pRL-TK vector expressing the *Renilla* luciferase reporter was transfected together with the firefly luciferase plasmids into HeLa cells as a control for luciferase activity, transfection efficiency, and cell viability. Individual firefly luciferase activity from transfected cells was normalized against the *Renilla* luciferase activity. Values were given in arbitrary luciferase units (one unit equals approximately 10^5 RLU) and expressed as the mean ± standard deviation of four independent repetitions. *a denotes statistically significant values ($p < 0.05$) compared to that of the -4008 construct. *b denotes statistically significant values ($p < 0.05$) compared to that of the -545 construct. *c denotes statistically significant values ($p < 0.05$) compared to that of the -488 construct. *d denotes statistically significant values ($p < 0.05$) compared to that of the -418 construct.

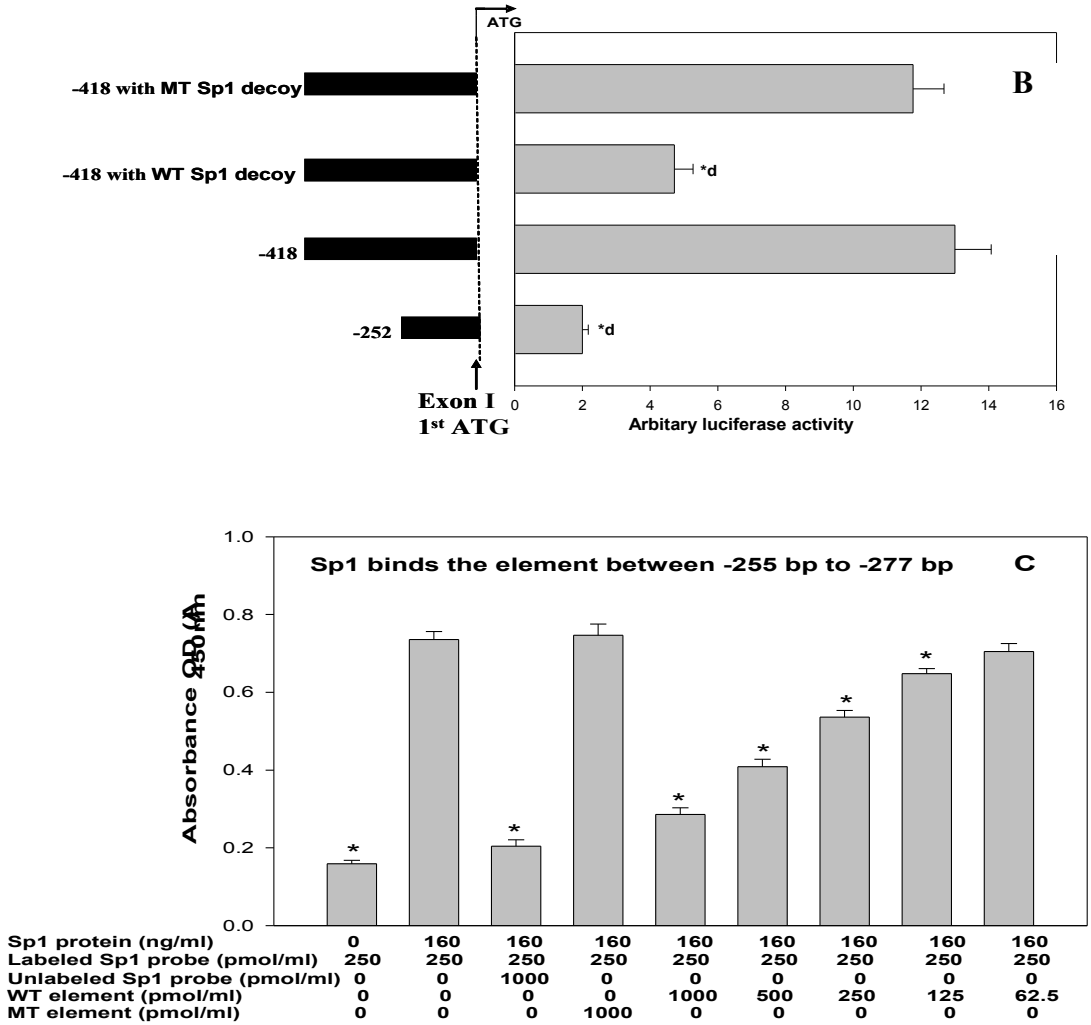

Fig 2.10. (*continued*) **(B)** Sp1 decoy oligonucleotides reduced transcription from the element between -252 to -418 bp. Double-stranded DNA oligonucleotides containing the consensus Sp1 binding sequence (underlined) were designated "Wild Type (WT) Sp1 decoys" and synthesized. Mutated (MT) Sp1 decoys were mutated at two positions in the WT Sp1 decoys (for sequences see "Materials and Methods" section). The decoy oligonucleotides were transfected together with the firefly luciferase plasmids at a molar ratio of 50:1 to compete for Sp1 binding. Luciferase activities values were given in arbitrary luciferase units (one unit approximately equals 10^5 RLU) and expressed as the mean ± standard deviation of three independent repetitions. *d denotes statistically significant values ($p < 0.05$) compared to that of the -418 construct. (**C**) Sp1 specifically binds to the element between -255 to -277 bp. The double-stranded DNA oligonucleotide, which resides between 255 to 277 bp upstream of the ATG start codon in exon I of the *plaa* gene, was designated "Wild Type (WT) element" and synthesized. Mutated (MT) element was altered at five positions in the WT element (for sequences see "Materials and Methods" section). The competitive binding assay was performed using a Sp1 ELISA kit. When indicated, the WT or MT element was used to compete with the Sp1 probe for Sp1 binding. A Sp1 probe without biotin label (unlabeled Sp1 probe) was used as positive control for the competitive binding assay. Values were shown as OD A_{450} and expressed as mean ± standard deviation of three independent repetitions. * denotes statistically significant values ($p < 0.05$) compared to that of the Sp1 binding without using competitor oligos.

Fig 2.11. DNA element between -418 to -252 bp upstream of the 1st ATG was screened using the online transcription factor binding site prediction tool "AliBaba2".

Discussion

Previous studies from our laboratory revealed that the expression of the *plaa* gene can be induced by stimuli such as TNF-α and LPS . However, the functional consequences of native PLAA induction have been elusive until our current study.

We performed microarray analysis to identify downstream effectors targeted by *plaa* gene induction to better understand cell signaling initiated by PLAA. Overexpression of the native *plaa* gene decreased expression of annexin A4 and clusterin and up-regulated IL-32 expression (**Table. 2.2 and 2.3**). Interestingly, in other microarray studies of synovial tissues from rheumatoid arthritis patients and rat model of arthritis, the expression of genes encoding PLAA , clusterin and IL-32 were also found to be altered. Annexin A4 belongs to the annexin family of proteins, which all possess calcium-dependent phospholipid binding activities and participate in membrane organization and trafficking . Several members of the annexin family, such as annexin A4/PP4-X/PAP-II , annexin A1/lipocortin I , and annexin A5/lipocortin V/PP4/PAP-I , are known to inhibit PLA_2 possibly by interfering its membrane binding activity . We confirmed that *plaa* ^{high} cells expressed less annexin A4 antigen than *plaa* ^{low} cells and showed that *plaa* ^{high} cells contained more PLA_2 activity in response to TNF-α stimulation (**Fig. 2.2**). The greater level of TNF-α-induced PLA_2 membrane binding in *plaa* ^{high} cells, compared to *plaa* ^{low} cells (**Fig. 2.4**), may at least partially result from less annexin A4 expression and hence more membrane exposure to PLA_2 in *plaa* ^{high} cells.

We demonstrated for the first time that overexpression of the native *plaa* gene increases the production of PGE_2 through induction of $cPLA_2$, $iPLA_2$ and COX-2 (**Fig. 2.3, 2.4, and 2.5**). We revealed that with TNF-α stimulation, the induction of PLAA is sufficient to increase PGE_2 production. Following TNF-α stimulation, *plaa* ^{high} cells showed increased activation and membrane translocation of $cPLA_2$ than did control *plaa* ^{low} cells. Interestingly, PLAA contains G protein beta domain (G_β) (amino acid residues 1- 250) , a known activator of phospholipase

C , in its amino terminal region. It is possible that the G_β domain in PLAA may contribute to the activation/membrane binding of $cPLA_2$ in a similar fashion. Furthermore, human PLAA contains a domain (amino acid residues 503-508) with 39% identity to melittin, a known activator of PLA_2 and phospholipase D . This melittin homology domain itself, when used to stimulate macrophages, can induce the expression of TNF-α and COX-2 . Therefore, PLAA might also activate PLA_2 directly through the melittin domain.

We revealed a novel link between the induction of PLAA and IL-32. Our results from microarray, real-time RT-PCR (**Table 2.3**) and ELISA (**Fig. 2.6**) demonstrated that overexpression of the native *plaa* gene is sufficient to induce the expression of IL-32. Stimuli such as TNF-α and LPS , have been shown to induce IL-32 expression in various cell types. In turn, IL-32 can perpetuate inflammatory responses and activate NF-κB and p38 MAP kinase , and induce the production of IL-6 , PGE_2 , TNF-α and IL-8 . Since overexpression of the *plaa* gene enhanced the activation of NF-κB (**Fig. 2.7**) and production of PGE_2 (**Fig. 2.3**) and IL-6 (**Fig. 2.8**) induced by TNF-α, the induction of IL-32 may contribute to these effects.

Overexpression of *plaa* promoted NF-κB activation induced by TNF-α (**Fig. 2.7**). Indeed, PLA_2 , COX-2 and metabolites from the eicosanoid production pathway are known to modulate NF-κB activation. Interestingly, murine PLAA was reported to interact with valosin containing protein (VCP, AKA cdc48p) , whose human homolog modulates ubiquitin-dependent degradation of I-κBα in B lymphocytes . Furthermore, UFD3/DOA1(which is 715-amino acid long), the yeast homolog of PLAA , also binds directly to cdc48p/VCP and modulates the degradation of yeast NF-kB-related transcription factor Spt23 . It is appealing to expect that PLAA could modulate NF-κB activity through ubiquitin signaling. However, caution must be taken since the homology between PLAA and UFD3/DOA1 is limited to only two regions in PLAA; region I resides within amino acid residues 10-407 which exhibits 58% overall similarity and region II resides within amino acid residues 479-706 which shows 43%

overall similarity . Domains in PLAA outside these two regions, and small domains inside the regions, such as the melittin homology domain (amino acid residues 503-538, 39% identity to melittin) , do not exist in UFD3/DOA1. The melittin homology domain, which has been shown to induce the production of TNF-α and IL-1β from macrophages , may modulate NF-κB activation.

Studies using mutated PLAA proteins and $PLAA^{-/-}$ knockout mice could shed light on its functions including influence on NF-κB activity. Our initial attempt to create $PLAA^{-/-}$ mice failed due to the infertility of heterozygous ($PLAA^{+/-}$) mice. Interestingly, defects in reproduction have been observed in $cPLA_2^{-/-}$ mice , COX-2 $^{-/-}$ mice and PGE_2 receptor EP4 $^{-/-}$ mice .

Overexpression of the *plaa* gene in HeLa cells specifically enhances IL-6 production induced by TNF-α (**Fig. 2.8**). Since NF-κB activation is also promoted by *plaa* overexpression, it is interesting that only IL-6, rather than other cytokines, was differentially expressed in *plaa* ^{high} cells. These data suggested that additional signaling in *plaa* ^{high} cells may contribute to IL-6 production. Indeed, an autocrine/paracrine loop of the IL-6/Stat3 and $cPLA_2$/COX-2/PGE_2 signaling pathways has been shown in human cholangiocarcinoma cells . PGE_2 can bind EP4 receptor and mediate production of IL-6, which in turn, enhances PGE_2 signaling through MAP kinase-mediated phosphorylation and activation of $cPLA_2$. Our data may represent a similar situation, since PGE_2 production in *plaa* ^{high} cells was also promoted by *plaa* overexpression (**Fig. 2.3**).

We demonstrated for the first time that induction of PLAA reduced the expression of clusterin, a novel regulator of PGE_2 production (**Fig. 2.9**). Extracellular clusterin is a lipid binding chaperone that protects cells against stress . Clusterin may act as a stress sensor and protects cells by binding proinflammatory lipids (e.g., PGE_2) for clusterin receptor (e.g.,

megalin) uptake and degradation. Exogenous clusterin antibody promoted PGE_2 production induced by TNF-α (**Fig. 2.9B**), mostly by blocking the interaction between clusterin and its receptor. Conversely, exogenous sCLU dose-dependently decreased the PGE_2 production induced by TNF-α (**Fig. 2.9C**). Once in the cytoplasm, clusterin may further reduce inflammation by inhibiting NF-κB activation , thus limiting the expression of COX-2 and proinflammatory cytokines . Indeed, disruption of the clusterin gene in cells promotes NF-κB activation and IL-6 production . The induction of NF-κB activation (**Fig. 2.7**) and IL-6 production (**Fig. 2.8**) observed in *plaa* ^{high} cells may partially be due to a reduction in the expression of clusterin.

De novo transcription of the *plaa* gene is required for the production of PGE_2 and AA . Actinomycin-D blocked PGE_2 production from smooth muscle-like cells , and antisense *plaa* inhibited AA production from macrophages . Further, the expression of the *plaa* gene is highly controlled and can be induced in macrophages within 10 min by LPS or CT . In order to characterize transcriptional regulation of the *plaa* gene, we mapped its 5' genomic region (**Fig. 2.10**). An inhibitory element, located between -901 bp to -1204 bp (upstream of the ATG start codon in exon I of the *plaa* gene), was found to be both sufficient and necessary to reduce the expression of the *plaa* gene. Further characterization is needed to identify regulatory transcription factors that bind to this inhibitory element, and such studies will be performed in our future research.

A stimulatory element, located between -252 to -418 bp (core promoter element resides between -252 to -293 bp), maintains basal transcription of the *plaa* gene and binds specifically with a Sp1 transcription factor (**Fig. 2.10**). Sp1 is a ubiquitously expressed general transcription factor which binds GC-rich elements in DNA . Consistent with our results, other proteins involved in eicosanoid production, such as $cPLA_2$, $sPLA_2$, and 12(S)-lipoxygenase, are also transcriptionally regulated by Sp1 . By *in silico* mapping of the stimulatory element (-252

to -418 bp) in the *plaa* gene, we identified a potential NF-κB binding site near one Sp1 binding site in the core promoter element (-252 to -418 bp) (**Fig. 2.11**). Interestingly, binding sites for NF-κB and Sp1 are also adjacent in the HIV-1 long terminal repeat, where they can cooperatively activate transcription . In the absence of activated nuclear NF-κB, Sp1 can maintain basal expression of NF-κB-dependent genes . The expression of the *plaa* gene probably resembles such an arrangement, since it can be induced by TNF-α and its basal expression is maintained by Sp1.

In summary, we demonstrated for the first time that induction of native PLAA promotes the production of PGE_2 and IL-6 and activation of NF-κB induced by TNF-α (**Fig.2.12**). Our microarray and functional studies revealed new inflammation-associated genes altered by the induction of PLAA. Overexpression of the *plaa* gene induces the expression of the proinflammatory cytokine IL-32 and reduces the expression of annexin A4 and clusterin. We confirmed the role of annexin A4 as an inhibitor of PLA_2 and demonstrated for the first time that extracellular clusterin limits the production of PGE_2. We showed that upon TNF-α stimulation, HeLa cells overexpressing the *plaa* gene revealed enhanced activation of $cPLA_2$ and $iPLA_2$, as well as increased expression of COX-2. Induction of PLA_2 and COX-2 resulted in increased production of PGE_2. Furthermore, we found a novel link between the induction of PLAA and the activation of NF-κB. Enhanced activation of NF-κB leads to induction of COX-2 and IL-6 . **Figure 2.12** summarizes the role of PLAA in inducing inflammation-associated targets demonstrated in this study. Moreover, we found that Sp1 maintains basal transcription of the *plaa* gene, whereas an inhibitory *cis*-acting element may limit its overexpression. Given the importance of PGE_2 and IL-6 in inflammatory signaling, these findings may provide knowledge for developing therapies against both acute and chronic inflammatory diseases.

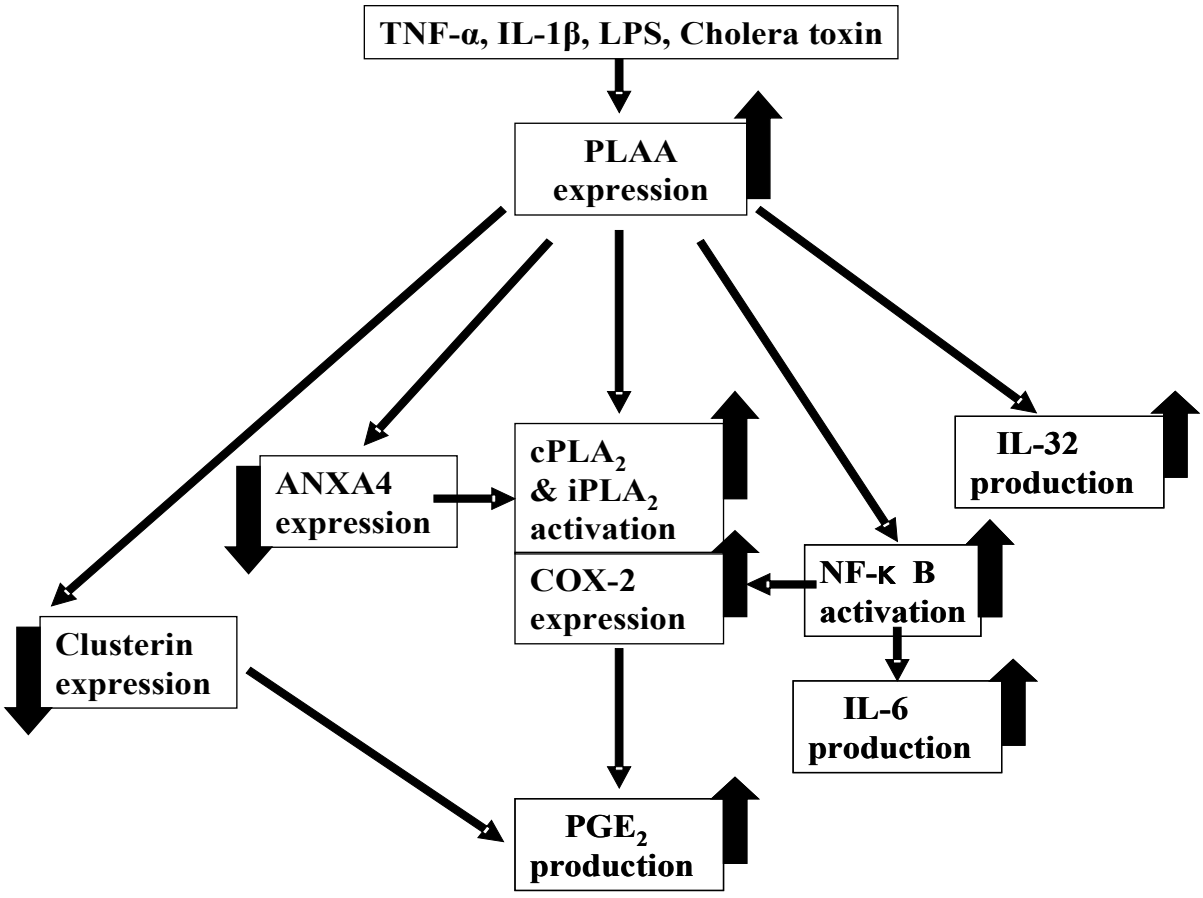

Fig 2.12. **Schematic diagram summarizing the role of PLAA in inducing inflammation.**

Chapter 3

PLAA ENHANCES CISPLATIN-INDUCED APOPTOSIS IN HeLa CELLS

Abstract

Phospholipase A_2 (PLA_2)-activating protein (PLAA) is a novel signaling molecule that regulates eicosanoid production and participates in inflammatory responses. In our current study, we revealed that PLAA production was induced by the chemotherapeutic drug cisplatin in HeLa cervical carcinoma cells. To determine the potential pro-apoptotic effects of PLAA induction by cisplatin, we utilized HeLa (Tet-off) cells overexpressing the *plaa* gene (*plaa* ^{high}) and compared them with control (*plaa* ^{low}) cells, which produce endogenous *plaa* from the chromosome. Cisplatin-stimulated *plaa* ^{high} cells contained significantly higher levels of DNA fragmentation, caspase 3, 8 and 9 activities, PLA_2 enzyme activity, and cytochrome *c* leakage from mitochondria than did the cisplatin-stimulated *plaa* ^{low} cells. Importantly, siRNA against PLAA (siRNA-PLAA) reduced the levels of cisplatin-induced PLAA, DNA fragmentation, and PLA_2 activation, while promoting cell viability in both *plaa* ^{high} and *plaa* ^{low} cells. Cisplatin induced-cytochrome *c* leakage in *plaa* ^{high} cells was reduced by siRNA-PLAA and restored by the addition of exogenous arachidonic acid (AA), suggesting to us that PLAA induction by cisplatin promoted cytochrome *c* leakage/mitochondrial damage partially by accumulating AA. In addition, cisplatin-stimulated *plaa* ^{high} cells produced less cytoprotecive clusterin than did the cisplatin- stimulated *plaa* ^{low} cells, and siRNA-PLAA promoted clusterin production from both *plaa* ^{high} and *plaa* ^{low} cells. We showed that clusterin reduced DNA fragmentation in cisplatin-stimulated *plaa* ^{high} and *plaa* ^{low} cells, which is consistent with the notion that clusterin promotes cancer chemo-resistance. Furthermore, cisplatin-stimulated *plaa* ^{high} cells produced more IL-32 (a pro-apoptotic protein) than did cisplatin-stimulated *plaa* ^{low} cells, and siRNA-PLAA reduced IL-32 production from both *plaa* ^{high} and *plaa* ^{low} cells. Finally, our proteomic analysis revealed that cisplatin-stimulated *plaa* ^{high} cells contained higher levels of phosphorylated JNK/c-Jun and FasL than did *plaa* ^{low} cells treated the same way. In summary, our data indicated that PLAA induction enhanced cisplatin induced-apoptosis through four pathways, namely by: 1) accumulation of AA and mitochondrial damage, 2) down-regulation of the cytoprotective

clusterin, 3) up-regulation of the pro-apoptotic IL-32, and 4) induction of JNK/c-Jun signaling and FasL expression.

Introduction

Cisplatin is a highly potent chemotherapeutic drug commonly used for a variety of human malignancies, such as testicular, prostate, ovarian, cervical, lung, and colon cancers . The cytotoxicity of cisplatin is primarily mediated by its ability to cause DNA damage and subsequent apoptotic cell death . However, tumors can develop cisplatin resistance by interfering with signal transduction from the nucleus to the apoptotic machinery . Additional cytotoxic effects of cisplatin include generation of toxic lipid metabolites , damage to cellular proteins , and other effects. These additional killing mechanisms, when targeted to resistant tumors in conjunction with modulation of relevant pathways, can potentially overcome resistance and restore apoptosis. When cisplatin causes toxic side effects in non-cancerous tissues, however, its cytotoxicity (e.g., nephrotoxicity and neurotoxicity) limits the efficacy of chemotherapy . In such as a case, to prevent this cytotoxicity, relevant cellular metabolism and signaling pathways could be modulated .

One potential cytotoxic mechanism of cisplatin may involve the generation of arachidonic acid (AA) and its metabolites . AA, generated by phospholipase A_2 (PLA_2) enzymes from glycerophospholipids, can cause apoptosis at low concentrations and necrosis at high concentrations . For example, in a cell line derived from the organ of Corti, cisplatin induced the overexpression of eight genes involved in AA metabolism , especially those of the PLA_2 group IVA (a cytosolic PLA_2); group V (a secreted PLA_2); and phospholipase A_2-activating protein (PLAA). Oxidative stress, potentially induced by oxidized metabolites of AA, was suggested to contribute to the cytotoxicity of cisplatin .

$cPLA_2$, $sPLA_2$ and $iPLA_2$ have all been implicated in apoptosis and $iPLA_2$ mediates cisplatin-induced renal cell apoptosis . AA accumulation, produced by PLA_2 activation, can induce apoptosis either directly *via* a mitochondrial-mediated pathway , or indirectly by inducing production of the cytotoxic ceramide . PLAA peptides are known to induce apoptosis in smooth muscle cells and tumor regression in animal models of glioma, lung and breast cancer .

Based on these previous studies, we believe induction of PLAA by cisplatin can partially mediate cytotoxicity in host cells . Transcriptional induction of PLAA together with $cPLA_2$ and $sPLA_2$ by cisplatin can potentially promote cytotoxicity by PLA_2 activation and AA accumulation. Additional lines of evidence suggesting PLAA's involvement in apoptosis lie in the location of the human *plaa* gene in chromosome 9p21 , a region frequently inactivated in various cancers, including melanoma, glioma, ovarian, lung and breast cancers and lymphoid leukemia . Interestingly, unpublished data from a study conducted by Peters *et al.* showed that carboplatin-sensitive ovarian cancer cells from patients expressed higher levels of PLAA than did their resistant control cells.

Further, clusterin and interleukin (IL)-32 , both of which are modulated by PLAA , are involved in apoptosis. PLAA induction downregulated the mRNA synthesis and antigen level of clusterin, while upregulating the mRNA and protein levels of IL-32 in HeLa cervical cancer cells . Clusterin is a cytoprotective protein with an established role in promoting tumor chemo-resistance , while IL-32 associated specifically with apoptotic T cells, and the ectopic expression of the *IL-32* gene in HeLa cells caused apoptosis .

However, it remains to be proven whether cisplatin-induced apoptosis is partially mediated by PLAA induction. The detailed mechanism by which PLAA induction modulates apoptosis deserves further investigation. We hypothesized that native PLAA promotes

cisplatin-induced apoptosis by modulating AA metabolism and expression/production of clusterin and IL-32. To test our hypothesis, we employed HeLa Tet (tetracycline)-off cells, which we previously used to overexpress the native *plaa* gene , and determined their apoptotic responses to cisplatin. HeLa cells were chosen because cervical tumor is a cisplatin-responsive tumor, while cervical tissues express the *plaa* gene , and respond to prostaglandins .

Materials and Methods

DNA fragmentation assay

The levels of DNA fragmentation in HeLa Tet-off (*plaa* ^{high} or *plaa* ^{low}) cells were determined by measuring cytoplasmic oligonucleosomes using the cell death detection ELISA^{plus} kit (Roche, Indianapolis, IN), following the manufacturer's instructions. After cisplatin stimulation, cells were resuspended in lysis buffer, and cytosolic extracts were harvested by centrifugation (200 x*g* for 10 min). Protein concentrations were determined and 60 μg cytosolic proteins were diluted in 20 μL lysis buffer for each assay. Subsequently, each cytosolic sample was incubated for 2 hr with biotin-conjugated-histone antibody in a 96-well plate coated with streptavidin and with Peroxidase (POD)-conjugated-DNA antibody. The plate was then washed 5 times, and the reaction was developed using ABTS (2,2′-Azino-*bis*[3-ethylbenzthiazoline-6-sulfonic acid]) as the substrate. The color reaction was measured in a microplate reader at 405 nm.

Caspase enzyme activity assays

The enzyme activities of caspase 3, caspase 8 and caspase 9 were measured by using colorimetric activity assay kits according to manufacturer's instructions (BioVision Inc., Mountain View, CA). After cisplatin stimulation, HeLa Tet-off (*plaa* ^{high} or *plaa* ^{low}) cells were resuspended in chilled lysis buffer, and cytosolic extracts were harvested by centrifugation

(10,000 x*g* for 1 min). Protein concentrations were measured and 200 μg of cytosolic proteins were diluted in 50 μL lysis buffer for each assay. Subsequently, 50 μl of reaction buffer (containing 10 mM dithiothreitol), and 5 μl of 4 mM peptide substrate of caspase was added to each sample, and it was incubated for 12-24 hr. The peptide substrates used were: DEVD-pNA for caspase 3, LEHD-pNA for caspase 9 and IETD-pNA for caspase 8. The absorbances of caspase enzyme reactions were read multiple times at 405 nm in a microplate reader during the 12-24 hr incubation. The results were recorded when sample absorbance from resting *plaa* ^{high} cells reached 0.2-0.3. Cell lysates from HeLa Tet-off cells, UV-treated for 5 min at maximum intensity in a Transilluminator (Fisher Biotech, Pittsburgh, PA), were used as positive controls.

siRNA transfection

Two siRNAs against PLAA were pre-designed and prepared by Ambion, Austin, TX. siRNA ID # s17934 and # s17935 (cat#4392420) were designated as Oligo#1 (O1) and Oligo#2 (O2) in our study. A scramble (scramb) siRNA (cat#AM4611) was also purchased from Ambion as a treatment control for *plaa* knockdown. siRNA transfection was performed by electroporation following established procedures with modifications. Briefly, 6 x 10^6 cells and 40 to 160 pmoles of siRNA were mixed in 400 μL of pre-chilled Cytomix electroporation buffer solution. The latter is an intracellular ionic strength- and pH-mimicking buffer with cytoprotective capabilities , and composed of: 120 mM KCl, 0.15 mM $CaCl_2$, 10 mM K_2 HPO_4 /KH_2 PO_4, 25 mM Hepes, 2 mM EGTA, 5 mM $MgCl_2$, 2 mM ATP and 5 mM glutathione (added just before electroporation). Further, Cytomix was pH adjusted to 7.6 with KOH. Cell suspensions were added in an electroporation cuvette with a 4-mm electrode gap (Bio-Rad, Hercules, CA), chilled on ice, and subsequently pulsed once at 260 v and 950 μF with a Gene Pulser electroporator II (Bio-Rad). After electroporation, cells were incubated on ice for 2 min, resuspended in pre-warmed medium and grown under standard tissue culture

conditions. Cisplatin stimulation was performed 48 hr after electroporation. Samples were taken 72 hr after electroporation (24 hr after cisplatin stimulation) for respective assays.

Measurement of cytochrome c release

The amount of cytochrome *c* in cell cytoplasm, released from the damaged mitochondria, was determined by using Western blot analysis. Cytosolic fractions without mitochondria were isolated following established procedures and were blotted with polyclonal antibody recognizing cytochrome *c* (Cell Signaling Technology Inc., Danvers, MA). Briefly, cisplatin-stimulated cells were resuspended in ice-cold isolation buffer (5 mM HEPES, pH 7.2 containing 210 mM mannitol, 70 mM sucrose, 1 mM EGTA, and 0.5% BSA (fatty acid-free, tissue/buffer ratio, 1:10 w/v) and homogenized by using three freeze-thaw cycles. Cell homogenates were then centrifuged at 8500 ×*g* for 15 min at 4 °C to eliminate mitochondria. Cytosolic fractions were then separated on 4-20% gradient SDS-polyacrylamide gels, and Western blot analysis for cytochrome *c* was performed. We used polyclonal antibody to β-tubulin (Santa Cruz Biotechnology, Inc., Santa Cruz, CA) as loading controls for host cell lysates.

Cell viability measured by MTT assay

An MTT [3-(4,5-dimethylthiazol-2-yl)-2,5-diphenyl tetrasodium bromide] assay was performed as instructed by the manufacturer (Chemicon-Millipore, Billerica, MA) to measure cell survival. HeLa Tet-off (*plaa* ^{high} or *plaa* ^{low}) cells were transfected with siRNA, adjusted to a concentration of 4×10^5 cells/ml, and plated in 96-well plates for incubation. After 48 hr, 30 μM cisplatin was supplied to cell culture for 24-hr stimulation. After cisplatin stimulation, 50 μg MTT was added to each well, and the plates were incubated for 3 hr at 37 °C. MTT is cleaved by mitochondrial reductase in living cells, generating dark-blue formazan crystals,

which were dissolved by adding 100 µl 0.04 N HCl in isopropanol. The absorbance was measured on a microplate reader at 570 nm.

KinetWorks proteomic analysis of apoptosis responses

Apoptosis responses from cisplatin-stimulated-*plaa* ^{high} and *plaa* ^{low} cells were analyzed by KinetWorks proteomic analysis (Kinexus Bioinformatics Corp., Vancouver, British Columbia, Canada). The KinetWorks analysis performed by the manufacturer (Kinexus), involved resolution of a single whole-cell lysate sample (500 µg) by SDS-polyacrylamide gel electrophoresis and subsequent immunoblotting with one primary antibody per channel in a multi-lane Immunetics Multiblotter. The antibody mixtures were carefully selected to avoid overlapping cross-reactivity with target proteins. Normalized trace quantity units (cpm) were arbitrary and based on the intensity of fluorescence detection for target immunoreactive proteins recorded with a Fluor-S MultiImager and quantified by using Quantity One Software (Bio-Rad). Kinexus performed all of the normalization and statistical analysis on the data.

Statistical analysis of the data

The data were analyzed using Student's t test, with a p value of < 0.05 considered significant.

Results

PLAA was induced by cisplatin and synergized with cisplatin to promote apoptosis

A HeLa Tet-off cell line that consistently overexpressed the native *plaa* gene was generated and characterized as reported in our previous publication and designated as *plaa* ^{high} in our current study. Another HeLa Tet-off cell line in which the *plaa* gene was inserted in the opposite orientation and exhibited the lowest level of *plaa* gene expression (representing expression of the native *plaa* gene in the HeLa cells) was referred to as *plaa* ^{low}, and used as a negative control in the following experiments. The growth and survival properties of *plaa* ^{high}

and *plaa* ^{low} cells were comparable to that of the normal HeLa cells. The expression level of *plaa* in *plaa* ^{high} cells is physiologically relevant, as a similar level of PLAA is observed in macrophages.

We first confirmed the cisplatin-induced expression of *plaa* in *plaa* ^{high} and *plaa* ^{low} cells **(Fig. 3.1A)**. Western blot analysis confirmed a significant increase in the expression of the *plaa* gene when unstimulated *plaa* ^{high} and *plaa* ^{low} cells were compared **(Fig. 3.1A)**. Stimulation with 30 μM of cisplatin for 12 hr differentially induced *plaa* gene expression, with *plaa* ^{high} cells producing 4- to 5-fold more PLAA than *plaa* ^{low} cells **(Fig. 3.1A)**. We used antibodies to β-tubulin as an internal control for equal protein loading.

We then compared the apoptotic response induced by cisplatin (30 μM for 12 to 24 hr) in *plaa* ^{high} and *plaa* ^{low} cells. DNA inter-chromosomal fragmentation, which generates oligonucleosomes, is an early hallmark of apoptosis. We performed an ELISA to measure oligonucleosome concentration, which correlates with the degree of DNA fragmentation . Although unstimulated *plaa* ^{high} and *plaa* ^{low} cells contained comparable amounts of DNA fragmentation **(Fig. 3.1B)**, stimulation with cisplatin differentially increased DNA fragmentation in *plaa* ^{high} and *plaa* ^{low} cells. The *plaa* ^{high} cells consistently contained 1.6-fold more oligonucleosomes than did *plaa* ^{low} cells at both 12 and 24 hr after cisplatin treatment **(Fig. 3.1B)**.

Elevated levels of apoptosis in cisplatin-stimulated *plaa* ^{high} cells suggested PLAA induction promoted cisplatin-induced apoptosis. To confirm this finding, we compared caspase activities in cisplatin-stimulated *plaa* ^{high} and *plaa* ^{low} cells. Caspase 3 is the executor caspase during apoptosis, whereas caspase 8 and caspase 9 are involved in Fas/FasL-mediated- and mitochondrial-mediated apoptosis, respectively . As shown in **Fig. 3.1C**, cisplatin stimulation differentially increased caspase 3 enzyme activity in *plaa* ^{high} and *plaa* ^{low} cells. The *plaa* ^{high}

cells contained 1.5 fold and 1.8 fold more caspase 3 activity than did the *plaa* ^{low} cells at 12 and 24 hr, respectively, after cisplatin treatment. Consistent with these data, in response to 12 and 24 hr cisplatin treatment, stimulated *plaa* ^{high} cells also contained significantly higher caspase 9 levels **(Fig. 3.1D)** and caspase 8 **(Fig. 3.1E)** activities than did *plaa* ^{low} cells.

To confirm PLAA's specific contribution to cisplatin-induced apoptosis, we performed siRNA knockdown of the *plaa* gene and determined the subsequent effect on the apoptosis response from cisplatin-stimulated *plaa* ^{high} and *plaa* ^{low} cells. Electroporation of 6 x 10^6 *plaa* ^{high} cells with 160 pmoles of siRNA against *plaa* 48 hr before cisplatin treatment effectively knocked down cisplatin-induced *plaa* gene expression to a level lower than that of the resting *plaa* ^{low} cells, as determined by Western blot analysis **(Fig. 3.2A, lanes 1 and 5)**. The knockdown of cisplatin-induced *plaa* gene expression by siRNA was dose-dependent **(lanes 5-7 versus lane 9)**. Scrambled siRNA to *plaa* (Scramb), which was used as a control, had no effect on *plaa* gene expression **(Fig. 3.2A, lanes 8 and 9)**. Importantly, the *plaa* ^{low} cells had a more reduced level of PLAA than did *plaa* ^{high} cells **(lanes 1 and 3)**. Moreover, 24-hr cisplatin treatment increased PLAA levels in *plaa* ^{low} cells to a level similar to that of the

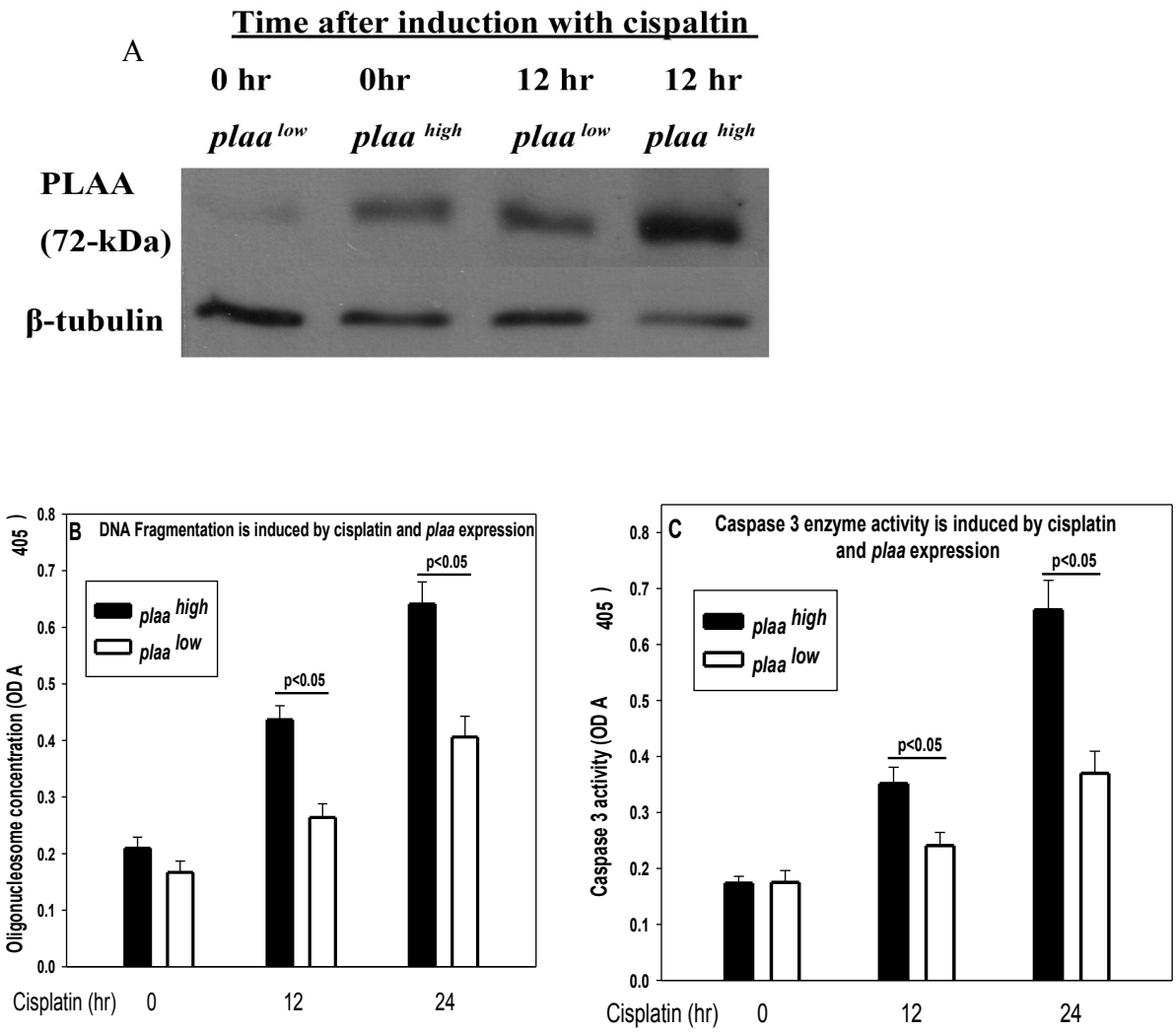

Fig. 3.1. PLAA induction by cisplatin promoted apoptosis in HeLa Tet-off cells. *plaa* ^{high} and *plaa* ^{low} cells were stimulated with 30 uM cisplatin for 12 to 24 hr**. (A)** Western blot analysis revealed that PLAA expression was induced by cisplatin in cells. Equal amounts of whole cell lysate (80 μg) were subjected to 4-20% SDS-PAGE, and the membranes probed with monoclonal antibody against PLAA. An antibody against β-tubulin was used to normalize protein loading. The blots presented are representative of three independent repetitions. **(B)** DNA fragmentation was induced by PLAA induction and cisplatin. Cisplatin-stimulated *plaa* ^{high} and *plaa* ^{low} cells were harvested, and equal amounts of whole cell lysates (100 μg) were used in a sandwich ELISA to measure the amount of oligonucleosomes, which indicates the degree of DNA fragmentation. The enzyme activities of caspase 3 **(C)**, caspase 9 **(D)** and caspase 8 **(E)** were induced by PLAA induction and cisplatin. Cisplatin-stimulated *plaa* ^{high} and *plaa* ^{low} cells were harvested, and equal amounts of whole cell lysates (200 μg) were used to measure the enzymatic activity of caspases. The plotted values denote the mean ± standard deviation (S.D.) of three independent repetitions.

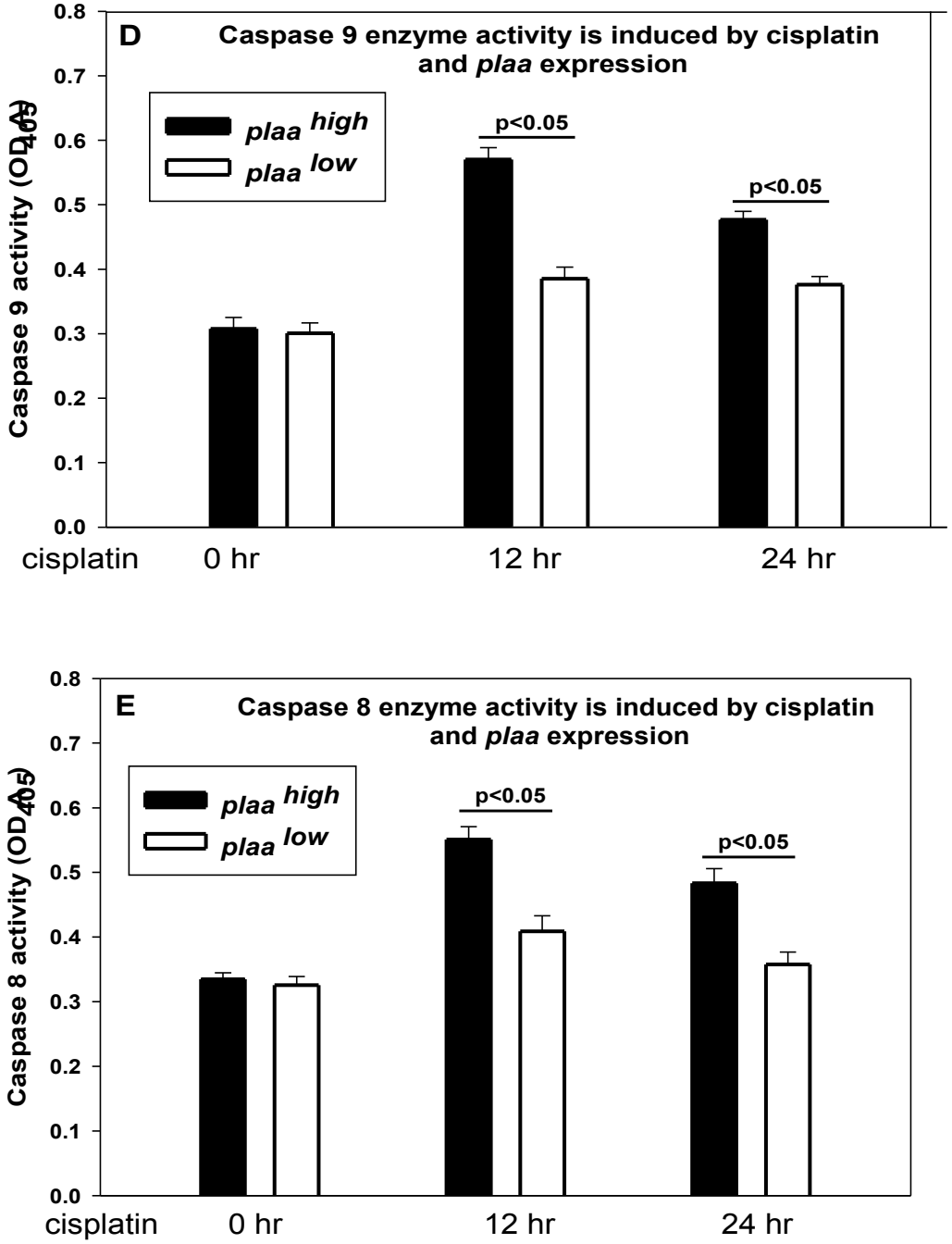

Fig. 3.1. PLAA induction by cisplatin promoted apoptosis in HeLa Tet-off cells. (*continued*)The enzyme activities of caspase 9 **(D)** and caspase 8 **(E)** were induced by PLAA induction and cisplatin. Cisplatin-stimulated *plaa* ^{high} and *plaa* ^{low} cells were harvested, and equal amounts of whole cell lysates (200 μg) were used to measure the enzymatic activity of caspases. The plotted values denote the mean ± standard deviation (S.D.) of three independent repetitions.

plaa ^{high} cells without cisplatin **(lanes 3 and 4)**. We used antibodies to β-tubulin as an internal control for equal protein loading.

Two different siRNAs (O1 and O2) to the *plaa* gene were used, and they exhibited equal efficiencies (only siRNA O1 was shown in **Fig. 3.2A**). In the following experiments, 80 pmoles of siRNA O1 and 80 pmoles of O2 were combined to obtain 160 pmoles of siRNA against *plaa* (siRNA-PLAA). As shown in **Fig. 3.2B**, pretreatment of cells for 48 hr with 160 pmoles of siRNA-PLAA before cisplatin (30 μM) stimulation statistically significantly reduced DNA inter-chromosomal fragmentation in both *plaa* ^{high} and *plaa* ^{low} cells, to a level lower than that of cisplatin-treated *plaa* ^{low} cells without the *plaa* knockdown at the 24-hr time point. These results suggested to us that PLAA was specifically required for optimal induction of apoptosis in cisplatin-stimulated HeLa cells.

PLAA induction by cisplatin promoted mitochondrial damage through PLA_2 activation and AA accumulation

We have previously shown that induction of native PLAA by TNF-α can activate PLA_2 enzymes in HeLa cells and macrophages . Since cisplatin can induce the expression of PLAA together with $cPLA_2$ and $sPLA_2$ in ear cells , and PLA_2 enzymes are involved in apoptosis **,** we determined whether PLA_2 enzyme activities were induced by PLAA and cisplatin. We compared PLA_2 activation in response to cisplatin in *plaa* ^{high} and *plaa* ^{low} cells **(Fig. 3.3A)**. Although unstimulated *plaa* ^{high} and *plaa* ^{low} cells contained comparable amounts of PLA_2 activities in zero-hr samples, stimulation with cisplatin differentially increased PLA_2 enzyme activity in *plaa* ^{high} and *plaa* ^{low} cells. The *plaa* ^{high} cells contained 1.8- and 1.9-fold more PLA_2 activity than did *plaa* ^{low} cells at the 12 and 24 hr time points after cisplatin treatment, respectively **(Fig. 3.3A)**.

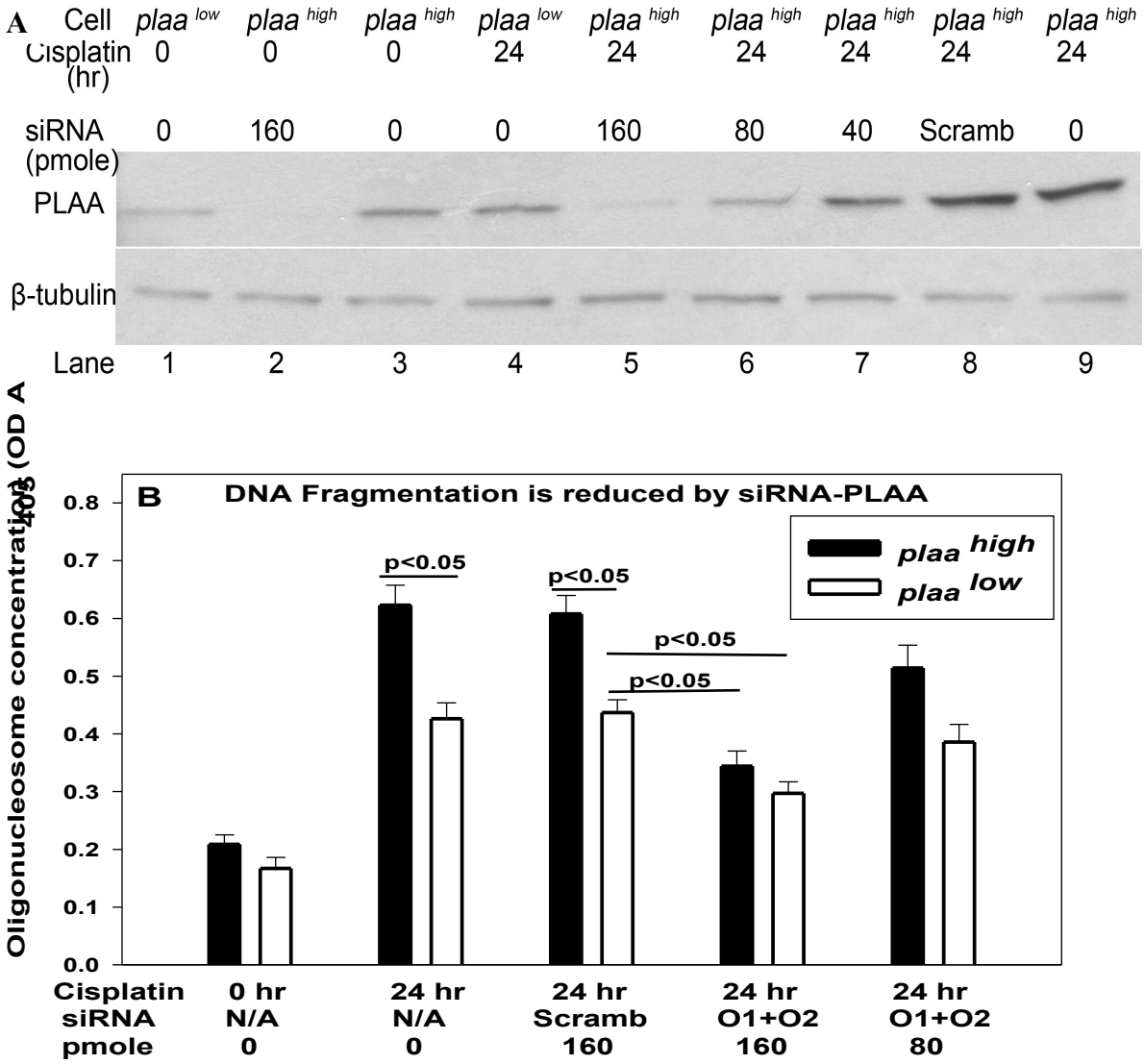

Fig. 3.2. Specific contribution of PLAA to cisplatin-induced apoptosisin HeLa Tet-off cells. *plaa* ^{high} and *plaa* ^{low} cells were left untreated or were treated with 30 μM cisplatin for 24 hr in the presence or absence of siRNA against *plaa.* Next, 40 to 160 pmole siRNA against *plaa* were electroporated into 6 x 10^6 cells 48 hr before cisplatin stimulation. Following the indicated treatment, cell lysates were prepared. **(A)** Western blot analysis revealed that PLAA induction by cisplatin was knocked down in both *plaa* ^{high} and *plaa* ^{low} cells. The blots presented are representative of three independent repetitions. **(B)** siRNA against *plaa* reduced DNA fragmentation induced by cisplatin. An aliquot (160 p moles of scrambled siRNA oligo [Scramb]) was used as a negative treatment control. Procedures were conducted in a manner similar to those used above (see legend, Fig. 1). The plotted values denote the mean ± standard deviation (S.D.) of three independent repetitions. Both of the siRNAs against *plaa*, O1 and O2, achieved similar efficacy of the *plaa* knockdown. Only Western blot using siRNA O1 to *plaa* was shown.

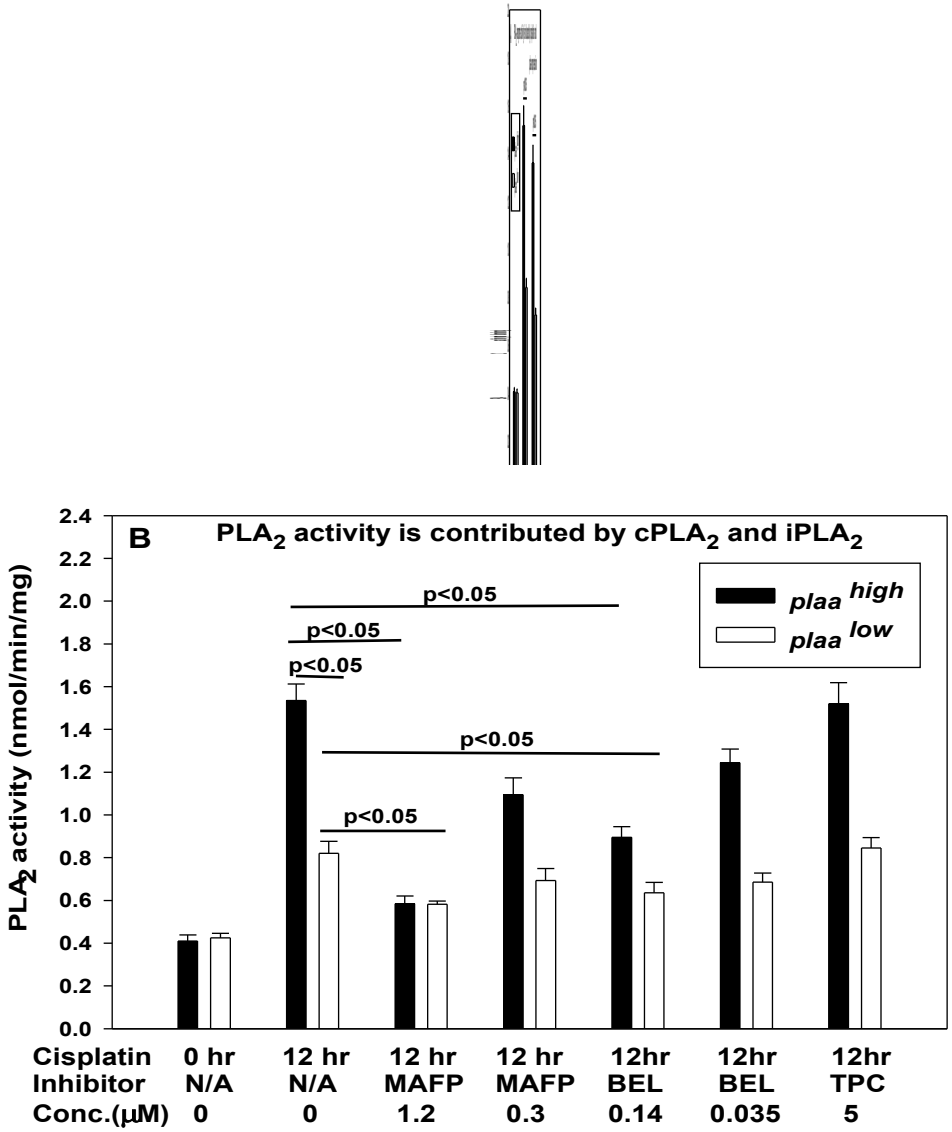

Fig. 3.3. **PLAA induction by cisplatin promoted PLA_2 activation and AA accumulation in HeLa Tet-off cells.** *plaa* ^{high} and *plaa* ^{low} cells were stimulated with cisplatin for 12 to 24 hr in the presence or absence of siRNA against *plaa.* **(A)** PLA_2 enzyme activities were induced by PLAA expression and cisplatin. Membrane fractions from stimulated cells were isolated and used as a source of PLA_2 enzyme in a PLA_2 activity assay. PLA_2 activity was expressed as μmol/ min/mg. **(B)** PLA_2 activation by cisplatin in *plaa* ^{high} and *plaa* ^{low} cells was contributed by $cPLA_2$ and $iPLA_2$. Similar procedures described in (A) were performed, except that isolated cell membranes were incubated with PLA_2 inhibitors for 30 min before we performed PLA_2 activity assay. DMSO was used as a vehicle control for the treatment. Included inhibitors were: $cPLA_2$ inhibitor MAFP (1.2 μM), $iPLA_2$ inhibitor BEL (0.14 μM), and $sPLA_2$ inhibitor TPC (5 μM). The inhibitors MAFP and BEL were titrated to confirm their specificities.

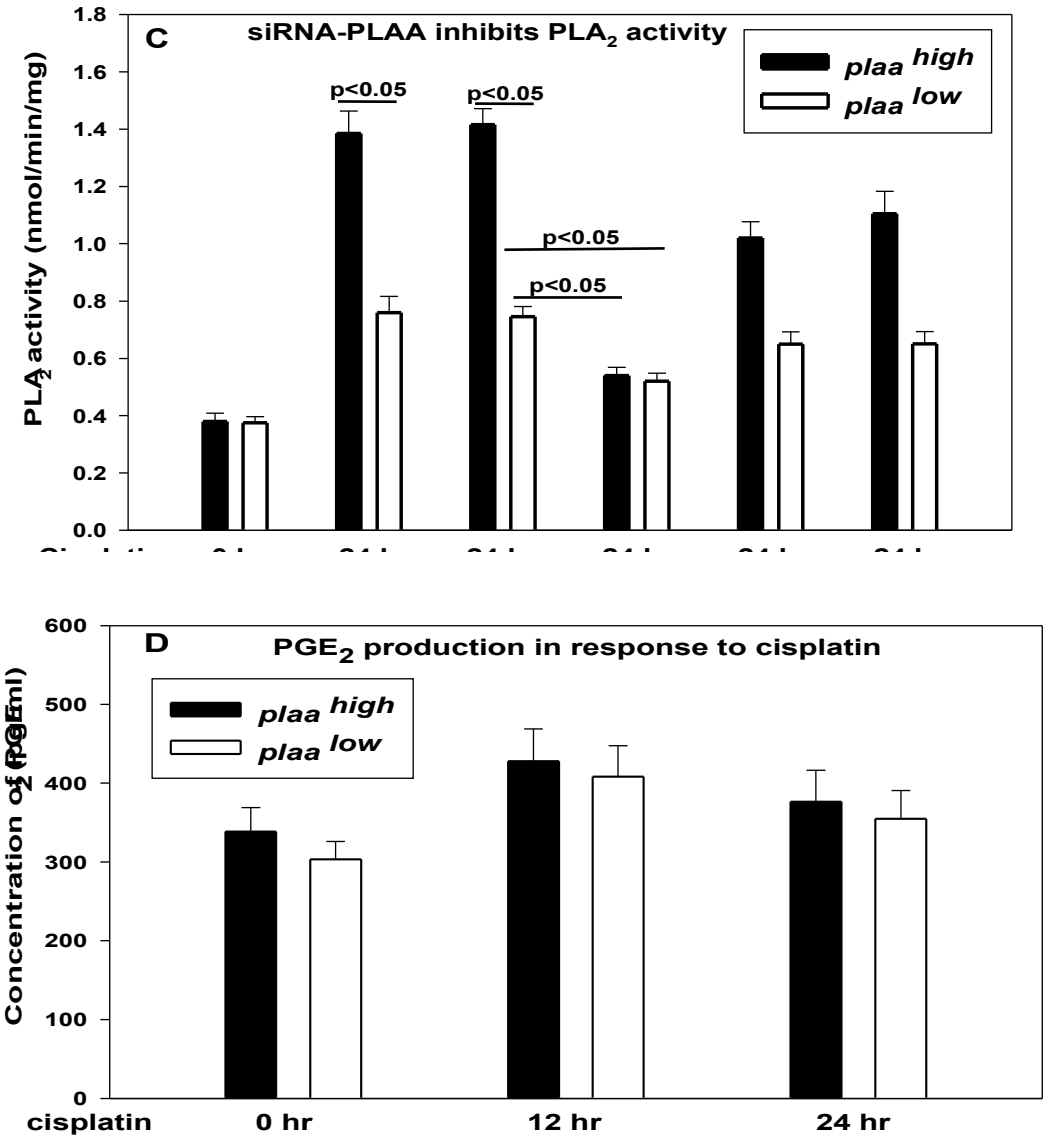

Fig. 3.3. **PLAA induction by cisplatin promoted PLA_2 activation and AA accumulation in HeLa Tet-off cells.** *(continued)* **(C)** siRNA against *plaa* inhibited PLA_2 activation by cisplatin in *plaa* ^{high} and *plaa* ^{low} cells. An aliquot (80 pmoles of siRNA (against PLAA) O1 and 80 pmoles of siRNA O2 were combined, designated as siRNA-PLAA, and then used in the following experiments. Cells were electroporated with or without siRNA-PLAA 48 hr before cisplatin stimulation. After 24-hr cisplatin treatment, PLA_2 activity assay was performed as described in (A). **(D)** *plaa* ^{high} and *plaa* ^{low} cells produced comparable amounts of PGE_2 (an AA metabolite) in response to cisplatin. PGE_2 levels were measured in cell culture supernatants by using an ELISA. The PGE_2 values were normalized to the amount of protein in the cell lysates. Values were plotted as the mean ± standard deviation following three independent experiments.

We next determined which PLA_2 subtypes were responsible for enzyme activities induced by PLAA and cisplatin in *plaa* ^{high} and *plaa* ^{low} cells **(Fig. 3.3B)**. The $cPLA_2$ inhibitor MAFP (1.2 μM) and the $iPLA_2$ inhibitor BEL (0.14 μM) were able to significantly reduce the PLA_2 activities associated with both *plaa* ^{high} and *plaa* ^{low} cells at the 12-hr time point. The inhibition of PLA_2 enzyme activities by MAFP and BEL was dose-dependent. However, the $sPLA_2$ inhibitor thioetheramide-PC (TPC) (5 μM) was not found to alter PLA_2 enzyme activities associated with cisplatin-stimulated *plaa* ^{high} and *plaa* ^{low} cells, compared to PLA_2 activities found in DMSO-treated and cisplatin-stimulated *plaa* ^{high} and *plaa* ^{low} cells **(Fig. 3.3B)**.

These data suggested that $cPLA_2$ and $iPLA_2$, and not the $sPLA_2$, were induced by PLAA and cisplatin. These findings were consistent with those showing that $iPLA_2$ is known to mediate cisplatin-induced renal cell apoptosis , and, moreover, our previous study indicated that PLAA modulated $cPLA_2$ levels in macrophages [18].

To confirm that cisplatin-induced PLA_2 activation is specifically mediated by PLAA, we determined the effect of siRNA-PLAA on PLA_2 activation in stimulated *plaa* ^{high} and *plaa* ^{low} cells. As shown in **Fig. 3.3C**, pretreatment of cells (for 48 hr) with 160 pmoles of siRNA-PLAA before cisplatin stimulation significantly reduced PLA_2 activation in both *plaa* ^{high} and *plaa* ^{low} cells to a level lower than that of cisplatin-treated *plaa* ^{low} cells without the *plaa* knockdown. The reduction of PLA_2 activation by siRNA-PLAA was dose-dependent **(Fig. 3.3C)**. Scrambled siRNA to the *plaa* gene (Scramb) had no effect on PLA_2 activity when compared to *plaa* ^{high} and *plaa* ^{low} cells that were treated with cisplatin but were not given the siRNA-PLAA.

To trace the metabolism of AA produced by PLA_2 activation in cisplatin-stimulated *plaa* ^{high} and *plaa* ^{low} cells, we examine the level of PGE_2, which is an AA metabolite . Cisplatin treatment slightly increased PGE_2 production from stimulated cells, with *plaa* ^{high} and *plaa* ^{low}

cells producing similar amounts of PGE_2 **(Fig. 3.3D)**. These results indicated to us that a higher amount of AA is likely to accumulate in *plaa* ^{high} cells than in *plaa* ^{low} cells, since *plaa* ^{high} cells contained higher levels of PLA_2 activity, while metabolizing AA at a rate similar to that of the *plaa* ^{low} cells.

AA accumulation in cells can cause mitochondrial damage and subsequent caspase 9-mediated apoptosis . Since we observed elevated caspase 9 and PLA_2 activation in cisplatin-stimulated *plaa* ^{high} cells, we determined the level of mitochondrial damage by measuring cytochrome *c* release from the mitochondria of cisplatin-stimulated cells. Cytochrome *c* was chosen because its release from the damaged mitochondria to the cytoplasm induces the formation of apoptosomes and subsequently activates caspase-9 . After 24 hr treatment with cisplatin, *plaa* ^{high} cells revealed significantly more cytochrome *c* leakage than did *plaa* ^{low} cells **(Fig. 3.4A, lanes 3 and 4)** or the normal HeLa cells **(Fig. 3.4B, lanes 1 and 6)** treated in the same fashion.

Pretreatment of host cells using 160 pmoles of siRNA-PLAA significantly reduced cytochrome *c* release induced by cisplatin from *plaa* ^{high} cells **(Fig. 3.4A, lanes 4-6)** and from normal HeLa cells **(Fig. 3.4B, lanes 1-3)**. Importantly, knockdown of the *plaa* gene in cisplatin-treated *plaa* ^{high} cells reduced cytochrome *c* release to a level lower than that of cisplatin-treated *plaa* ^{low} cells **(Fig. 3.4A, lanes 3 and 6)** and cisplatin-treated normal HeLa cells **(Fig. 3.4B, lanes 1 and 8)** without the *plaa* knockdown. The effect of siRNA-PLAA on cytochrome c release was dose-dependent **(Fig. 3.4A, lane 4 versus lanes 6-8).** Scrambled siRNA had no effect on cisplatin-induced cytochrome *c* release in *plaa* ^{high} cells when compared to its appropriate control **(Fig. 3.4A, lanes 4 and 5 and Fig. 4B, lanes 6 and 7)** and in normal HeLa cells (**Fig. 3.4B, lanes 1 and 2**). Arachidonic acid (AA), which can be reduced by knocking down PLAA is a known inducer of mitochondrial damage . We noted that cytochrome *c* levels were restored in the *plaa*-knockdown cells when we supplied exogenous

AA to the culture medium of *plaa* ^{high} cells **(Fig. 3.4B, lanes 8 and 9)** or normal HeLa cells **(Fig. 3.4B, lanes 3 and 4)**. Scrambled siRNA did not reduce cisplatin-induced cytochrome *c* release in *plaa* ^{high} cells **(Fig. 3.4B, lanes 6 and 7)** or normal HeLa cells **(Fig. 3.4B, lanes 1 and 2).** Importantly, the *plaa* ^{low} cells and normal HeLa cells had similar levels of cytochrome *c* release in the cytoplasm from host cell mitochondria after cisplatin treatment **(Fig. 3.4B, lanes 1 and 5).** Taken together, these results suggested to us that PLAA induction promoted mitochondrial-mediated apoptosis through PLA_2 activation and AA accumulation in cisplatin-stimulated HeLa cells.

To determine whether siRNA-PLAA could restore mitochondrial integrity and cell viability following cisplatin stimulation, we performed an MTT assay to measure the viability of cisplatin-treated *plaa* ^{high} and *plaa* ^{low} cells. The MTT assay is a colorimetric method that allows one to measure the mitochondrial reductase activity located inside intact mitochondria from living cells. A higher MTT reduction indicates more intact mitochondria and more viable cells . We noted that 24-hr cisplatin stimulation differentially reduced cell viability/mitochondrial integrity in *plaa* ^{high} and *plaa* ^{low} cells, while *plaa* ^{high} cells had significantly lower cell viability/mitochondrial integrity than did *plaa* ^{low} cells **(Fig. 3.4C)**. These results were consistent with our previous data **(Fig. 3.4A)** in that *plaa* ^{high} cells exhibited more cytochrome *c* release generated by mitochondrial damage. Pretreatment of *plaa* ^{high} and *plaa* ^{low} cells with 160 pmoles of siRNA-PLAA restored cell viability/mitochondrial integrity in cisplatin-stimulated cells. Importantly, siRNA-PLAA promoted MTT reduction/cell viability to a level higher than that of cisplatin-treated *plaa* ^{low} cells without the *plaa* gene knockdown **(Fig. 3.4C)**. The effect of siRNA-PLAA on cytochrome *c* release was dose-dependent, and the scrambled siRNA had no effect. These results further confirmed the role of PLAA in cisplatin-induced cell death and suggested to us that siRNA-PLAA could be used to reduce the toxic side effects of cisplatin.

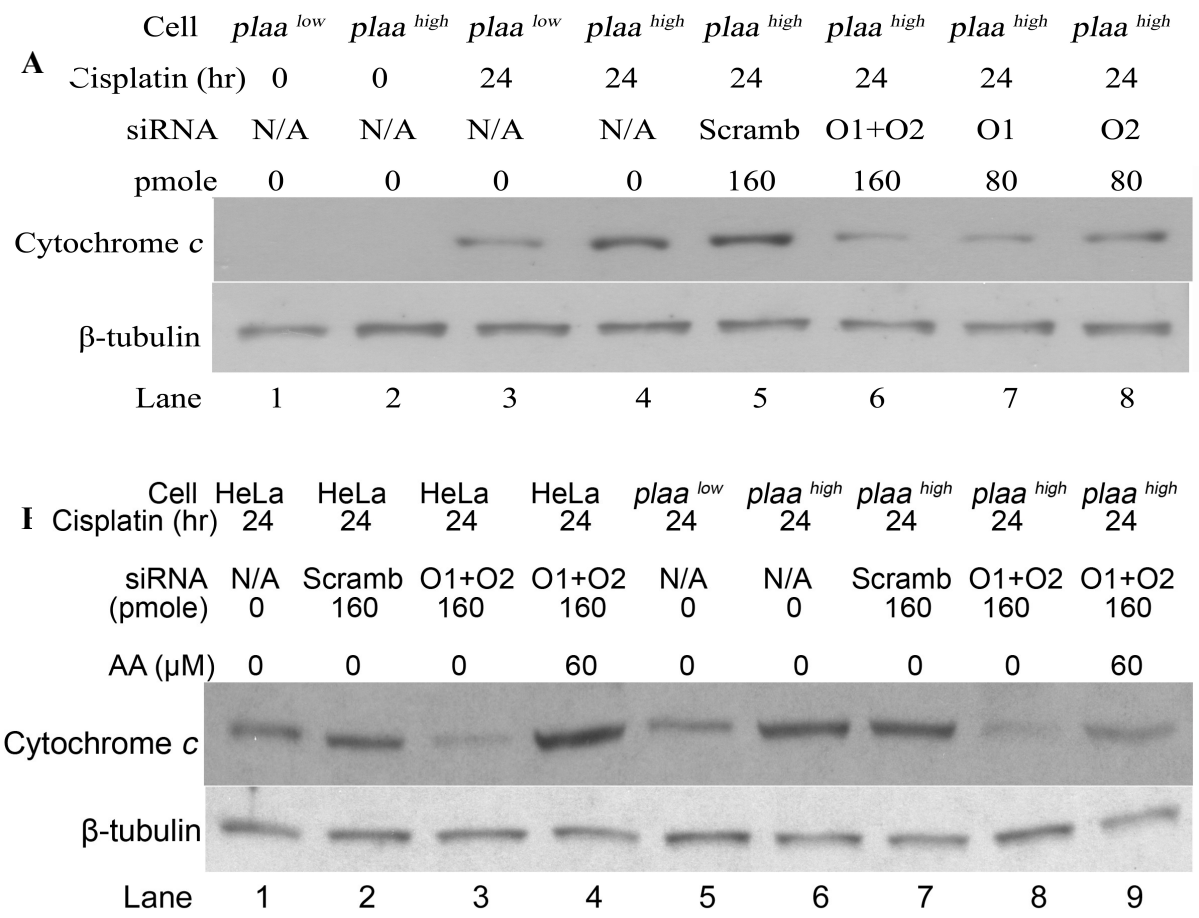

Fig. 3.4. PLAA induction by cisplatin caused mitochondrial damage through AA accumulation. *plaa* ^{high} cells, *plaa* ^{low} cells and normal HeLa cells were stimulaed with cisplatin for 24 hr in the presence or absence of siRNA against *plaa.* **(A)** Western blot analysis revealed that cytochrome *c* release/mitochondrial damage was induced by cisplatin and that siRNA-PLAA (80 pmole of siRNA O1 combined with 80 pmole of siRNA O2) reduced cytochrome *c* release from *plaa* ^{high} cells. Cells were electroporated with or without siRNA-PLAA at 48 hr before cisplatin stimulation. After 24 hr of cisplatin treatment, a cytosolic fraction of host cells without mitochondria was prepared and analyzed in a Western blot by using polyclonal antibody to cytochrome *c*. An antibody against β-tubulin was used to normalize protein loading. **(B)** Western blot analysis revealed that siRNA-PLAA reduced cytochrome *c* release from normal HeLa cells and that exogenous AA restored cytochrome *c* release in both HeLa and *plaa* ^{high} cells treated with siRNA-PLAA. An aliquot (60 μM) of exogenous AA was added together with cisplatin to the supernatant. Other procedures were conducted similarly as described in (A). The blots presented are representative of three repeated independent experiments.

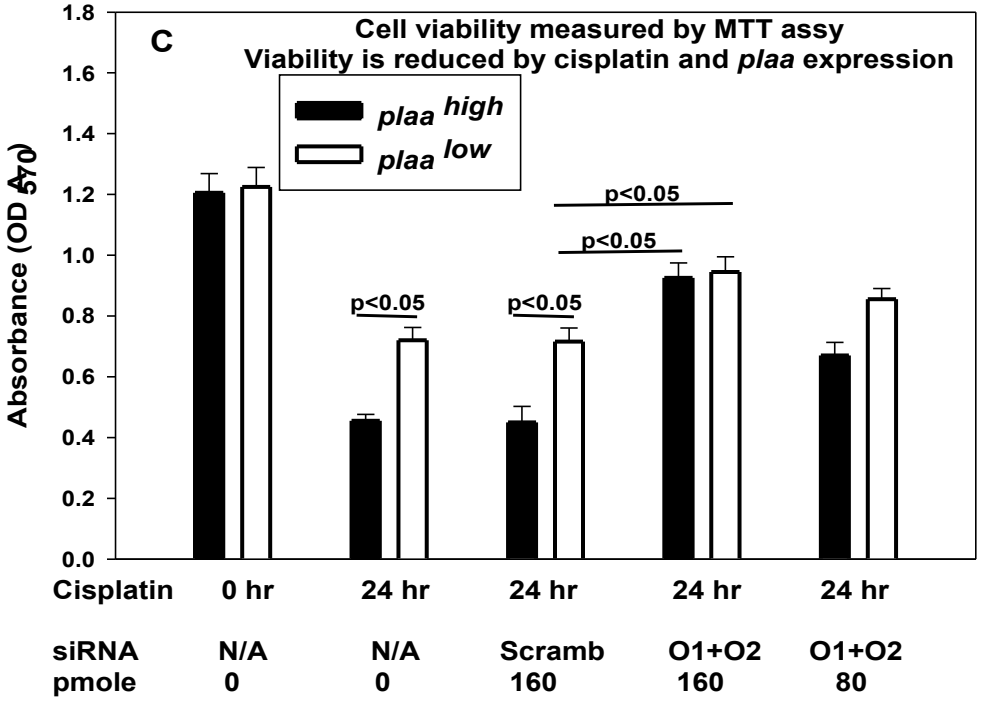

Fig. 3.4. PLAA induction by cisplatin caused mitochondrial damage through AA accumulation. (*continued*) **(C)** siRNA-PLAA restored cell viability in cisplatin-stimulated cells. Equal numbers of *plaa* ^{high} and *plaa* ^{low} cells were transfected with or without siRNA-PLAA 48 hr before cisplatin treatment. After 24 hr of cisplatin stimulation, MTT was added to cells as a color-producing substrate to measure mitochondrial reductase activity, which correlates with the number of living cells. Values were plotted as the mean ± standard deviation of three independent repetitions.

PLAA induction by cisplatin reduced chemo-resistance by downregulating expression of the cytoprotective clusterin

Clusterin is a cytoprotective chaperone protein that protects host cells against oxidative stress and chemotherapeutic agents . We have previously shown that resting *plaa* ^{high} cells produced significantly less clusterin than did resting *plaa* ^{low} cells, and reduction of clusterin contributed to a pronounced inflammatory response to TNF-α . Since clusterin is known to promote tumor chemoresistance , we examined the effect of cisplatin and *plaa* induction on clusterin expression. We confirmed that resting *plaa* ^{low} cells produced around 1.9-fold more clusterin in the supernatant and cytoplasm than did *plaa* ^{high} cells **(Fig. 3.5A)**. Cisplatin stimulation promoted clusterin production from treated *plaa* ^{high} and *plaa* ^{low} cells to more than 2-fold of their respective, un-stimulated levels. Consistently, stimulated *plaa* ^{low} cells produced around 1.7 fold more clusterin in the supernatant and cytoplasm than did *plaa* ^{high} cells **(Fig. 3.5A)**.

Interestingly, antisense oligonucleotides against clusterin are being used in phase I clinical trials as an adjuvant to promote apoptosis/chemosensitivity in prostate and breast tumors . We next determined whether PLAA induction mediated cisplatin-induced apoptosis specifically by downregulating clusterin. As shown in **Fig. 3.5B**, siRNA-PLAA promoted clusterin production in the supernatant from both resting and cisplatin-stimulated *plaa* ^{high} and *plaa* ^{low} cells. In both cisplatin-stimulated and resting cells, PLAA knockdown in *plaa* ^{high} and *plaa* ^{low} cells resulted in comparable clusterin production; both *plaa* ^{high} and *plaa* ^{low} cells treated with siRNA-PLAA produced more clusterin than did *plaa* ^{low} cells without PLAA knockdown **(Fig. 3.5B)**. siRNA-PLAA upregulated clusterin production in cisplatin-treated *plaa* ^{high} and *plaa* ^{low} cells to a comparable level. The effect of siRNA-PLAA on clusterin production was dose-dependent, and scrambled siRNA had no effect. These results suggested that PLAA induction specifically downregulated clustrin production, which may play a role in chemoresistance.

To confirm clustrin's chemoresistance-promoting role , we determined whether exogenous clusterin could protect cells against cisplatin-induced apoptosis. Indeed, 0.8 to 1.6 μg/ml of exogenous clusterin significantly reduced DNA fragmentation in cisplatin-stimulated *plaa* ^{high} and *plaa* ^{low} cells **(Fig. 3.5C)**. The protection conferred by exogenous clusterin against cisplatin was more pronounced in stimulated *plaa* ^{high} cells, which produced less clusterin. The effect of clusterin was dose-dependent, and exogenous bovine serum albumin (BSA) had no effect on DNA fragmentation **(Fig. 3.5C)**. Exogenous supplied clusterin is known to reduce TNF-α cytotoxicity in prostate cancer cells , and this is consistent with our data.

To confirm that PLAA induction promoted cisplatin-induced apoptosis by downregulating clusterin, we next examined whether neutralizing clusterin could promote apoptosis in cells treated with siRNA-PLAA. Indeed, cisplatin. siRNA-PLAA reduced DNA fragmentation, whereas 2.4 μg/ml of neutralizing antibody against clusterin (αCLU) significantly promoted DNA fragmentation in *plaa* ^{high} and *plaa* ^{low} cells treated with siRNA-PLAA and cisplatin **(Fig. 3.5D)**. The apoptosis-promoting effect of αCLU was dose-dependent and exogenous neutralizing antibody against β-tubulin (αTUB) had no effect **(Fig. 3.5D)**. Consistent with our results, neutralizing antibody against clusterin has been reported to enhance chemosensitivity/apoptosis in osteosarcoma cells . These data indicated that PLAA induction by cisplatin enhanced apoptosis by dowregulating clusterin-mediated chemoresistance.

PLAA induction by cisplatin upregulated IL-32 expression

IL-32 is a novel cytokine implicated in inflammation , and cell death . IL-32 is known to associate specifically with apoptotic T cells and ectopic expression of IL-32 in HeLa cells causes apoptosis . We have shown previously that PLAA induction by TNF-α upregulated IL-32 expression in HeLa cells . In our current study, we examined whether

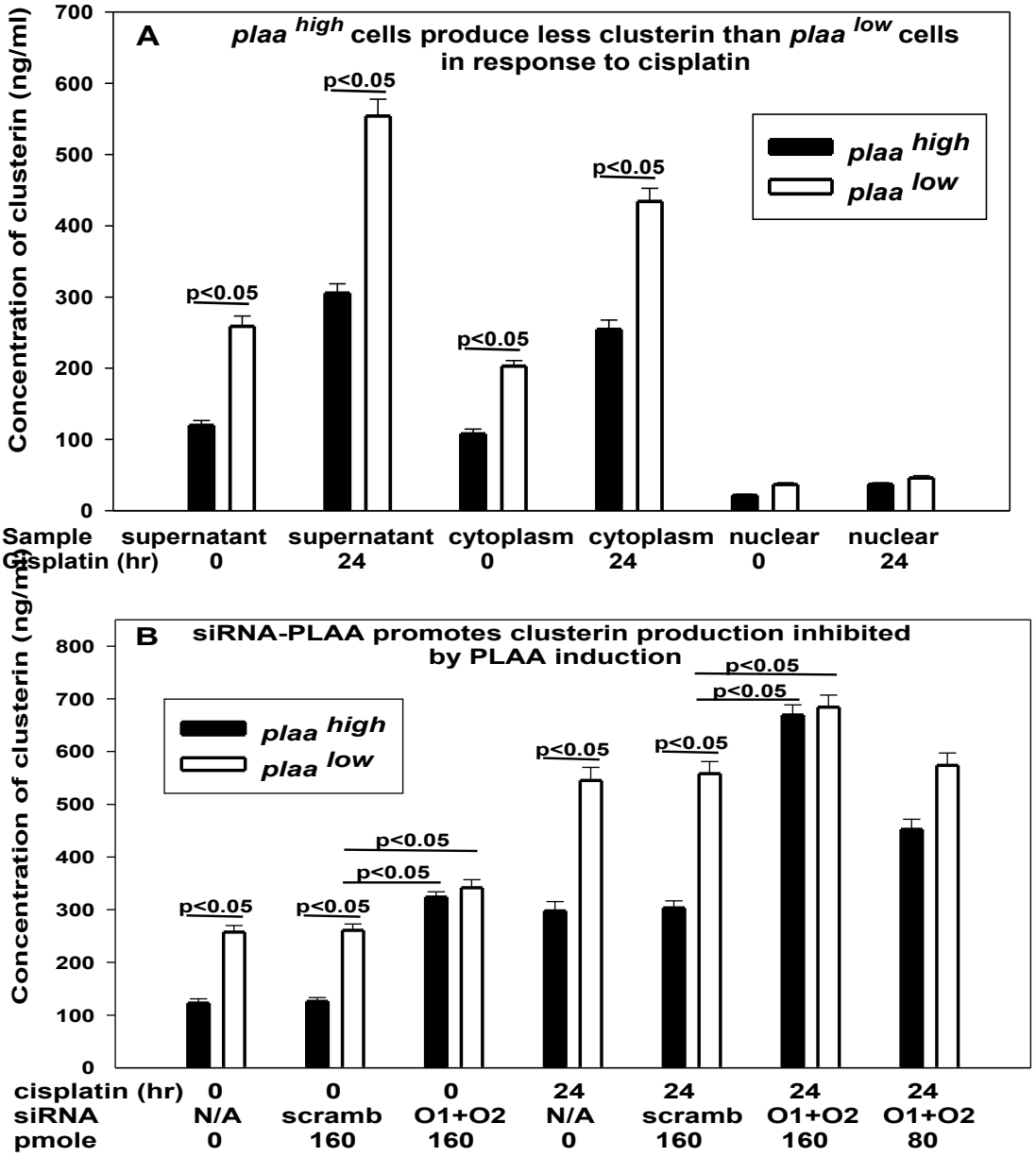

Fig. 3.5. PLAA induction by cisplatin reduced chemoresistance by downregulating expression of the cytoprotective clusterin in HeLa Tet-off cells. (A) *plaa* ^{high} cells produced less clusterin than did *plaa* ^{low} cells in response to cisplatin. After 24 hr cisplatin treatment, supernatant, cytoplasm and nuclear fractions of host cells were prepared, and concentrations of cluserin in each fraction were analyzed by sandwich ELISA. Each ELISA sample was prepared to contain an equal amount of total protein. **(B)** siRNA-PLAA (80 pmole of siRNA O1 combined with 80 pmole of siRNA O2) restored clusterin production inhibited by PLAA induction. Both *plaa* ^{high} and *plaa* ^{low} cells were transfected with or without siRNA-PLAA for 48 hr before cisplatin stimulation. After 24 hr of cisplatin treatment, concentrations of clusterin in the cell culture supernatant were analyzed as described in (A).

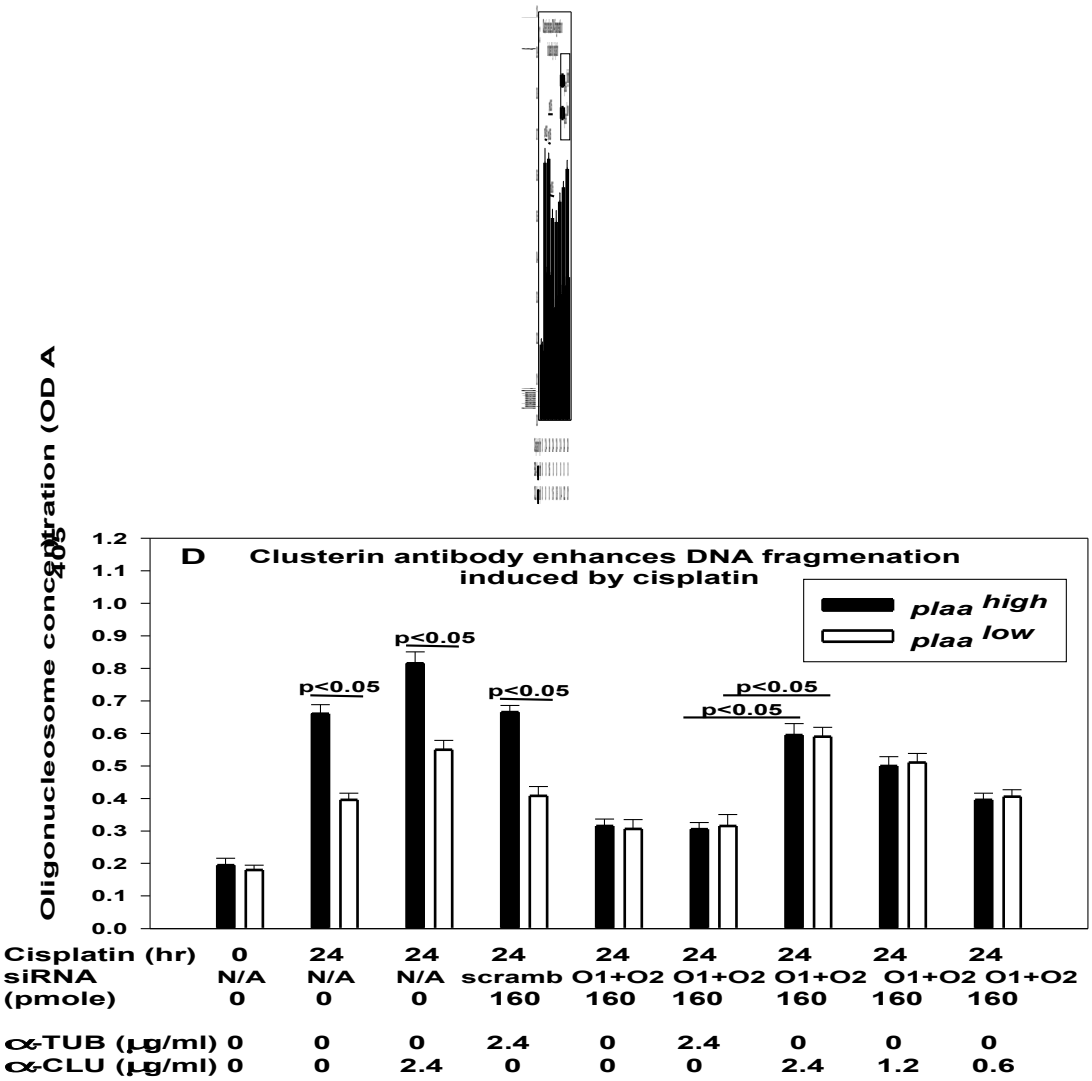

Fig. 3.5. PLAA induction by cisplatin reduced chemoresistance by downregulating expression of the cytoprotective clusterin in HeLa Tet-off cells. *(continued)* **(C)** Exogenous clusterin reduced DNA fragmentation in cisplatin-stimulated *plaa* ^{high} and *plaa* ^{low} cells. Exogenous clusterin (CLU) was supplied to cell supernatants to indicated concentrations at 4 hr before cisplatin stimulation and was present throughout the 24 hours' stimulation. BSA was used as a negative treatment control. After cisplatin treatment, DNA fragmentation in cells was measured as described in Fig. 1B. **(D)** Exogenous clusterin antibody promoted DNA fragmentation in *plaa* ^{high} and *plaa* ^{low} cells treated with cisplatin and siRNA-PLAA. *plaa* ^{low} cells were transfected with or without siRNA-PLAA (80 pmole of siRNA O1 combined with 80 pmole of siRNA O2) for 48 hr before cisplatin stimulation. At 44 hr after siRNA transfection (4 hr before cisplatin stimulation), exogenous clusterin antibody (α-CLU) was supplied to the cell supernatants to indicated concentrations before cisplatin simulation and was present throughout the 24-hour cisplatin stimulation. Antibody against β-tubulin (α-TUB) was used as a negative treatment control. After cisplatin treatment, DNA fragmentation in cells was measured as described in Fig. 1B. Values were plotted as the mean ± standard deviation of three independent repetitions.

PLAA induction by cisplatin specifically upregulated IL-32 expression **(Fig. 3.6)**. Resting *plaa* ^{high} cells contained significantly more IL-32 in the cytoplasm than did *plaa* ^{low} cells. Cisplatin differentially upregulated IL-32, with *plaa* ^{high} cells containing 1.4 fold more IL-32 than *plaa* ^{low} cells **(Fig. 3.6)**. In both cisplatin-stimulated and resting cells, siRNA-PLAA significantly reduced IL-32 expression in *plaa* ^{high} and *plaa* ^{low} cells to a comparable level, which was lower than that of *plaa* ^{low} cells without PLAA knockdown. The effect of siRNA-PLAA on IL-32 expression was dose dependent and scrambled siRNA had no effect.

Interestingly, Goda *et al.* reported that ectopic expression of IL-32 in HeLa Tet-off cells induced apoptosis, whereas downregulation of IL-32 by siRNA rescued HeLa cells from apoptosis . It is very likely that PLAA induction by cisplatin could promote apoptosis by upregulating IL-32 expression, and siRNA-PLAA could reduce apoptosis by downregulating IL-32.

PLAA induction by cisplatin promoted proapoptotic proteomic changes in the JNK/c-Jun-FasL-caspase 8 pathway and mitochondrial-caspase 9 pathway

To characterize the signaling cascade changes induced by PLAA and cisplatin, we compared protein phosphorylation profiles of *plaa* ^{high} and *plaa* ^{low} cells treated with cisplatin. We performed Bioplex phosphorylation analysis to measure phosphorylation levels of NF-κB (p65 and I-κBα), ERK-1, p38 MAPK, JNK, c-jun, CREB, Akt, GSK 3α and β, TrkA, HSP27, and histone 3. Our results revealed that only phosphorylated (phosphor)-JNK and phosphor-c-Jun were differentially induced between cisplatin-stimulated *plaa* ^{high} and *plaa* ^{low} cells **(Fig. 3. 7).** Resting *plaa* ^{high} and *plaa* ^{low} cells contained comparable amounts of phosphor-JNK (T183+T185) **(Fig. 3.7A)** and phosphor-c-Jun (S63) **(Fig. 3.7C)**. Twelve- to twenty-four-hour cisplatin stimulation differentially upregulated the phosphorylation of JNK and c-Jun in *plaa* ^{high} and *plaa* ^{low} cells; stimulated *plaa* ^{high} cells contained 2.2 fold more phosphor-JNK **(Fig. 3.7A)** and 3.1 fold more phosphor-c-Jun than did *plaa* ^{low} cells **(Fig. 3.7C)**. The

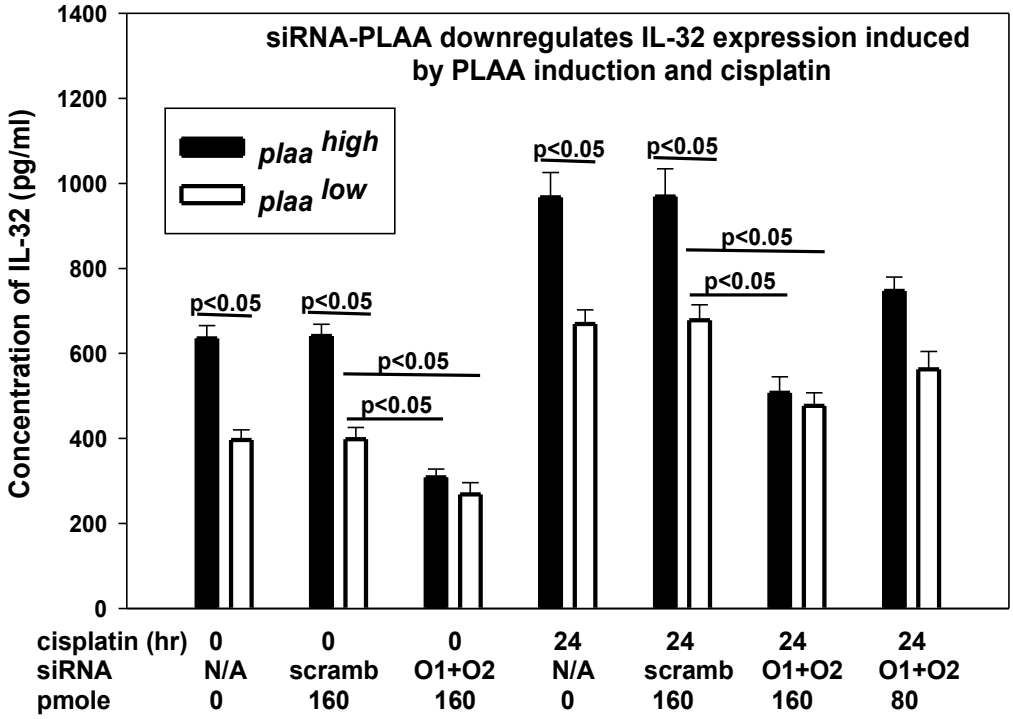

Fig. 3.6. PLAA induction by cisplatin promoted IL-32 expression in HeLa Tet-off cells. *plaa* ^{high} cells expressed more IL-32 than did *plaa* ^{low} cells in response to cisplatin and siRNA-PLAA (80 pmole of siRNA O1 combined with 80 pmole of siRNA O2) downregulated IL-32 expression. *plaa* ^{low} cells were transfected with or without siRNA-PLAA for 48 hr before cisplatin stimulation. After 24 hrs' cisplatin treatment, concentrations of IL-32 in the cell cytoplasm were analyzed by sandwich ELISA. Each ELISA sample was prepared to contained equal amounts of total protein. Values were plotted as the mean ± standard deviation of three independent repetitions.

amounts of total JNK **(Fig. 3.7B)** and total c-Jun **(Fig. 3.7D)** remained comparable between *plaa* ^{high} and *plaa* ^{low} cells. Interestingly, activation of the stress-responsive JNK/c-Jun pathway is known to induce FasL expression and activates FasL-caspase 8 pathway in cisplatin-induced apoptosis .

To characterize the proteomic changes mediated by PLAA in cisplatin-induced apoptosis, we compared cisplatin-treated (for 12 hr) *plaa* ^{high} and *plaa* ^{low} cells by using an antibody screen provided by Kinexus **(Fig. 3.7E)**. The screening results revealed that *plaa* overexpression indeed enhanced apoptosis. Activation of Fas/Fas ligand (FasL)-caspase 8-mediated apoptosis pathway was demonstrated by FasL induction (114%), and activation of caspase 8 was evidenced by the reduction in pro-caspase 8 (74% reduction) in *plaa* ^{high} cells over that in *plaa* ^{low} cells. Furthermore, activation of the JNK/c-Jun pathway, which can induce FasL expression , was confirmed by increased phosphorylation of JNK (298%) and c-Jun (703%). These data confirmed our results from Bioplex phosphorylation screening **(Fig. 3.7)** and suggested to us that PLAA promoted cisplatin-induced apoptosis through the JNK-c-Jun-FasL-caspase 8 pathway.

Activation of the mitochondrial-caspase 9-mediated apoptosis pathway was evidenced by the increased ratio of Bax/Bcl2 (63% increase over *plaa* ^{low} cells), which is associated with compromised integrity/leakage of the mitochondria . Further, an activation of caspase 9 was revealed by the reduction of pro-caspase 9 (79% reduction) in *plaa* ^{high} cells. These results confirmed the activation of the caspase 9 **(Fig. 3.1D)** and caspase 8 pathways **(Fig. 3.1E)**.

Although expression of pro-caspase 3 was not altered at 12 hr-cisplatin treatment, increased cleavage of caspase 3 targets, namely DNA fragmentation factor (DFF)-45 (46% reduction) and DFF-35 (45% reduction) , was noted. Importantly, after

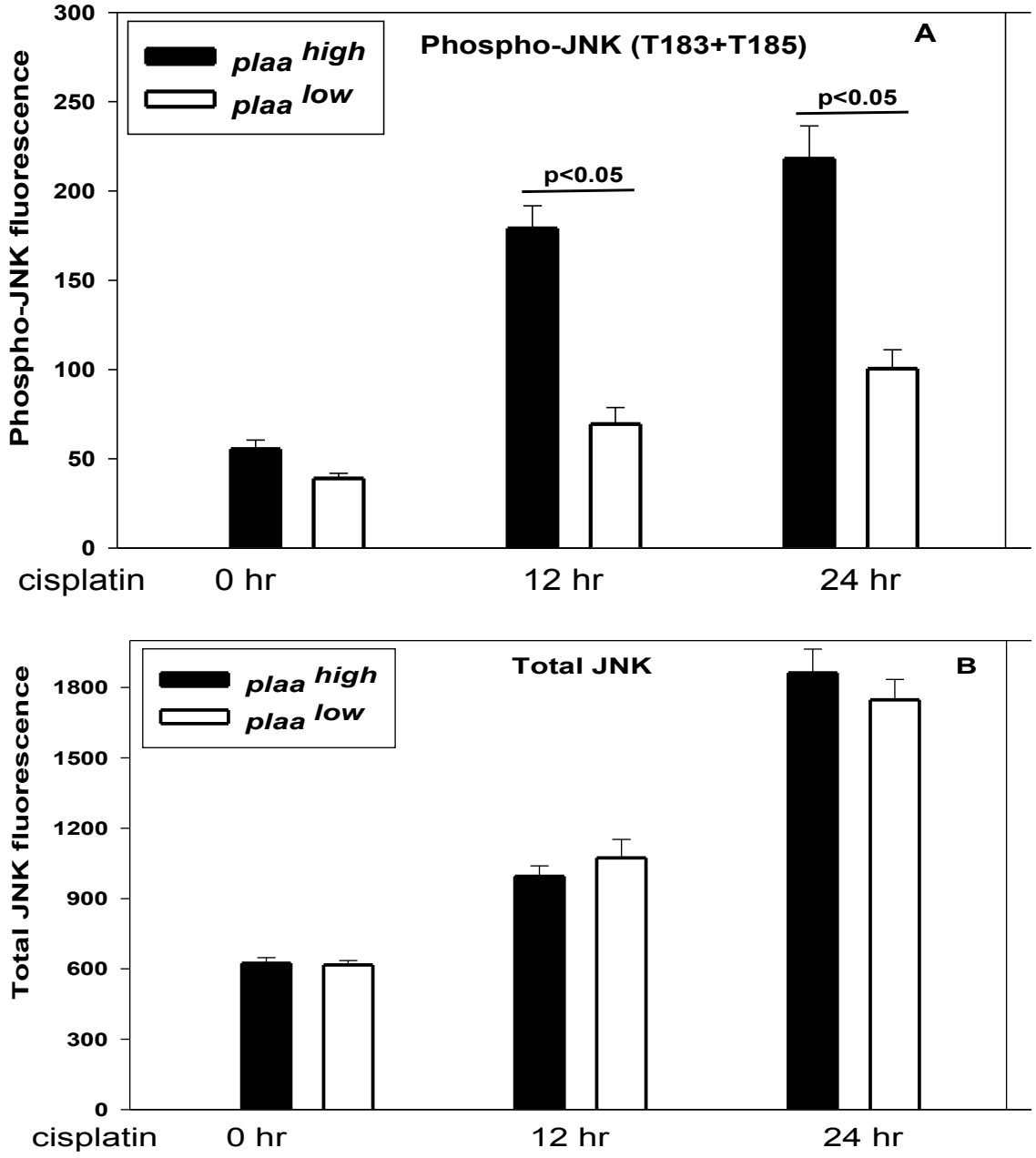

Fig. 3.7. PLAA induction by cisplatin promoted proapoptotic proteomic changes in the JNK/c-Jun-FasL-caspase 8 pathway and mitochondria-caspase 9 pathway in HeLa Tet-off cells. (A-D) *plaa* ^{high} cells contained significantly more phosphorylated JNK (phosphor-JNK) **(A)** and phospho-c-Jun **(C)** than did *plaa* ^{low} cells. The phosphorylation status of JNK/c-Jun was determined by using a Bio-plex phosphoprotein assay. Phosphorylated protein standards were used in the assay. The amount of phosphor-JNK **(A)**, total JNK **(B)**, phosphor-c-Jun **(C)** and total c-Jun **(D)** was measured in the same whole cell lysate samples. Values were given as relative fluorescence units, and bars represent the means ± standard deviation of three independent repetitions.

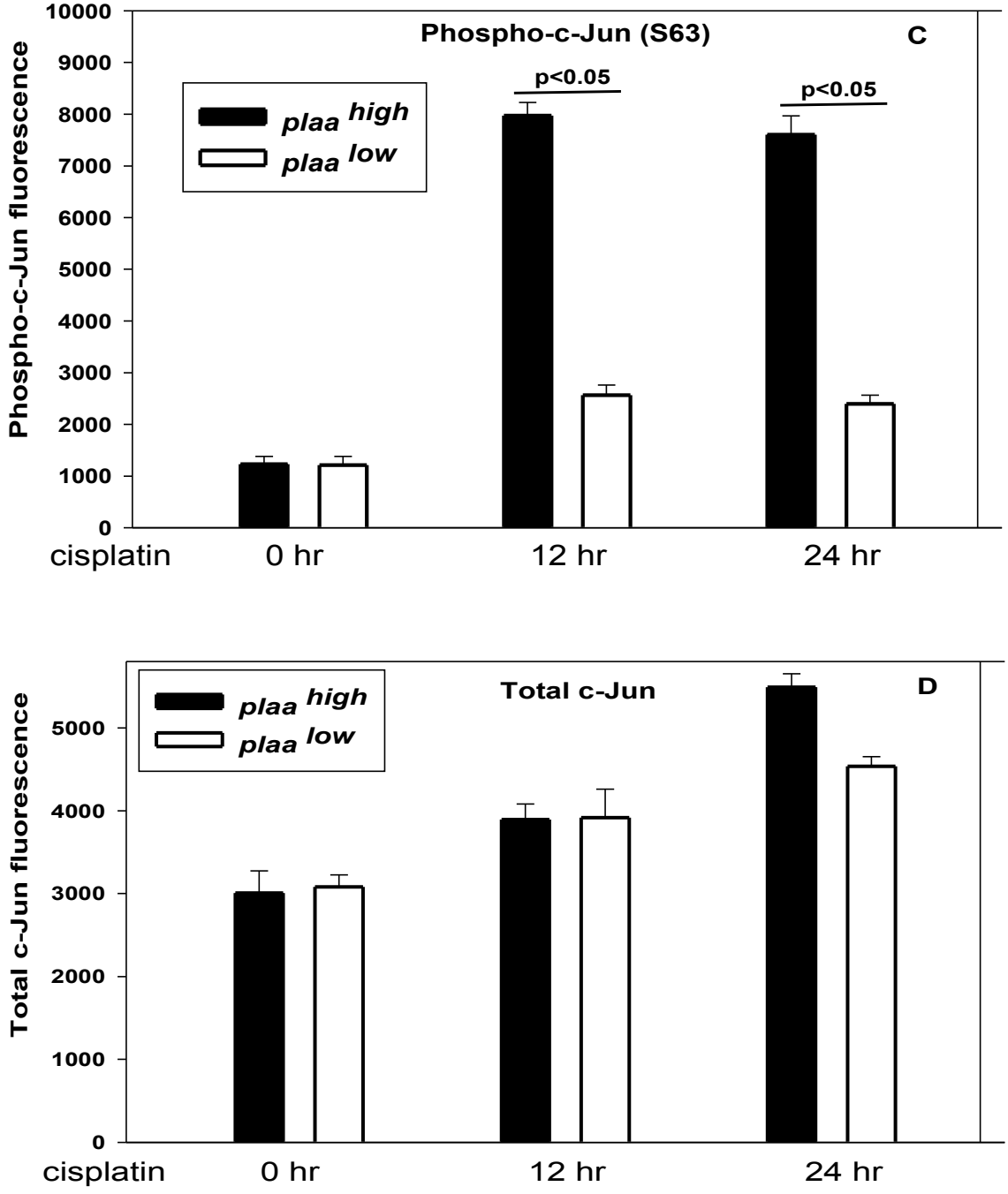

Fig. 3.7. PLAA induction by cisplatin promoted proapoptotic proteomic changes in the JNK/c-Jun-FasL-caspase 8 pathway and mitochondria-caspase 9 pathway in HeLa Tet-off cells. *(continued)* The amount of phosphor-JNK **(A)**, total JNK **(B)**, phosphor-c-Jun **(C)** and total c-Jun **(D)** was measured in the same whole cell lysate samples. Values were given as relative fluorescence units, and bars represent the means ± standard deviation of three independent repetitions.

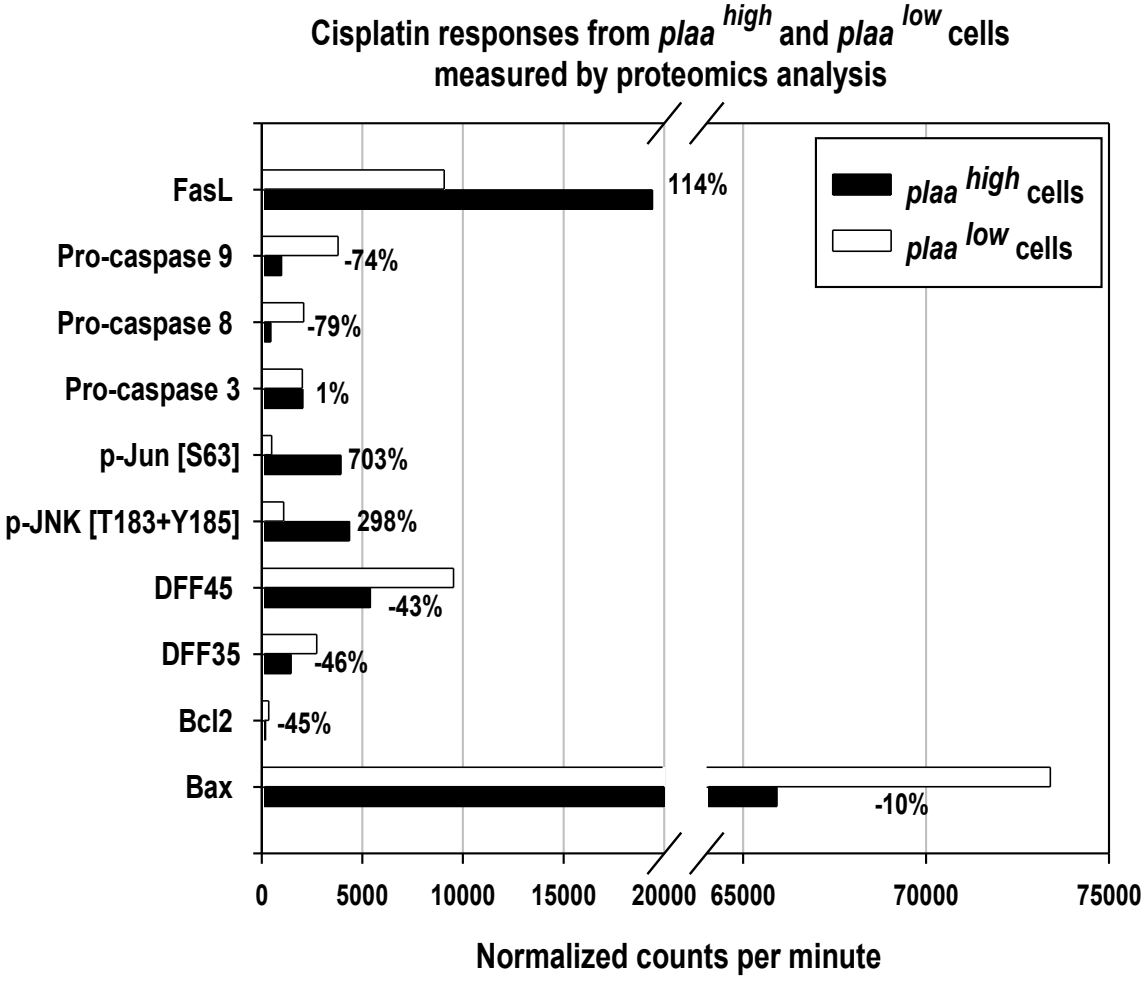

Fig. 3.7. PLAA induction by cisplatin promoted proapoptotic proteomic changes in the JNK/c-Jun-FasL-caspase 8 pathway and mitochondria-caspase 9 pathway in HeLa Tet-off cells. *(continued)* **(E)** Whole-cell lysate protein samples (500 μg) from cisplatin treated *plaa* ^{high} and *plaa* ^{low} cells were analyzed by using KinetWorks apoptotic screen according to the manufacturer's instructions (for details, see methods section). Kinexus provided all of the immunoblotting, normalization and statistical analysis data. Normalized trace quantity units (cpm) were based on the intensity of fluorescence detection for the target immunoreactive proteins.

24 hr treatment with cisplatin, *plaa* ^{high} cells contained 73% more caspase 3 activity than did *plaa* ^{low} cells **(Fig. 1C)**.

Discussion

Based on our data, we believe that PLAA induction promotes cisplatin-induced apoptosis in HeLa cells. Enhanced PLAA expression by cisplatin resulted in induction of PLA_2 activation **(Fig. 3.3)** and IL-32 expression **(Fig. 3.6)**, as well as inhibition of clusterin expression **(Fig. 3.5)**. Induction of PLA_2 and IL-32 , as well as downregulation of clusterin , have all been shown by other groups to promote apoptosis and in our current studies as well **(Fig. 3.8)**.

AA accumulation, generated by PLA_2 activation, is known to cause mitochondrial damage and apoptosis . We believe that PLAA promoted cisplatin-induced apoptosis in HeLa cells partially through AA accumulation. Expression of the *plaa* gene is required for producing AA, since antisense against PLAA significantly reduced the amount of AA in macrophages treated with lipopolysaccharide and Chinese hamster ovary cells treated with oxytocin (unpublished data from our laboratory). In our current study, cisplatin significantly induced *plaa* expression (**Fig. 3.1A**), in concurrence with $cPLA_2$ and $iPLA_2$ activation (**Fig. 3.3**) in HeLa Tet-off cells. Compared to the control *plaa* ^{low} cells treated in the same way with cisplatin, *plaa* overexpressing (*plaa* ^{high}) cells exhibited elevated levels of $cPLA_2$ and $iPLA_2$ activation **(Fig. 3.3)**, mitochondrial damage/cytochrome *c* release **(Fig. 3.4)**, DNA fragmentation **(Fig. 3.1B)** and caspase activation **(Figs. 3.1C, 3.1D, 3.1E and 3.7E)**. The siRNA-PLAA reduced PLA_2 activation **(Fig. 3.3C)**, mitochondrial damage/cytochrome *c* release **(Figs. 3.4A & 3.4B)** and DNA fragmentation **(Fig. 3.2B)**, while it partially restored cell viability after cisplatin stimulation **(Fig. 3.4C)**. Supplementing AA to *plaa* knockdown cells treated with cisplatin reversed the effect of siRNA-PLAA by promoting mitochondrial damage/

cytochrome *c* release **(Fig. 3.4B)**, which was indicative that siRNA-PLAA protected cells against mitochondrial damage partially by reducing AA accumulation.

PLAA induction also contributed to cisplatin-induced apoptosis by downregulating the cytoprotective protein clusterin **(Fig. 3.5)**. Antisense oligonucleotides against clusterin are being used in phase I clinical trial to confirm its efficacy as an apoptosis-promoting agent in prostate and breast tumors . We found that *plaa* ^{high} cells expressed significantly less clusterin than did the control *plaa* ^{low} cells **(Fig. 3.5A)** and exhibited a higher degree of apoptosis responses to cisplatin **(Fig. 3.1)**. These results supported clusterin's established role in promoting chemoresistance for various tumors, notably those of the prostate, lungs and kidneys . We demonstrated that siRNA-PLAA promoted clusterin expression in HeLa Tet-off cells **(Fig. 3.5B),** and exogenously supplied clusterin reduced cisplatin-induced DNA fragmentation **(Fig. 3.5C)**. On the contrary, neutralizing antibodies against clusterin promoted DNA fragmentation in both *plaa* ^{high} and *plaa* ^{low} cells treated with siRNA-PLAA and cisplatin **(Fig. 3.5D)**. Neutralizing antibody against clusterin enhanced chemosensitivity in osteosarcoma cells , and exogenously supplied clusterin reduced TNF-α sensitivity in prostate cancer cells , findings which were consistent with our results **(Figs. 3.5B and 3.5C)**. Interestingly, clusterin can protect cells against mitochondrial damage by interacting with the proapoptotic mitochondrial protein Bax . Accordingly, we noted in *plaa* ^{high} cells an elevated level of mitochondrial damage/cytochrome *c* release **(Fig. 3.4A)** and a reduction of Bcl-2/Bax ratio, compared to equivalent findings in the control *plaa* ^{low} cells **(Fig. 3.7E)**.

Upregulation of IL-32 by PLAA induction in cisplatin-treated HeLa cells can potentially promote apoptosis **(Fig. 3.6)**. We demonstrated that *plaa* ^{high} cells expressed more IL-32 than did the control *plaa* ^{low} cells and showed a higher level of cisplatin-induced apoptosis. The siRNA-PLAA reduced IL-32 expression **(Fig. 3.6)** and apoptosis (**Fig. 3.2B**). IL-32 was initially designated as natural killer cell transcript 4 (NK4) and known to be induced at mRNA

level by anticancer drug 8-chloroadenosine in neuroblastoma cells . In a later study, IL-32 was found to associate specifically with T cells undergoing activation-induced apoptosis . Goda *et al* reported that ectopic expression of IL-32 in HeLa cells induced apoptosis whereas downregulation of IL-32 by siRNA rescued HeLa cells from apoptosis , and this is consistent with our findings.

In addition to their importance in cancer chemotherapy, PLAA and IL-32 are also potential targets that can be employed for chemotherapy to treat autoimmune diseases such as rheumatoid arthritis and systemic lupus erythematosus. Both PLAA and IL-32 mediate inflammatory responses and are highly expressed in the immune system, e.g., in the spleen and thymus. Induction of PLAA and IL-32 following chemotherapy can potentially reduce pathogenic immune cells by apoptosis.

Another possible mechanism by which *plaa* induction promotes apoptosis is by activating of JNK/c-Jun signaling. It is well documented that the latter, which can be induced by cisplatin, is a key pro-apoptotic mediator in various cancer cells, including those of the cervix (i.e., HeLa cells), ovaries, lungs, colon and stomach . FasL is an established target regulated by the JNK/c-Jun signaling that mediates cisplatin-induced apoptosis in a JNK/c-Jun-dependent fashion . Consistently, *plaa* ^{high} cells exhibited significantly more JNK/c-Jun activation **(Fig. 3.7A, 3.7C and 3.7E)**, FasL induction **(Fig. 3.7E)** and caspase 8 activation **(Fig. 3.1E and 3.7E)** than did *plaa* ^{low} cells. The detailed mechanism by which PLAA induction promotes cisplatin-induced JNK/c-Jun signaling deserves further investigation. Since PLAA peptides can activate MAP kinase ERK1/2 in smooth muscle cells , native PLAA may directly enhance JNK/c-Jun activation in response to cisplatin. Alternatively, the AA metabolites generated by PLAA induction and PLA_2 activation may activate JNK/c-Jun signaling .

In summary, our data demonstrated that induction of PLAA promoted cisplatin-associated apoptosis in cervical carcinoma HeLa cells by the following four pathways **(Fig.**

3.8): a) activation of PLA_2 and accumulation of AA, which causes mitochondrial damage; b) downregulation of clusterin, a cytoprotective protein which promotes chemoresistance; c) upregulation of IL-32, whose induction has been shown to cause apoptosis in HeLa cells ; and d) activation of JNK/c-Jun signaling, which is an established inducer of FasL expression and death receptor mediated-apoptosis.

Our results suggest that modulation of the PLAA-PLA_2 pathway may provide therapeutic benefits in cisplatin-based chemotherapy. In cisplatin-resistant tumors, PLAA peptides and/or a PLA_2 enzyme agonist could be used to enhance the cytotoxicity of cisplain. Indeed, peroxisome proliferator-activated receptor γ (PPARγ), one of the receptors activated by AA and its metabolites, has been demonstrated to synergize with carboplatin in ovarian and lung cancer cells, as well as in a mouse model of colon cancer . Interestingly, unpublished data from the same study also demonstrated that carboplatin-resistant ovarian tumors expressed significantly less PLAA than did the control carboplatin-sensitive tumors . The high expression level of native PLAA in the prostate and cervical tissue may contribute to the effectiveness of cisplatin in prostate and cervical cancers. In addition, the high expression of PLAA in the immune system can also be employed via chemotherapy to suppress autoimmunity by reducing the pathogenic leukocytes through apoptosis. On the other hand, downregulating cisplatin-induced PLAA may reduce the toxic side effects of chemotherapy in non-cancerous tissues. Accordingly, siRNA against PLAA and/or an antagonist of PLA_2 enzymes can be employed to reduce the neurotoxicity and nephrotoxicity of cisplatin.

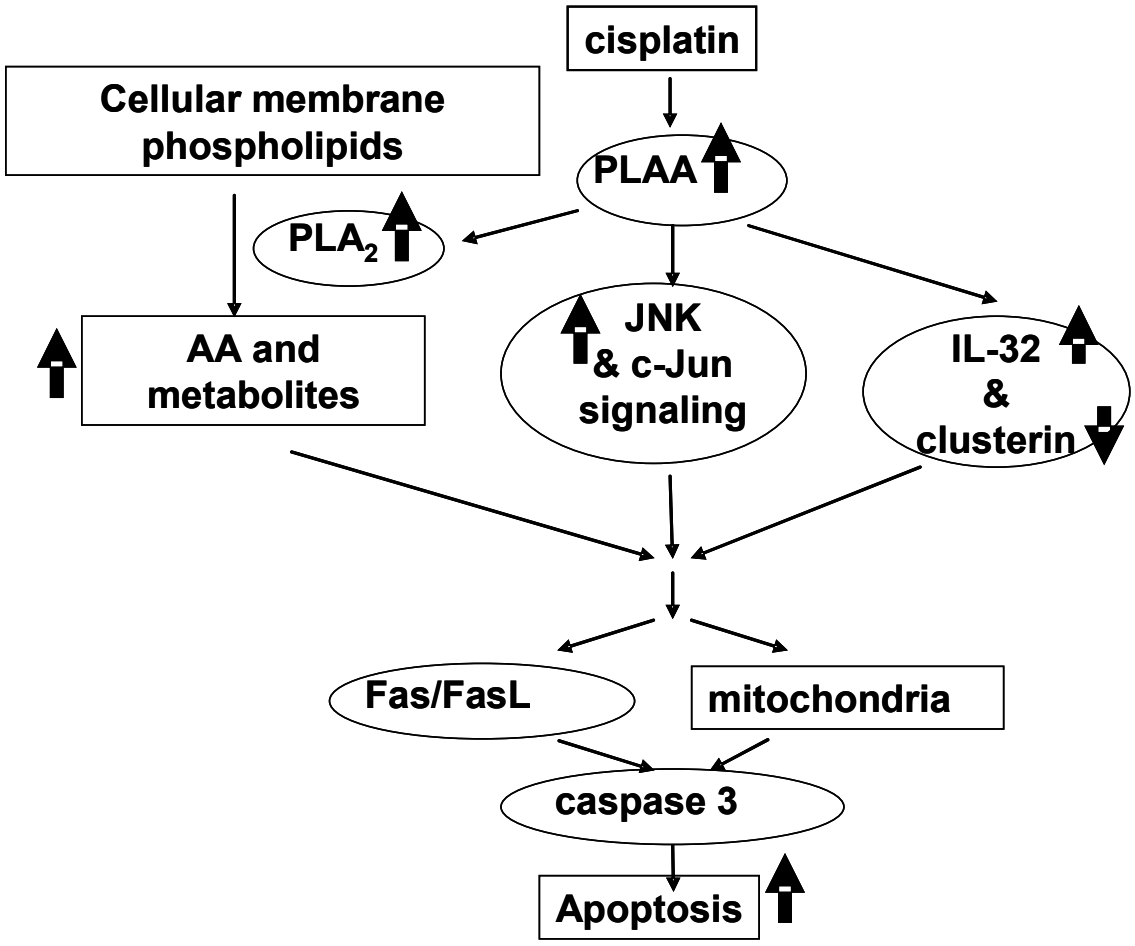

Fig. 3.8. Proposed role of PLAA induction by cisplain during apoptosis.

Upward arrows denoted upregulation and downward arrows denoted downregulation of the indicated genes.

Chapter 4

FUTURE DIRECTIONS OF PLAA RESEARCH

Due to the difficulties in purifying full length PLAA, genetic manipulation (knock-down/ knockout or knock-in/overexpression) of the native *plaa* gene is the preferred approach to elucidate its functions. Short hairpin RNA (shRNA) against *plaa* (commercially available from Open Biosystems) can be used to knock-down *plaa* expression in host cells. Since PLAA seemed to be involved in mouse fertility (unpublished data from our laboratory), we may need to generate conditional knock-out mice or mice with organ-specific knock-down of PLAA. Lentiviral vector-based shRNA, which has been used by different groups to successfully knock down gene expression in mice , can be used to knock down *plaa* in mice.

Subsequently, global effect of PLAA knock-down can be studied in specific disease models using genomic (GeneChip analysis), proteomic (e.g., two-dimensional gel electrophoresis), biochemical (e.g., phosphorylation/signaling analysis) and histopathological approaches. As an example, the role of PLAA in the pathogenesis of IBD can be investigated by knocking down *plaa* in a mouse model of colitis (e.g., IL-10 $^{-/-}$ mice infected with *Helicobacter hepaticus*). Disease progression in PLAA knock-down mice and control mice can be induced and compared with each other using specific pathological parameters. Using mouse model of colitis as an example, PLAA $^{-/-}$ colitic mice can be compared with control colitic mice in: 1) epithelial integrity of colonic epithelium; 2) degree of colonic inflammation; 3) tissue production (from the cecum and proximal colon) of cytokines and other inflammatory mediators (e.g., PGE_2); 4) apoptosis of T cells from the lamina propria, mesenteric lymph nodes and spleen. Specific signaling events underlining the pathological changes (e.g., MAP kinase, PLA_2 and NFκB activation) can also be compared between PLAA knock-down mice with disease and control mice with disease.

Further, peptide fragments of PLAA in the length of 300-500 amino acids have been successfully expressed in *E. coli* and purified by other group(s). Protein-protein interaction between PLAA and its binding partners can be studied using these PLAA peptides. We may also use these PLAA peptides and examine their biological responses in the host cells. As an example, we could treat macrophages with PLAA peptides and determine TNF-α production . Alternatively, tumor cells can be stimulated with PLAA peptides and apoptotic responses can be examined. However, caution should be taken when interpretating these results, since the native PLAA resides as an intracellular protein and is only found in extracellular space under certain pathological conditions (e.g., rheumatoid arthritis or cell lysis). PLAA peptide concentration used to stimulate cells should be pathologically relevant. The pathological concentration of extracellular PLAA protein remains to be determined. In addition, when using PLAA peptides purified from *E. coli,* LPS should be removed from these peptides to rule out the effects from contamination on such biological effects.

LIST OF ABBREVIATIONS

TNF-α	tumor necrosis factor α
siRNA	small interference RNA
IL-32	interleukin 32
COX-2	cyclooxygenase 2
NF-κB	nuclear factor κB
JNK	c-Jun N-terminal kinases
MAPK	mitogen-activated protein kinase
ERK1/2	extracellular signal-regulated kinases
GSK3β	glycogen synthase kinase 3β
PKC	protein kinase C
MAPK	mitogen-activated protein kinase
PI3K	phosphatidylinositol 3-kinase
Bcl-2	B cell lymphoma 2
RT-PCR	Reverse Transcriptase Polymerase Chain Reaction